VOLUME 86 NO. SM6
DECEMBER 1960
PART 1

JOURNAL of the

Soil Mechanics and Foundations Division

PROCEEDINGS OF THE

AMERICAN SOCIETY OF CIVIL ENGINEERS

BASIC REQUIREMENTS FOR MANUSCRIPTS

Original papers and discussions of current papers should be submitted to the Manager of Technical Publications, ASCE. Authors should indicate the technical division to which the paper is referred. The final date on which a discussion should reach the Society is given as a footnote with each paper. Those who are planning to submit material will expedite the review and publication procedures by complying with the following basic requirements:

1. Titles must have a length not exceeding 50 characters and spaces.

2. A summary of approximately 50 words must accompany the paper, a 300-word synopsis must precede it, and a set of conclusions must end it.

3. The manuscript (an original ribbon copy and two duplicate copies) should be double-spaced on one side of 8½-inch by 11-inch paper. Three copies of all illustrations, tables, etc., must be included.

4. The author's full name, Society membership grade, and footnote reference stating present employment must appear on the first page of the paper.

5. Mathematics are recomposed from the copy that is submitted. Because of this, it is necessary that letters be drawn carefully, and that special symbols be properly identified. The letter symbols used should be defined where they first appear, in the illustrations or in the text, and arranged alphabetically in an Appendix.

6. Tables should be typed (an original ribbon copy and two duplicate copies) on one side of 8½-inch by 11-inch paper. Specific illustrations and explanation must be made in the text for each table.

7. Illustrations must be drawn in black ink on one side of 8½-inch by 11-inch paper. Because illustrations will be reproduced with a width of between 3-inches and 4½-inches, the lettering must be large enough to be legible at this width. Photographs should be submitted as glossy prints. Explanations and descriptions must be made within the text for each illustration.

8. The desirable average length of a paper is about 12,000 words and the absolute maximum is 18,000 words. As an approximation, each full page of typed text, table, or illustration is the equivalent of 300 words.

9. Technical papers intended for publication must be written in the third person.

10. The author should distinguish between a list of "Reading References" and a "Bibliography," which would encompass the subject of his paper.

This Journal is published bi-monthly by the American Society of Civil Engineers. Publication office is at 2500 South State Street, Ann Arbor, Michigan. Editorial and General Offices are at 33 West 39 Street, New York 18, New York. $4.00 of a member's dues are applied as a subscription to this Journal. Second-class postage paid at Ann Arbor, Michigan.

The index for 1959 was published as ASCE Publication 1960-10 (list price $2.00); indexes for previous years are also available.

EM,HY,SA,SM.

Journal of the

SOIL MECHANICS AND FOUNDATIONS DIVISION

Proceedings of the American Society of Civil Engineers

CONTENTS

December, 1960

Papers

(Over)

Note.—Part 2 of this Journal is the 1960-46 Newsletter of the Soil Mechanics and Foundations Division.

DISCUSSION

Journal of the

SOIL MECHANICS AND FOUNDATIONS DIVISION

Proceedings of the American Society of Civil Engineers

COMPUTER SOLUTION OF PRESSURE DISTRIBUTION PROBLEM

By U. W. Stoll,[1] M. ASCE

SYNOPSIS

A general computer method for solving vertical pressure distribution problems encountered in applied soil mechanics is presented. The attempt is made to retain a direct equivalence between the physical problem and the required computer notation and logic. A possible computer flow diagram and a specific Fortran program for use on the computer used are given.

INTRODUCTION

A recurring problem in applied soil mechanics is that of determining the distribution of vertical pressures at some depth due to the application of loads at some higher plane. This problem might be conceived to be as shown in Fig. 1, and the solution may take the form of the general equation

$$P\,V = \sum_{i=1}^{i=n} K_i\,P_i \quad \text{. . . . .} \quad (1)$$

and C Z equals the radius of area within which loads have significant effect on pressure at PV.

The coefficient K is generally considered to be a function of relative position of applied load and the pressure point, and also is a function of the relation be-

Note.—Discussion open until May 1, 1961. To extend the closing date one month, a written request must be filed with the Executive Secretary, ASCE. This paper is part of the copyrighted Journal of the Soil Mechanics Division, Proceedings of the American Society of Civil Engineers, Vol. 86, No. SM 6, December, 1960.

[1] Instr., Civ. Engrg., Univ. of Michigan, Ann Arbor, Mich.

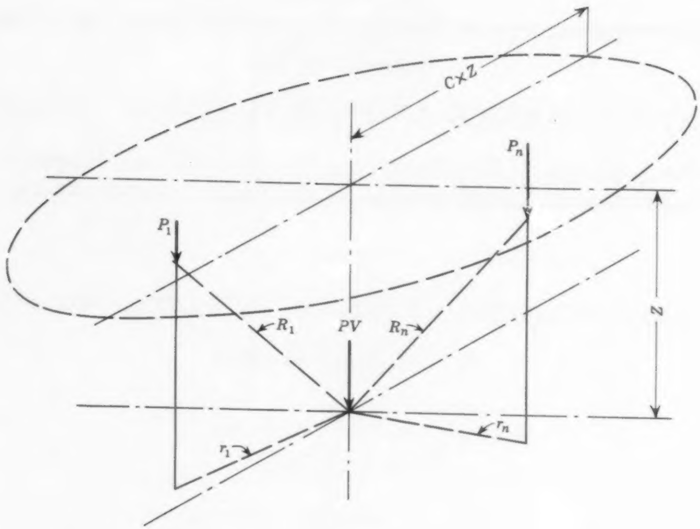
C×Z
P_n
P_1
Z
R_1
PV
R_n
r_n
r_1

FIG. 1

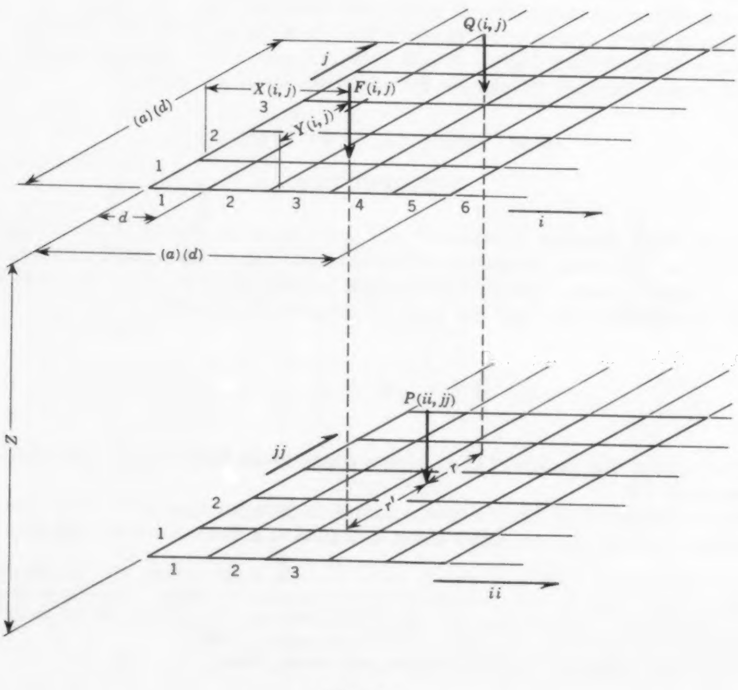
Q(i, j)
j
X(i, j)
F(i, j)
(a)(d)
3
Y(i, j)
2
1
1
2
3
4
5
6
d
i
(a)(d)
Z
P(ii, jj)
jj
r
r'
2
1
1
2
3
ii

FIG. 2

tween elastic properties of the pressure transmitting medium, that is, soil mass. The required number and form of individual solutions for a given problem depends on how detailed and mathematically precise a picture of pressure variations is desired.

Two of the more widely used expressions of the distribution parameter, K, (Eq. 1) are the Boussinesq equation for homogeneous, isotropic, semi-infinite elastic mass

$$K = \frac{3}{2\, Z^2\, \pi \left[1 + \left(\frac{r}{Z}\right)^2\right]^{\frac{5}{2}}} \quad \ldots\ldots\ldots\ldots\ldots (2a)$$

and the Westergaard equation[2] for a horizontally layered elastic mass, infinitely rigid in the horizontal direction

$$K = \frac{1}{Z^2\, \pi \left[1 + 2\left(\frac{r}{Z}\right)^2\right]^{\frac{3}{2}}} \quad \ldots\ldots\ldots\ldots\ldots (2b)$$

Another useful form of the pressure distribution equation is one proposed by J. A. Griffith and O. K. Froehlich[3,4]

$$P_v = \frac{N\, P}{2\, \pi\, R^2}\ \frac{Z^N}{R^N} \quad \ldots\ldots\ldots\ldots\ldots (3)$$

in which N = 3 is equivalent to Boussinesq (Eq. 2a) and N = 6 is empirically applicable to concentrated loads transmitted through a shallow granular stratum bearing against a rigid support.

M. A. Biot[5] and K. Wolf[6] have also developed precise elastic solutions of considerable complexity for varying supporting boundary conditions and degrees of anisotropy. Evaluation of the former's relationships indicates that these largely fall within the range of values given by the preceeding equations.

It has been generally recognized that elastic pressure relationships have only limited applicability in soil mechanics and are generally inaccurate and misleading when applied to plastically-deformed zones, particularly near the point of load application. However, soils under moderate stress and at points remote from the zone of load application do appear to react in an elastic manner. In such instances, the Boussinesq equation has been usefully employed for estimating values of distributed pressures.

Although it is possible to obtain solutions to the Boussinesq or other equations by summing the component reactions using slide rule and desk computers,

---

2 "Soft Material Reinforced by Numerous Strong Horizontal Sheets," by A. M. Westergaard, Contributions to the Mechanics of Solids, Stephen Timoshenko 60th Anniversary Vol., 1938.

3 "Pressure Under Substructures," by J. A. Griffith, Engineering and Contracting, March, 1929, pp. 113-119.

4 "Drukverdeeling in Bouwgrond," by O. K. Froelich, De Ingenieur, April 15, 1932, p. B-52.

5 "Effect of Certain Discontinuities on Pressure Distribution in a Loaded Soil," by M. A. Biot, Physics, Vol. VI, December, 1935.

6 "Ausbreitung der Kraft in der Halbebene und in Halbraum bei anisotropem Material," by K. Wolf, Zeitschrift fur angewandte Mathematik und Mechanik, Vol. XV, No. 5, 1935.

this is practical only for the more modest problems. Most widely used for the typical practical problem concerning area loadings for buildings or embankment foundations is the Newmark influence diagram.[7] This method requires visual integration of influence areas and incidental computations. Some data leveling may also be required to bring problems to a manageable form.

DEVELOPMENT OF COMPUTER PROGRAM

It was necessary to determine the pressure distribution beneath a large mat-supported power house in connection with long time settlement observations and forthcoming revisions of loading schedules. The stratum being considered lay from 33 ft to 25 ft below the building mat, covering an area of approximately 300 ft by 700 ft with foundation mat loads ranging from 0.3 to 3.0 kip per sq ft and involving about 700 columns, unsymmetrically arranged, delivering from 4 to 2,000 kips each. It was apparent that the conventional methods would involve a large expenditure of time to obtain even the sketchiest picture of the overall distribution at the desired depth.

To solve this problem, the writer developed the computer program that will be outlined here. For convenience, a general example of the method will be carried through, with particular attention devoted to assigning physical meaning to the symbols and operations as they are introduced and discussed. In addition to a general flow diagram, a specific Fortran language instruction is presented in the Appendix.

The first step is to establish an appropriate square grid that is laid out on a scaled plan of the area being studied. In general, the basic grid dimension may be set equal to 1/3 or less that of the depth from the load plane to the pressure plane. In addition, it will be advantageous to limit the grid dimension to less than the minimum spacing between significant concentrated loads.

After the properly scaled square grid system has been drawn, coordinate values are assigned to each grid element, numbering from left to right (the X or i direction) and from bottom to top (the Y or j direction), making reference to column load, slab weight, and floor load schedules, assigning appropriate values to each grid element. It will be convenient to prepare a standard data form, leaving space for: (a) Uniform loads, Q (i, j) - that is, equivalent concentrated load acting at the center of the grid element; (b) Concentrated loads, F (i j); (c) X coordinate of F, X (i, j); and (d) Y coordinate of F, Y (i, j). Reading these items in sequence (a) through (d) for each grid element, from left to right, bottom to top. If a concentrated or uniform load is absent, the appropriate item is set equal to zero and recorded in proper sequence.

Using the notation of the grid element coordinates to identify the location of the load data, and a parallel and related coordinate system to identify the location of the pressure point, Eqs. 1 and 2a may now be written (Fig. 2).

$$P\,(ii,jj) = C \sum \frac{Q\,(i,\,j)}{\left[1 + \left(\frac{r}{Z}\right)^2\right]^{\frac{5}{2}}} + C \sum \frac{F\,(i,\,j)}{\left[1 + \left(\frac{r'}{Z}\right)^2\right]^{\frac{5}{2}}} \quad \ldots\ldots \quad (4)$$

in which Z is the depth from load plane (i - j) to pressure plane (ii - jj) where

[7] "Influence Charts for the Computation of Stresses in Elastic Foundations," by N. M. Newmark, Univ. of Illinois Engrg. Experiment Sta. Bulletin 338, 1942.

i varies from $\left| ii - \frac{a-1}{2} \right|$ to $\left| ii + \frac{a-1}{2} \right|$ and j varies from $\left| jj - \frac{a-1}{2} \right|$ to $\left| jj + \frac{a-1}{2} \right|$; a denotes the number of grid elements in both the left-right and bottom-top directions, spanning the area within which loads have a significant effect on the value of P (ii, jj); and in which

$$r = d\sqrt{(ii - i)^2 + (jj - j)^2} \quad \ldots\ldots\ldots\ldots\ldots\ldots \quad (5)$$

and

$$r' = \sqrt{\left[X(i, j) - d \times (ii) + \frac{d}{2}\right]^2 - \left[Y(i, j) - d \times (jj) + \frac{d}{2}\right]^2} \quad \ldots (6)$$

d refers to the dimension of individual grid element; and $C = \frac{3\pi}{2 Z^2}$.

Fig. 2 indicates the physical equivalents of the notation introduced previously. It shows that in computing a value P (ii, jj), only a limited and definable block of grid elements with concomitant loads are being directly involved in the computations. The essence of the computer program is to not only determine and sum the component pressure values, but to index the pressure point over the desired area, redefining the block of grid elements to encompass the loaded area of significance. In addition, for a large program, it will be necessary to reorganize and replace the data as the program proceeds.

A possible flow diagram for the general program is shown in Table 1.

Insofar as is feasible, the notation of Fig. 2 has been retained in the flow diagram. The following comments will help explain certain additional terms or substitutions, in the order they appear in the flow diagram. The factors M and N are the number of grid elements in the left-right and bottom-top directions, respectively. The factor JY defines the coordinate, in the j or y direction, of the pressure point being evaluated. Factor KEND defines the left hand grid column coordinate of the grid block considered in computing the pressure points to the extreme right. The factor K, which is initiated at a value of 1 and is indexed as each pressure point is computed and tabulated, controls the proper minimum and maximum values of i to be used in calling for the load and coefficient data. When K reaches the value KEND, the data in the core memory is rearranged, currently applicable load and coordinate data are substituted for data no longer required, and the factor K is initiated once again. It will be noted that the pressure point PV is identified in a non-subscripted form. The values of KK, JY, and Z, which are written in conjunction with a specific value of PV, adequately identify the coordinates (location) of the pressure value. Since PV is set equal to zero after each "write" statement, there is no danger of overloading the memory with redundant output data.

The above flow diagram and the Fortran program shown in the Appendix are not purported to be the optimum procedure from the standpoint of computer efficiency. However, they do retain a reasonably close equivalence to the physical representation shown in Fig. 2. It will be noted that a special sub-routine has been inserted between statements 23 and 36 in the Fortran program. By limiting the precise computation of radial distances to just those loads falling within grid elements most proximate to the pressure point (in the example, within two grid blocks from the pressure point), one can significantly reduce the computation

TABLE 1.—FLOW DIAGRAM

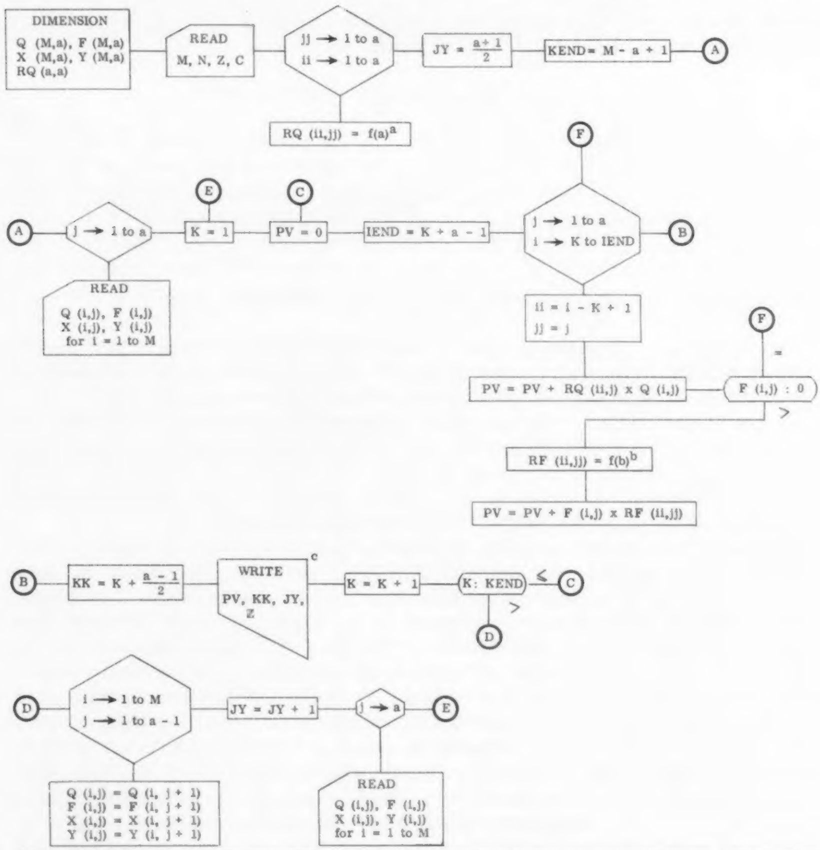

[a] $$RQ\ (ii,jj) = \frac{C}{Z^2 \left\{1 + \frac{[r\ (ii,jj)]^2}{Z^2}\right\}^{\frac{5}{2}}}$$

$$r\ (ii,jj) = d\sqrt{\left(ii - \frac{a+1}{2}\right)^2 + \left(jj - \frac{a+1}{2}\right)^2}$$

[b] $$RF\ (ii,jj) = \frac{C}{Z^2 \left\{1 + \frac{[r'\ (ii,jj)]^2}{Z^2}\right\}^{\frac{5}{2}}}$$

$$r'\ (ii,jj) = \sqrt{\left[X\ (i,j) - d\left(K + \frac{a-1}{2}\right) + \frac{d}{2}\right]^2 + \left[Y\ (i,j) - d \times JY + \frac{d}{2}\right]^2}$$

[c] PV = current value of P (ii,jj)
KK = current value of ii
JY = current value of jj

time. More remote concentrated loads are considered to act at the grid element mid-point and the precomputed radial distances, that is, RX (ii, jj) and related pressure coefficients, are used. Other problems might suggest further economies or require additional refinements.

To indicate the amount of computer time required to execute the program outlines, the following experience might be considered as a guide: for 484 separate pressure points involving a 15 by 15 block of loaded grid elements for each pressure point, the time required for execution was 5.8 min. A significant portion of this time involved rearrangement and transfer of data from tape to magnetic memory. Thus, smaller programs not requiring this step would require even less time than that indicated by a single proportion between number of pressure points and grid block elements.

LIMITATIONS

One limitation on the program outlined is that pressures are computed only at mid-points of grid elements, which may not be the loci of maximum pressures if a large concentrated load located within the element does not fall at the center. This discrepancy, of course, is rapidly diminished by reducing the dimensions of the grid element. An alternate method would be to program a sub-routine to compute the pressure directly beneath any concentrated load greater than some specified value, this involving the recomputation of the radial distances and related pressure coefficients of the surrounding loaded grid elements.

Any error introduced by considering uniform loads to be equivalent concentrated loads acting at the centers of the elements would be small and consistent. For example, when d (element width) is less than 1/3 Z (depth), the concentrated load yields pressure values less than 5% above equivalent uniform load values.

CONCLUSION

Experience indicates that the computer method and the specific program presented is sufficiently flexible and economical to be considered for solving lengthy or complex pressure distribution problems.

ACKNOWLEDGMENTS

The development of the computer program was carried on under a University of Michigan Research Institute project sponsored by the Cleveland Electric Illuminating Company, with Mr. W. S. Housel acting as project supervisor. The writer wishes to acknowledge the counsel and review given by Mr. Glen V. Berg, F. ASCE, of the University of Michigan (Ann Arbor) Civil Engineering Department, concerning the development of the Fortran program.

APPENDIX.—FORTRAN PROGRAM FOR IBM 704 COMPUTER

```
      DIMENSION Q(57,15),Y(57,15),X(57,15),F(57,15),RX(15,15)
      WRITE OUTPUT TAPE 6,102
  102 FORMAT (62H1          DELPV     X        Y          Z          Q
     X      F)
      READ INPUT TAPE 7,100,M,N,Z,C
  100 FORMAT (215,F5.0,F6.5)
      ZSQ = Z*Z
      DO 15 J = 1,15
      DO 15 II = 1,15
      A = 10.*(FLOATF((II-8)**2+(J-8)**2))**.5
   15 RX(II,J) = C/(ZSQ*(1.+(A*A)/ZSQ)**2.5)
      JY = 8
      KEND = 43
      DO 101 J = 1,15
  101 READ INPUT TAPE 7,103,(Q(I,J),Y(I,J),X(I,J),F(I,J),I = 1,M)
  103 FORMAT(12F6.1)
    5 K = 1
    8 DELPV = 0.
      IEND = K+14
      DO 20 J = 1,15
      DO 20 I + K,IEND
      II = I-K+1
      DELPV = DELPV+RX(II,J)*Q(I,J)
      IF (F(I,J)) 20,20,10
   10 P = 0
      P = X(I,J)-(FLOATF(K+7)-.5)*10.
      IF (ABSF(P)-25.)11,11,13
   11 R = 0
      R = Y(I,J)-(FLOATF(JY)-.5)*10.0
      IF (ABSF(R)-25.)12,12,13
   12 RF = 0
      RF = ((X(I,J)-10.*FLOATF(K+7)+5.)**2+(Y(I,J)-10.*FLOATF(JY)+5.)**2)*
     X*.5
      WRITE OUTPUT TAPE 6,50,RF,F(I,J),Q(I,J)
   50 FORMAT (3F8.1)
      DELPV = DELPV+C*F(I,J)/(ZSQ*(1.+RF**2/ZSQ)**2.5)
      GO TO 20
   13 DELPV = DELPV+RX(II,J)*F(I,J)
   20 CONTINUE
      KK = K+7
   21 WRITE OUTPUT TAPE 6,6, DELPV,KK,JY,Z
    6 FORMAT (F12.2,2I10,F10.0,2F10.1)
      K = K+2
      IF(K-KEND)8,8,7
```

```
  7 DO 30 I = 1,M
    DO 30 J = 1,13
    Q(I,J) = Q(I,J+2)
    F(I,J) = F(I,J+2)
    X(I,J) = X(I,J+2)
 30 Y(I,J) = Y(I,J+2)
    JY = JY+2
    DO 104 J = 14,15
104 READ INPUT TAPE 7,103,(Q(I,J),Y(I,J),X(I,J),F(I,J),I = 1,M)
    GO TO 5
```

Journal of the
SOIL MECHANICS AND FOUNDATIONS DIVISION
Proceedings of the American Society of Civil Engineers

TUTTLE CREEK DAM OF ROLLED SHALE AND DREDGED SAND

By K. S. Lane,[1] F. ASCE, and R. G. Fehrman,[2] M. ASCE

SYNOPSIS

To fit available materials, the design of Tuttle Creek Dam in central Kansas includes major volumes of shale-limestone constructed as a rolled fill, and of sand deposited by dredging directly into place two types of fill not commonly employed in present-day earth dam construction. The reasons for choosing this design are explained, together with experiences learned during construction. The paper covers primarily the earthwork and foundation aspects of the project, of which the other more unusual features are closure "in the wet" and handling an area of weak clay foundation partly by excavation and partly by exceptionally wide berms.

INTRODUCTION

With a volume of about 21,000,000 cu yd, Tuttle Creek ranks as one of the world's largest earth dams (only recently displaced from 7th to 9th in size by start of construction of Trinity and Navajo Dams). After the giant Oahe Dam, it is the next largest embankment currently under construction by the Corps of Engineers. Started in 1952, suspended during 1954 when the views of reservoir landowners curtailed appropriations, the embankment has risen progressively since 1955 and is scheduled for completion in 1960. Construction has been accomplished by 5 major contracts: 2 all earthwork, 2 for the outlet works structures with some earthwork included, and 1 for the spillway structure. Now that diversion and closure have been accomplished in the summer

Note.—Discussion open until May 1, 1961. To extend the closing date one month, a written request must be filed with the Executive Secretary, ASCE. This paper is part of the copyrighted Journal of the Soil Mechanics Division, Proceedings of the American Society of Civil Engineers, Vol. 86, No. SM 6, December, 1960.

1 Chf., Geology, Soils & Materials Branch, Mo. River Div., Corps of Engrs., Omaha, Nebr.

2 Civil Engr., Dams & Foundations Sect., Kansas City Dist., Corps of Engrs., Kansas City, Mo.

of 1959, success seems sufficiently assured that the design and construction lessons learned can be recorded for information of the earth dam building profession.

A particularly interesting lesson has been the demonstrated practicality of dredging some 6,300,000 cu yd of sand directly into place in a modern earth dam. Although dredging and its companion method of hydraulicking for

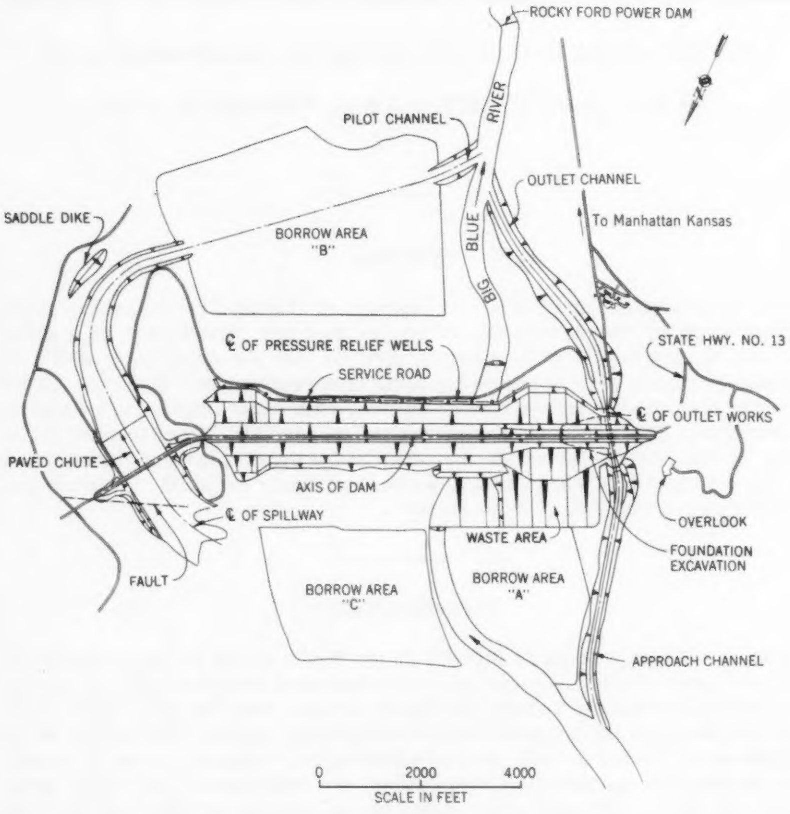

FIG. 1.—GENERAL LAYOUT OF DAM

gradational sorting are old methods, they have been little used for dams since about 1940 with Ft. Peck, Sardis, Kingsley, and Knightville Dams representing about the last of the hydraulic fill era in dam construction. In part, this is believed due to concerns of designers following the slide on Ft. Peck Dam[3] and in part to equipment improvements making rolled fill cost generally the cheaper. While Tuttle Creek was designed primarily for rolled fill construc-

[3] "Fort Peck Slide," by T. A. Middlebrooks, Transactions, ASCE, Vol. 107, 1942.

tion, the site conditions indicated that placing of the pervious sand by rolling methods or by dredging methods could be a "standoff" in cost. Hence the specifications allowed a dredging option, which even then might not have been utilized had it not been for the combination of a progressive contractor plus an alert Resident Engineer with wide experience in the techniques of hydraulic fill. To the authors' knowledge, Tuttle Creek is the world's only major dam outside the Iron Curtain where the dredging method is currently being used for placing a major portion of the main embankment.

DESCRIPTION OF PROJECT

Located on the Big Blue River about 12 mi. upstream of its confluence with the Kansas River at Manhattan, Kansas, Tuttle Creek Dam is a vital unit in controlling the Kansas River and one of the key dams in the comprehensive inter-agency developed plan for the entire Missouri River Basin.[4] Its functions are multi-purpose with its total storage of 2,346,000 acre-ft (to flood pool at el 1,136) being divided between flood control and conservation to supplement low flow. The need has long been recognized for evening out the widely varying flows of the Kansas River, of which the Big Blue is a major tributary, and this has been strikingly emphasized in recent years. The year 1951 saw the disastrous flood of record amounting to over 500,000 cfs on the Kansas River to which the Big Blue contributed about 100,000 cfs. This was promptly followed by a drought period from 1952 to 1956 when the flow in the Kansas River at times dropped below 200 cfs at Topeka, Kansas and greatly restricted normal uses of water for municipal and industrial water supply, for irrigation, and for reduction of pollution.

The general layout is shown by Fig. 1. The earth embankment is about 7,500 ft long and has a maximum height of 157 ft above stream bed. The outlet works is located at the base of the right abutment and consists of twin 20-ft horseshoe-shaped conduits, an intake tower with two gate passages for each conduit, and a stilling basin which includes a center wall to divide the flow from the two conduits. The spillway is cut into the shale and limestone bedrock of the left abutment and consists of a gated weir structure discharging into a paved chute. A state highway is carried across the top of the dam and crosses the spillway on a bridge. Presently estimated project cost totals $85,000,000, of which about $26,000,000 represents cost of the dam itself, with the remainder being divided between real estate acquisition and relocation-protection work in the reservoir.

FOUNDATION CONDITIONS

Foundation conditions are shown in generalized form on Fig. 2. At the dam site the flood plain is about 5,000 ft wide, with alluvial deposits in this reach varying in thickness from 40 ft to about 100 ft. The upper 8 ft to 27 ft forms the flood plain natural blanket which consists of silt (ML) and clay (CL, CH, and OH). This is underlain by the valley sand for a thickness of 25 ft to 50 ft, sand and gravelly sand (SM, SP, and SW). One buried valley was encountered in the bedrock as shown on Fig. 2; here thickness of sand increased to 80 ft. Pumping tests on pressure relief wells indicate an average permeability of $1,800 \times 10^{-4}$ cm per sec for the valley sand.

[4] "Missouri River Basin Plan in Operation," by W. E. Johnson, Transactions, ASCE, Vol. 122, 1957.

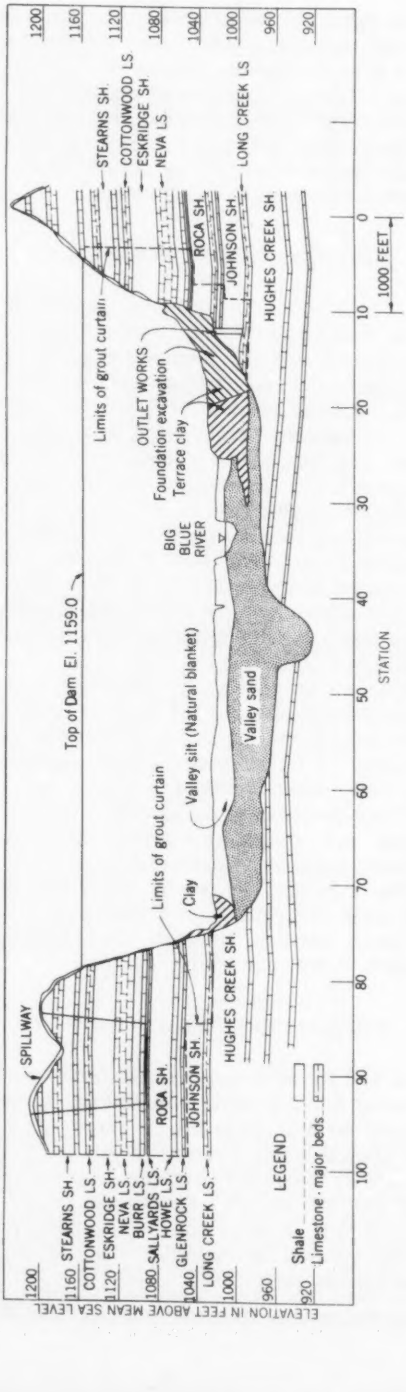

FIG. 2.—GEOLOGICAL PROFILE ALONG AXIS (LOOKING DOWNSTREAM)

At a slightly higher elevation on the right bank of the river is an alluvial terrace (1,500 ft wide) composed principally of weak, wet clay, termed the terrace clay. Nearer the river, the terrace consists of 40 ft of clay (CH, OH, CL and including a 6-ft thick intermittent peaty deposit) underlain by about 10 ft of sand at the base. Higher on the terrace a 10 ft to 40 ft thickness of clay (CH and CL) exists above a small amount of discontinuous sand. The terrace clay averaged 35% clay-size material with moisture content as high as 40%. An early test fill showed this material so wet that it could only be placed as uncompacted berm or channel fill. Near the foot of the left abutment an old channel deposit was encountered, consisting of about 20 ft of weak clay similar to the terrace clay. This is not expressed topographically and is rather small in extent compared to the right bank terrace.

The rocks encountered at Tuttle Creek are alternating beds of shale and limestone of Permian age, underlain by over 2,000 ft of similar materials of Pennsylvanian age. Generally, the limestones may be described as argillaceous and the shales as calcareous. While many of the beds have their own personality traits, the limestones are generally medium bedded hard rocks, and with one exception have been cooperative by not exhibiting any marked solution cavities. The limestones vary from about 2 ft to 18 ft thick, are generally medium hard to soft, most are shaly, some are dolomitic, and some contain chert nodules. Cottonwood and Long Creek limestones are quite sound and were used for riprap. Advantage was taken also of the favorable location of Long Creek limstone in the right abutment as a foundation for conduit and intake tower. Other numerous limestone beds are less durable or too thin for separate excavation. Weathering of the interbedded limestones is characterized by iron stain along joints and somewhat porous solution-formed honeycomb zones, some partially clay filled which was most pronounced with part of the Neva limestone. The limestones are only feebly permeable, principally from leakage along joints. Contrastingly the shales are substantially impervious.

Shale beds vary from 2 ft to about 36 ft in thickness, and most are relatively fine textured, with massive highly compacted clay being the most abundant type. Nearly all are limey and some parts are laminated and fissile. Some of the limey layers in the shale beds are several feet thick and approach the hardness of limestone. Generally the unweathered shales are firm to subfirm, but disintegrate somewhat by crumbling or slaking if exposed to air drying, and alter to soft plastic clay by long continued weathering. Only the upper 5 ft to 10 ft of shale bedrock was thoroughly altered to plastic clay.

The range of hardness, consolidation, and cementation of the rocks at Tuttle Creek is from fissile moderately hard shales at one extreme and to hard limestone at the other. Where unweathered, the shales required systematic drilling and blasting, both to facilitate removal and to obtain proper fragmentation, and generally broke chunky. In the weathered areas, the shales and thin limestones were excavated with power shovels without blasting, but desired uniformity of breakage for use in the embankment and cost for processing on the fill limited this method.

EMBANKMENT DESIGN

Key factors in the embankment design were handling different foundation conditions and utilizing maximum amounts of local materials from required excavations. The former principally influenced external slope design. The

latter was a main consideration determining the internal zoning with the objective to use different materials at the time expected from excavation in an orderly construction program. Required excavation contributed about 60% of total volume of the dam and the remainder was obtained from valley borrow.

The valley embankment section as shown on Fig. 3(a) was used for longest reach of dam. Impervious material for the central core was obtained for the most part from borrow areas, placed in 8-in. lifts, usually wetted, and compacted with tamping rollers. With required excavation contributing about 8,000,000 cu yd of shale-limestone, it was important to use this material. This required special techniques which are discussed later. Shale-limestone was placed principally in the upstream shell. Top part of the upstream shell was placed as a rock fill, partly to allow steeper slopes, but primarily to use about 1,000,000 cu yd of Neva limestone from the bottom of the spillway excavation. Since this material was excavated last, it was desirable to arrange its use near the top of the dam.

One of the job headaches was discovering the "fickleness" of the 18-ft thick Neva limestone bed. Roughly, the upper 9 ft was a moderately durable limestone, fine-grained, thick-bedded, of nearly riprap quality, and when used alone, resulted in an excellent rock fill. However, the lower half of the Neva bed was plagued with inconsistency, except for a 1-ft bed at the base of sound limestone. In major areas of the spillway, excavation revealed the remaining 8 ft as essentially decomposed to clay with only a fair percentage of insoluble rock fragments floating in the clay matrix. To avoid opening up a quarry, the upper and lower portions of the Neva, were mixed in excavation except where the latter completely lacked rock fragments. Operations in placing the rock fill were controlled so as to obtain rock-to-rock contact and to avoid overfilling voids with clay-like material. Material was traffic compacted in 3-ft lifts (5 ft when material was essentially all limestone). While the result was hardly a textbook rock fill, it was considered adequate for its prime function as a high shear strength fill. The outer 5 ft of the rock fill was constructed entirely of limestone for slope protection. (The Lower Neva was originally visualized as consisting of extensive clay filled solution cavities in fairly soft limestone. This interpretation was based on 2-in. and 6-in. diameter core drilling, largely concentrated in area of spillway structures, plus a large outcrop about 10 mi. away where upper Neva was sound and lower Neva a soft limestone. While the original interpretation was correct in a considerable part of the excavation, it was disappointing, to say the least, to find adjacent major areas so thoroughly decomposed. The lesson for the future is believed to indicate the desirability of 30-in. or 36-in. calyx holes for close inspection of suspected similar conditions. While the borehole camera probably would also be tried, it seems questionable if it could distinguish between the assumed clay filled cavities and the actual rock pieces surrounded by clay.)

The downstream shell was largely pervious fill, dredged in place. As discussed later, the specifications allowed the contractor an option of rolled or dredge methods for placing pervious materials. For rolled fill design, pervious was limited to a 15-ft horizontal drainage blanket and an inclined zone (chimney drain) next to the impervious core, with bulk of shell being random fill (Fig. 3). Above the random zone, a shale-limestone zone was used to accommodate the volume available. A berm fill zone (largely for counterweight functions) was provided to use low shear strength and wet materials. It was traffic compacted in 2-ft lifts and consisted of excess shale-limestone, wet channel excavation, and terrace clay.

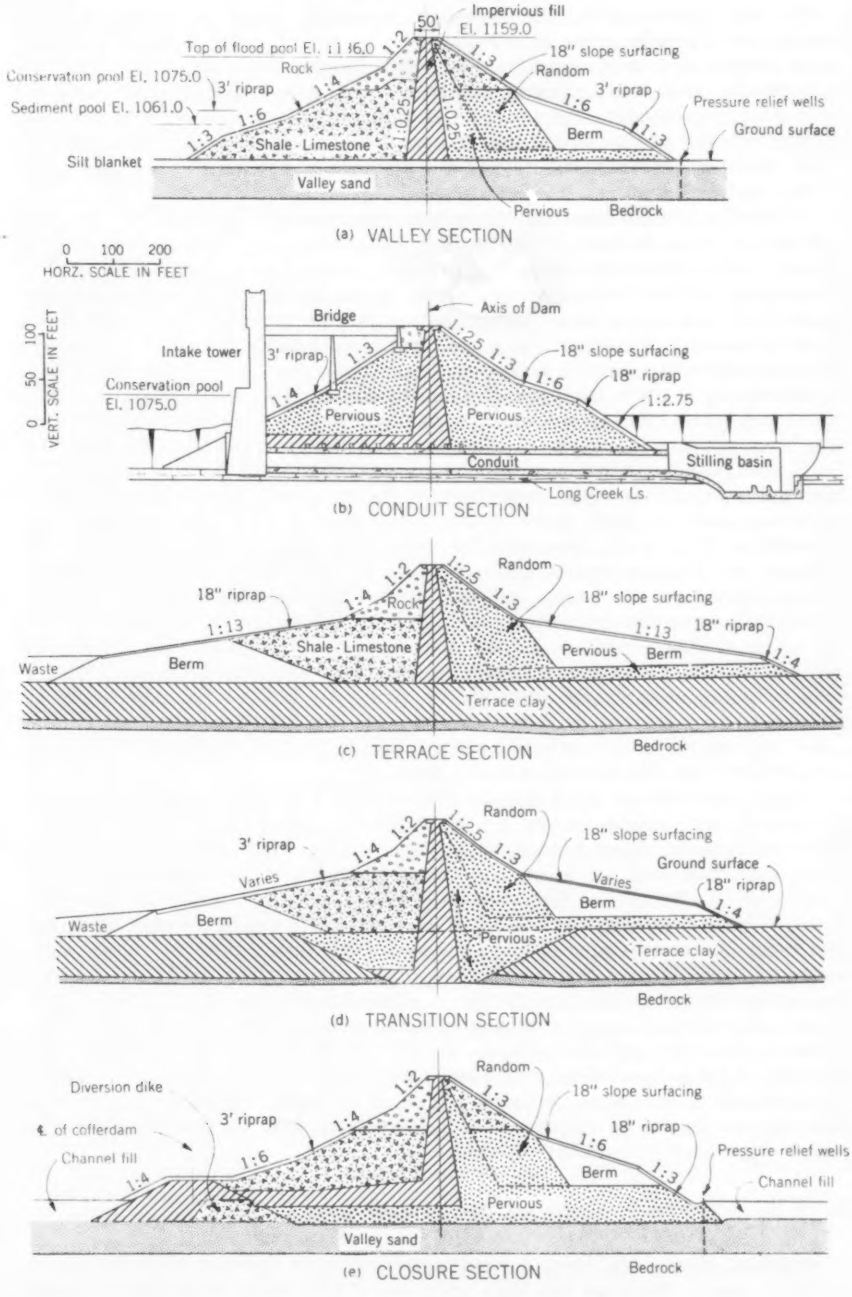

FIG. 3.—TYPICAL EMBANKMENT SECTIONS

In the conduit area, the strongest material (sand) was utilized in the shells on both sides of the impervious core to permit steepening the embankment slopes and thus minimize the conduit length. As shown in Fig. 3(b), the impervious zone was extended upstream around the conduit while pervious was used downstream. The conduit and intake tower were founded on the Long Creek bed, one of the harder limestones. Outlet channel grades were adjusted so as to use it as the channel floor for a distance of about 1,300 ft downstream of the stilling basin.

A relatively wide embankment section was used over the weak terrace clay foundation area to obtain stability (Fig. 3(c)). Unusually wide berms (1 on 13 slope) were necessary since the analysis allowed for development of pore pressures in the thick foundation clay layer during construction. Limited measurements during construction indicated pore pressure developed at the rate of about 1 ft of water for each foot of embankment load. This was approximately equivalent to a pore pressure equalling 50% of the added load, comfortingly a little less severe than the 55% to 65% range assumed in stability analyses. A waste area upstream served as a further counterweight and thus slightly improved the stability over that counted on in the analysis.

In the transition reach between the conduit section and the terrace section, the clay foundation was excavated to bedrock and backfilled with semipervious sand on both sides of the impervious core to provide a stronger foundation (Fig. 3(d)). Beneath the narrowest embankment adjacent to the conduit, the foundation excavation was the widest. The foundation excavation was narrowed as the berms widened so that the same safety factor was obtained throughout the transition reach (Fig. 1). To lessen the potential cracking effect of differential settlement, the foundation excavation was terminated on a flat 1 on 5 slope and the impervious core was placed 2% to 3% wetter than optimum moisture to improve its flexibility. Settlement gage observations to date, adjacent to this area, indicate that the differential settlement after completion of the embankment is likely to be of the order of 1.5 ft over a length of about 400 ft along the dam axis.

Slope protection on the upstream consisted of 3 ft of Cottonwood limestone as quarry run riprap below the rock fill zone. For filter action, a 12-in. layer of crushed stone bedding was placed under the riprap where the embankment consisted of sand, but omitted where it was formed of shale-limestone fill. Since the flat 1 on 13 berms provided considerable beaching action, riprap here was reduced to 18 in. Rock fill at top of the dam was protected by selective placing of more durable of the Neva limestone on the outer surface. Protection of the downstream slope was provided by 18 in. of slope surfacing for which the specifications allowed a mixture of low grade limestone and limey shale as a means of using material intermediate in quality between rock fill and shale-limestone fill. While the result contained considerable shale, the coarse fragment content has appeared adequate to fulfill its function of resisting erosion. This downstream slope treatment was selected as likely to require less maintenance than for the alternate of a turfed slope needing periodic mowing.

SHALE-LIMESTONE FILL

Although there has been considerable usage of the soft rock variety of shales in dams (such as the huge volumes of clay shale excavated by earth

moving equipment and rolled into Garrison[5] and Oahe Dams[6]), there has been comparatively little experience in utilizing the harder type of shales which are generally excavated by blasting. Youghiogheny Dam is one of the few recorded cases.[7] There shale chunks were reduced to minus 6-in. size by a crusher, delivered to the dam by a belt conveyor, and then compacted by tamper rollers. With the good experience in subsequent years using a heavy rubber tire roller for compacting granular soils containing aggregate to cobble size, it was believed entirely practical to utilize as compacted fill some 7,300,000 cu yd of bedrock excavated from the spillway. As shown by Fig. 2, this consisted mostly of shale but also included numerous limestone beds, which it was neither practical nor desirable to excavate separately.

The problem was approached by constructing several test fills with a variety of shales and compaction equipment,[6] and then by including about 1,000,000 cu yd of shale-limestone fill in the first contract to serve as a large scale test embankment. The methods evolved and used in the subsequent major embankment contracts were essentially as follows, with the objective being a well-graded dense fill. The shale-limestone mixture was placed in 18-in. lifts and compacted by 3 passes of a rubber tire roller carrying 100,000 lb on 4 wheels. To prepare the lift for rolling, the specifications required that the material be "conditioned" by removing over-size pieces and by breakage in blasting and/or on the fill to produce a well-graded mixture with sufficient fines to substantially fill the voids. Over-size pieces (those exceeding the lift thickness) were raked to the outer slope of the dam directly behing the riprap using a large rock rake capable of raking to full depth of the lift. The rake included 4 teeth, 5 in. thick, spaced 24 in. apart, and weighing about 400 lb per tooth. A dual drum spike-toothed roller, weighing about 55,000 lb or 4,500 lb per lineal foot of drum, was used for breakage on the fill. Drums were 6 ft in diameter and each was equipped with 36 spikes consisting of a 12-in. long triangular section of 4-in. plate. Generally it and the spreading bulldozer served to break most of the shale chunks, leaving only larger pieces of limestone and hard limey shale to be raked out as over-size. However, the real secret of conditioning the material was in good breakage during blasting. This was accomplished with 4-in. blast holes usually on 12-ft x 14-ft centers, although the pattern was varied some with the rock conditions. Powder was ammonium nitrate and consumption averaged 0.5 lb per cu yd. With thorough breakage in blasting, the slow and more costly breakage on the fill was greatly minimized, and the material could be rolled promptly after placing, as no moisture control was required.

Results were excellent and exceeded expectations. A very dense fill was produced with only a minor amount of visible voids, as revealed by occasional test pits. Such were hand dug since a power auger proved unable to penetrate through the dense chunky fill. Dry density averaged about 115 lb per cu ft, and was determined by excavating a hole of about 1 cu ft size, lining it with a plastic membrane and then filling with water to determine the volume. Bulking factor from excavation to embankment was only about 5%. Costs for the two main earth-work contracts were $0.15 per cu yd for placing on the

5 "Embankment Soil Characteristics, Garrison Dam," Corps of Engrs. Report, Garrison Dist., June, 1951.

6 "Materials and Compaction Methods, Missouri Basin Dams," by P. T. Bennett, Transactions, 6th World Congress on Large Dams, 1958. Data presented for Tuttle Creek Dam is largely that from the test fills.

7 "Belt Delivers Fill for Earth Dam," by Engrg. News Record, December,3, 1942.

fill and $0.45 per cu yd for excavation, including haul from spillway to left bank embankment in which the latter figure increased to $0.61 for the longer haul to the opposite bank involved in the second contract.

For analysis purposes, two limiting cases were assumed and the dam designed to be safe for either condition. First, it was considered the shale-limestone could act as a highly pervious fill and produce full reservoir pressure at upstream side of the central core. Second, it was assumed the material would ultimately weather to a clay, for which effective shear strength was assumed as a 24° friction angle and zero cohesion. After seeing the fill actually produced plus the relatively minor slaking of the shale on the excavated slopes, it now seems that the second assumption was unnecessarily conservative. For such a dense fill, it seems more likely that circulation of the weathering agents, air and water, will be relatively minor so that the time required for the great bulk of the mass to weather to a clay would be measured in hundreds of years and possibly thousands. Hence, for the useful life of the project, it would seem reasonable to assume strength and permeability gradually reduced by weathering only in the outer part of the fill, and for the inner portion to assume a strength perhaps only slightly lower than that for a normal granular material. (As a word of caution, there are other types of shale for which this assumption would be unsound. Examples are those which slake severely, and the weaker clay shales which soften and swell when unloaded in the presence of water.) Possible economies from such approach are now being explored for two other dams in the Kansas City District involving similar shale, and the concept seems realizable with some selection to avoid the weaker shales, using such in berm fill.

DREDGED SAND

Conditions in the two main borrow areas, A and B, were substantially, as shown by the left bank portion of the geologic profile on Fig. 2, a 6-ft to 10-ft flood plain blanket of silt and lean clay overlying 35 ft to 40 ft of sand, becoming coarser with depth. The water table varied with river level and was generally 8 ft to 10 ft below top of the sand. Considering these borrow conditions, the specifications allowed two optional methods for handling the pervious fill. The first contemplated placement as rolled fill; the quantity of pervious was minimized by using a large random section for construction as a mixture of silt and fine sand; and sufficient borrow area was provided to permit obtaining the pervious by dragline excavation extending only a few feet below the water table. The second method allowed placement of both pervious and random zones by dredging sand directly into place, subject to certain restrictions to avoid any ponding on the fill and any undesirable trapping of fines in critical portions of the pervious zone. Both methods contemplated removal of the silt blanket and its use as impervious fill.

Pervious fill was started in 1955 as a rolled fill. Sand was obtained by draglines excavating a face extending about 8 ft above water and an equal distance below. Close fitting doors were required on the bottom dump Euclids to haul the resulting semi-fluid sand-water mixture. The material was spread in 12-in. layers and compacted by tractors whose vibration brought the excess water to the surface. Since the underlying flood plain silt blanket prevented drainage downward, and since the relatively flat surface of the initially wide fill retarded runoff, most of this water remained on the surface. Here it

mixed with the already semi-fluid sand of the next lift and caused the Euclids to "bog down." Essick vibrating rollers were tried and produced results similar to the tractors. In effect, both types of equipment compacted the sand by vibration with the excess water coming to the surface; the excess representing the difference between water required for saturation in the inital loose state and that for saturation in the compacted state. After trying several other variations in methods, the contractor changed to dredge placement.[8] A method proposed, but not tried, was to keep the fill surface sloping sufficiently so the excess water would drain off as it was vibrated to the surface during compaction by the tractors. About 1 1/2 years later such a method was used at Swift Dam for handling a far less free draining material in a high rainfall climate. It proved so successful there that rain seldom stopped the work and was often a preferred weather condition.[9]

Fig. 4 shows a typical dredging operation. With the dredge in the downstream borrow pit, the discharge header was carried up a ramp which also served as a haul road for handling the impervious core material from the same borrow area. From Y-branches in the header, stub lines discharged on the beach with the return water flowing parallel to the dam axis to reach the dredge spillway. This was a morning glory type spillway, flared at the top to a 16-ft diam, which conveyed the return water to the embankment toe through a vertical riser and horizontal leg of 36-in. corrugated metal pipe. This pipe remained in the embankment and was sluiced full of sand. For work on the left bank, the discharge header was located at about the middle of the 3,800-ft length of embankment. With a spillway at each end, this permitted dredging on one of the 1,900-ft beaches while rearranging the stub discharge lines on the other.

For the shorter right bank embankment, a single dredge spillway was located at the river end and the discharge header was placed near the outlet works (Fig. 5) making the downstream beach reach about 1,600 ft. To take advantage of the shorter pumping distance, the sand portion of the right bank embankment was dredged from the adjacent upstream borrow area. Since the central impervious core was always kept ahead of the dredged sand shells, this required temporarily carrying the discharge header through the central core to reach the downstream sand shell. This was accomplished by running the header through a larger sleeve pipe extending across the top of the core. Then to raise the discharge header as the core and dredged sand grew around it, a wide trench was cut through the core to remove the header, and the core section was carefully restored by backfilling the trench with impervious.

In the dredge borrow areas, the surface silt and clay were excavated ahead of the dredge, except for the bottom 1 ft to 2 ft of this natural blanket material which served to support the hauling equipment. The dredge cut was then full face. Typically it consisted of 8 ft to 10 ft of sand above water, capped with about 1 ft to 2 ft of silt, plus 30 ft to 40 ft of sand below water. The sand was frequently gravelly at the bottom and occasionally contained intermediate thin beds of silt and clay. To prevent strata of impervious fines in the pervious zone, specifications required the dredge water be kept flowing with no ponding on the embankment. For the first contract involving dredging, discharge from

---

[8] "Dam Builder Switches to Dredge," Engrg. News Record, November 29, 1956.

[9] "World's Highest Earth Fill Dam Completed," Civil Engrg., November, 1958; and information presented by H. H. Burke at the Spring 1958 ASCE Convention, Portland, Oreg.

FIG. 4.—DREDGING ON LEFT BANK

FIG. 5.—DREDGING ON RIGHT BANK

bottom traps in the dredge line was specified. Objective was to carry bulk of the fines beyond the open traps and thence back to the borrow pit through a return line discharging outside the embankment. Work was started with trap discharge pipe laid on a wood trestle. However, it was soon shifted to open end pipe discharge when this method was found to give equally good results. The open end discharge required only a baffle at the end of the pipe to spread out the jet, and eliminated the trestle as the pipe rested directly on the fill surface. A key factor in success of the open end discharge method was to keep the return water constantly flowing with a velocity sufficient to continually rewash the top few inches of material on the beach. Generally this was accomplished with a beach slope of about 1 on 10 where the coarser material was deposited near the discharge pipe. This gradually flattened to a slope of around 1 on 30 leading to the spillway.

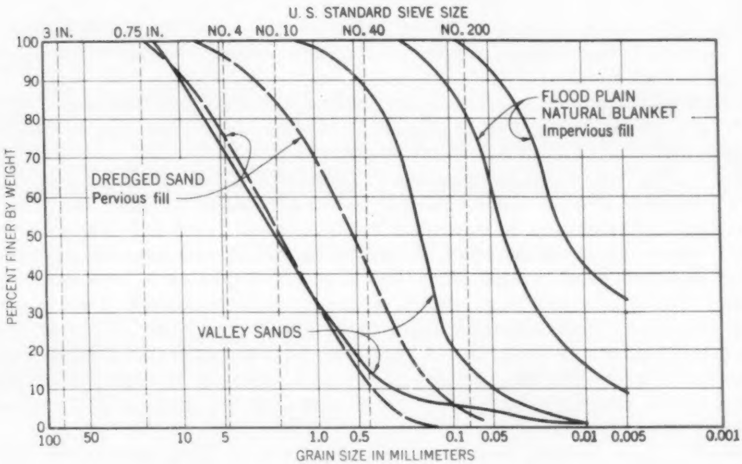

FIG. 6.—GRADATION CURVES

A dozer was operated near the discharge pipe to distribute the flow. The impervious core was carried ahead of the dredged sand shell and supported by a flat-topped wedge of compacted sand, dozed up from the dredge beach and compacted by the dozer tractor. Clay balls were occasionally produced from intermittent clay layers in the sand pit. When these were considered excessive, the clay ball—sand mixture was dozed to the downstream portion of the dredged sand (random zone area shown in Fig. 3). As the beach advanced in front of one stub line, discharge was shifted to the adjacent stub. These stub lines from the discharge header were about 100 ft apart (± 25 ft), and the number varied as the width of the dredged zone decreased with elevation. As the discharge shifted between stubs, and wherever velocity caused local deposition of fines, low training dikes were dozed up to concentrate the flow and thus wash away the fines.

These procedures reduced the fines to the extent that the dredged fill contained slightly less fines than the natural sand in the borrow pit. This is shown by Fig. 6 which compares the gradation range of several hundred control samples with that of the natural sand and also with that of the silt blanket used for impervious. Several series of tests attempted to determine the change in gradation at different distances away from the discharge point. After leaving the region of coarser material deposited near the discharge point, there was remarkably little difference in gradation along the entire length of the beach. Principal exception was a tendency in early work for thin silt lenses in immediate proximity of the spillway, but this was largely eliminated by using a spiral approach channel to maintain velocity near the spillway (Fig. 7). Numerous shallow inspection pits showed the principal stratification to consist of tongues and rivulet channels of pea gravel and coarse sand within a mass of medium sand. Tongues of fines occurred less frequently and were seldom continuous for any significant distance. This was attributed to the continual rewashing on the beach surface which tended to cut through any fine stratum while simultaneously promoting continuity in the rivulet channels of coarser material.

Densification was entirely from seepage forces as the water drained downward and outward to the embankment toe. No rolling was specified for the dredged sand; except where it was excavated and replaced for construction convenience, rolled fill methods were required for the refilling. Fill density tests required special care to locate the sample in reasonably uniform nonstratified material and to wait until the free water level had drained at least a foot below the sampling level. From the more reliable results, dry density of the dredged sand ranged from 105 lb to 120 lb per cu ft. The rather wide range is due to changes in gradation so that a better measure of compactness is in terms of relative density. This generally ranged from 55% to 80% relative density and was determined by the Providence Vibrated Density test.[10] Perhaps a more graphic picture of the compactness is that self-propelled rubber-tired scrapers were able to operate over the surface of the dredged sand without difficulty.

While the placement techniques exceeded those for a more conventional dredged fill, they were considered desirable to insure the caliber of stability and permeability required of the pervious shell of a dam. In the latter respect, the specifications required high permeability material in a vertical band downstream of the core (a "chimney drain") and in the horizontal drainage blanket at base of the dam, with less permeable material being allowed for the balance of the dredged sand shell. Actually the borrow pits yielded such good sand that the dredged fill was relatively uniform throughout.

DREDGE EQUIPMENT

Two 20-in. electric powered dredges were used, both erected on the job and designed to permit disassembly and transport. The first dredge was used for the left bank embankment and utilized 2 pumps in series powered by one 1,500 and one 1,250 hp motors. For higher lifts it was supplemented by a booster pump powered by a 1,500 hp motor. It originally functioned as a straight suction dredge but output was low, partly because the sand did not

10 "Providence Vibrated Density Test," by K.S. Lane, Proceedings Second Internatl. Conf., Soil Mech. and Foundation Engrg., Vol. IV, Rotterdam, 1948.

FIG. 7.—DREDGE SPILLWAY

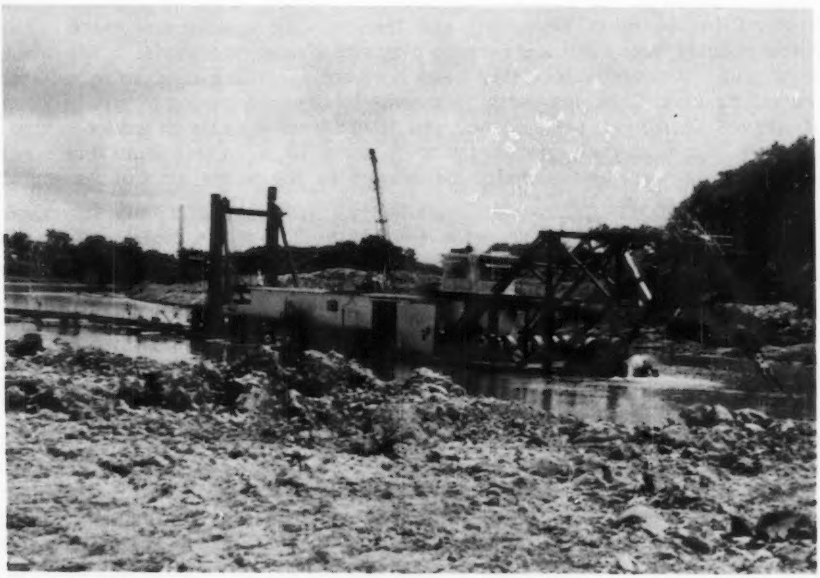

FIG. 8.—DREDGE ROCKY FORD

cave readily. Production was considerably improved by addition of an endless chain agitator on each side of the suction head. When the same contractor obtained the following contract, the second dredge was constructed (using some parts from the first) and was used for the right bank embankment and closure reach. Since the second dredge, the "Rocky Ford," profited from experience on the prior contract, it was the more interesting of the two dredges. Fig. 8 is a photo of the Rocky Ford.

To fit the site conditions, the Rocky Ford included a 6-ft diam rotary cutter head. This was mounted on a 25-in. suction pipe so that both the cutter head and the suction pipe were rotated by a 400 hp motor, an arrangement which permitted keeping nearly the whole cutter head buried and distributed the wear over the circumference of the suction pipe. The ladder was arranged for digging depths up to 50 ft. This was a single pump dredge, with a 78-in. impeller and a 20-in. discharge line, powered by a 3,000 hp slip ring motor. Where the lift exceeded around 50 ft with the length of discharge line over 3,000 ft, the addition of a booster pump driven by a 2,000 hp motor permitted lifting up to 100 ft above the dredge pool through around 5,000 ft of line. In sand, affording reasonably good digging, production was about 1,000 cu yd per hr although the percentage of solids seldom was estimated over 10%. Considerable of the material was a gravelly sand, particularly near the bottom of the borrow deposit, which required a line velocity of about 20 fps to move the coarser particles. Wear of the pipe line and pumps was combated by frequent renewal of hard-facing and by using pump liners and casings of a specially hard metal, "Ni-Hard."

With the dredge on the job, it was also used for some portions of the required excavation largely below the water table which might otherwise have been allocated to draglines, principally a portion of the approach channel dredged to upstream berm fill and the extreme downstream reach of the outlet channel where silt and terrace clay were dredged to waste. In the latter excavation, the available cutter head frequently became clogged in tackling the sticky clay. This was partly overcome by over-deepening to mix in a bed of gravel at top of the bedrock and to undercut the clay to induce caving. Cobbles and flat rock pieces up to 9 in. to 12 in. in size from this basal gravel layer were occasionally discharged on the waste area at the end of about 4,500 ft of pipe line.

DIVERSION AND CLOSURE

Provision for constructing lower portion of the closure embankment "in the wet" without unwatering the river bed was another of the projects's less conventional features. For the particular site conditions, this method was considered satisfactory in lieu of the common practice of pumping out the river channel between cofferdams. Foundation conditions were one of the major reasons for this choice, although some savings in time and cost were also realized. Since the dam was located essentially at the head of the pool formed by Rocky Ford Dam (Fig. 1), it was originally anticipated that a thick muck deposit would be present from the 50 odd yr of aggradation behind this small power dam, and that this would require unwatering the channel for its removal. However, borings in the channel showed the river generally running on the foundation sand. The muck was found to be largely concentrated along the banks as a 3-ft to 5-ft thickness of organic silt, and was only inches thick

in the channel proper. It appeared that a modest amount of under-water muck excavation would make the foundation in the channel area at least as good as that beneath the embankment on adjacent banks. Hence, closure in the wet was considered satisfactory and the design was prepared accordingly.

The resulting embankment section for the closure reach is shown on Fig. 3(e). Below the cofferdam an under-water pervious fill was utilized to reach above water surface. Upstream of the central core was covered with an impervious blanket which joined with the impervious fill of the upper cofferdam and with that of the channel fill upstream to match the natural blanket of impervious silt found on each bank. Otherwise zoning was the same as for the valley embankment section.

Diversion was timed to avoid periods of maximum flood potential. While the Big Blue River has produced floods in every month of the year, the flood potential has been most likely in May and June, although occasionally in the 62 yr of record, this flood period extended to mid-July. Hence, diversion was planned for the latter half of July. Completion of the cofferdam was required by mid-August in preparation for fall floods, which have occurred as early as August 15.

Diversion was accomplished on July 20, 1959 following the aftermath of a small flood in early July which reached bank full stage, about 30,000 cfs. The river cooperated splendidly by flowing only around 2,500 cfs which greatly simplified the diversion operation. The diversion dike was constructed by end dumping shale and limestone from stockpiles on both banks, and the flow was thus diverted through the conduits. The contractor did a fine job in concentrating equipment in the cramped work area of the 230,000 cu yd cofferdam which resulted in its completion in about 8 days time. Impervious material formed the bulk of the cofferdam. This was traffic compacted in 12-in. layers, utilizing upstream borrow area C on the left bank, and on the right bank a stockpile of clay which had dried reasonably in the 3 yr since its excavation from the outlet works channels.

About the only unscheduled event was the slow progress of the dredge in excavating the tenacious clay in the short downstream reach of the outlet channel which had been left for dredging. Hence, draglines were put to work excavating this reach to water level and opening up a partial width channel along one side. Since studies showed the lack of full channel section would have only a minor effect on the pool level, diversion proceeded and the dredge succeeded in completing the channel to full section shortly after the cofferdam was finished. A small inconvenience was the need to construct a roadway across the riprap to reach the trash fenders of the intake tower for removing drift. This had by-passed a log boom and accumulated to the extent that it added about $1\frac{1}{2}$ ft to the pool level. Future designs could easily avoid this by providing for such access in initial construction.

As the cofferdam approached completion, draglines excavated the muck along both sides of the river. Simultaneously the banks were trimmed to a flatter slope to reduce differential settlements in the closure reach embankment. The dredge then moved in and removed the remainder of the muck, pumping it over the cofferdam to waste area 1 on the right bank. The specifications did not require the removal of thin muck layers (of the order of 6 in. such as those in the center of the channel) since they would consolidate rapidly under the embankment load. Actual result was even better as the dredge swept the channel twice and its practical depth of cut frequently ex-

tended into the underlying foundation sand. A light aluminum sounding rod readily indicated the depth of muck and checked its removal.

A prime problem in placing the under-water pervious fill by dredging was to avoid any sizeable deposition of dredge fines that would tend to accumulate in the quiet water ahead of the advancing fill. The following combination of techniques handled the problem so well that the accumulation of silt fines was far less than the 12-in. thickness established as a tolerable maximum. To minimize fines in the material pumped, the dredge operated in a portion of the borrow pit from which the silt blanket had been thoroughly stripped to the top of the sand. The dredge line was carried across the river on pontoons and was equipped with bottom discharge traps. These traps were opened progressively with only one trap being open at a time. In the area immediately upstream of the trapline, a dragline re-worked the sand to break up any silt lenses. The dredge line terminated on the bench at toe of the embankment on right bank of the river and here deposited a stockpile by open end discharge. Keeping a reasonably steep beach here produced a narrow stockpile of comparatively clean sand which was dozed laterally into the river, thus working out the fill from the right bank. Return water was carried by a ditch on the right bank to deposit the fines in the channel fill area below the construction bridge.

As soon as the dredged pervious reached above water level, it was topped with an 18 in. lift of sand placed in the dry, and then heavily rolled to explore for any soft spots in the under-water fill. No soft spots were found and the balance of the closure embankment proceeded in the dry with the pervious shell placed by dredge. Discharge of the return water was through a gloryhole spillway similar to Fig. 7, and was controlled so that the dredge fines deposited to build up the lower portion of the downstream channel fill. The principal function of this channel fill was to increase embankment stability and to support a service road. For the latter purpose, about 8 ft of rolled fill was placed above river level to carry the road over the dredged fines. At no time was a downstream cofferdam needed and the river cooperated in fine style by producing no flood against the upstream cofferdam. For the optional hauled fill method of placing the under-water pervious, a downstream cofferdam was specified to protect placement operations from high tailwater during a flood discharge. However, it was felt that the dredge method would be much less delayed by such tailwater conditions so that for this option the specification allowed omission of the downstream cofferdam.

SPILLWAY

The spillway was excavated in the shale-limestone bedrock of the left abutment and arranged to discharge into the downstream borrow area with a pilot channel from there to the river (Fig. 1 for layout plan). Control structure is a concrete weir with eighteen 40-ft by 20-ft tainter gates discharging into a paved chute. Spillway design flood was based on an inflow of 800,000 cfs with the reservoir at top of flood control pool which resulted in a spillway design discharge of 580,000 cfs after allowing for surcharge operation.

Considering the infrequent use anticipated for the spillway, the concrete chute was extended 600 ft and then terminated in a flip bucket. However, the design was arranged to facilitate adding a stilling basin if experience or a change in operation should show such desirable. In the meantime, the large

permanent pool remaining in the borrow area as a result of dredging is expected to provide significant stilling action for moderate discharges; for discharges approaching the design flood, the entire valley would be flooded to a depth of about 20 ft. Between the paved chute and borrow area pool, a small valley between two bedrock hills provided an economical location for the discharge channel, which condition was a primary factor in selection of project site. (This has also been the case at other dams in the Missouri Basin where it is not uncommon to find spillway cost approaching that of the embankment.) Surplus bedrock from structural excavation, mostly limestone and harder shale, was placed in a broad top dike, as shown on Fig. 1, to fill a low saddle well above water surface for the design discharge.

Fig. 9 shows a longitudinal section through the spillway structure. The concrete weir was founded on the $2\frac{1}{2}$-ft thick Sallyards bed of hard limestone overlying the 23-ft thick Roca shale, a generally massive and firm shale with thin limestone horizons. This foundation level was adopted principally to set the weir below the Legion shale, a $1\frac{1}{2}$-ft bed of black waxy shale between the Sallyards and overlying Burr limestones, and decidedly the weakest formation in the entire spillway area from the standpoint of sliding resistance. Bottoming the excavation on the Sallyards limestone required only minor foundation cleanup and protection, and minimized the need for protecting the very fissile Legion shale which slaked severely in a matter of hours after exposure. Slaking of other shales varied from moderate in most beds to minor in the well cemented Esksridge shale. Slaking on vertical and steeply sloping foundation surfaces was handled by preventing the shales from drying, either by keeping them moist or by spraying with a bituminous shale sealer. This sealer worked effectively on reasonably dry surfaces, but did not adhere where the shale was moist. Since slaking results from drying, a sealer is not needed on continuously moist surfaces. Hence, where seepage was insufficient to prevent drying, it was supplemented with water spraying. Horizontal and gently sloped foundation surfaces on shale were protected with a 2-in. minimum thickness of lean concrete, placed promptly after foundation cleanup.

The chute was paved with an 18-in. continuously reinforced slab which covered an area about 830 ft wide and 530 ft long. It was constructed in 25-ft longitudinal lanes; reinforcement was continuous through the joints and consisted of 0.2% steel in each direction, located at middle of the slab. Expansion joints were provided where the slab abutted the weir, flip bucket, and side walls, and included waterstops. The slab was anchored to the foundation with hooked anchors on 10-ft centers, each consisting of a no. 11 bar terminating with a 4-in. plate in a grout filled hole. Anchor holes generally extended 12 ft into the foundation, but were deepened to 20 ft near the weir to reach below its excavation level. Those bottoming in limestone for 2 ft or more were drilled to a 6-in. uniform diameter; those bottoming in shale were belled to an 18-in. diameter to offset the much lower bond between grout and shale. This slab design was similar to the continuously reinforced concrete slabs used on much larger areas at Fort Randall and Garrison Dams, except for a frost blanket of pervious material under the slab which was considered unnecessary for the milder climate at Tuttle Creek Dam.

The flip bucket included a downstream scour key extending some 25 ft to the Howe limestone plus an upstream key wall for stability in event of deep scour. Downstream of the flip bucket, the 4-ft Burr limestone was left in place for a distance of about 100 ft for the small benefit it would contribute as a channel flooring. Side walls of the chute utilized a flat base where founded

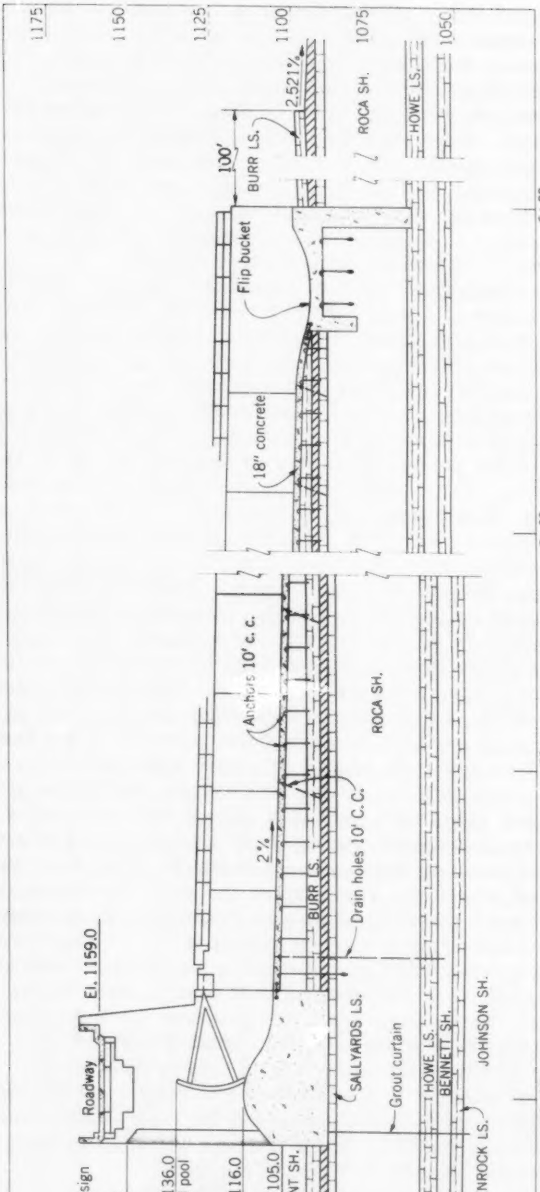

FIG. 9.—SECTION-SPILLWAY STRUCTURE

on limestone with a key added where the foundation was shale (Fig. 10). For minimum earth pressure, the walls were backfilled with pervious sand, except for a top cover of impervious to reduce infiltration.

With the shales generally impervious, seepage and uplift problems at the spillway were concerned mainly with the more open jointed limestone beds. Principal treatment was a stage-grouted curtain extending from the dam across the spillway as shown by Fig. 2. The curtain continued roughly 300 ft beyond east end of the spillway to intersect a fault (Fig. 1). This formed a convenient termination for the grouting since the 30± ft throw of the fault effectively interrupted continuity of seepage in the limestones. To control uplift from leakage through the grout curtain, 3-in. diameter drain holes were provided on 10-ft centers downstream of the weir (Fig. 9) and extended along each side wall for about 180 ft. These were filled with pea gravel to support the walls of the hole in shale beds, and were arranged to discharge into the underslab drainage system. The latter consisted of a system of half-round openings (formed by half-section 12-in. cmp) at the base of the slab spaced transversely on approximately 60-ft centers. Shallow drain holes penetrating only the upper limestones also discharged into these half-round drains. This drainage system discharged through 4 collectors into the flip bucket with auxiliary discharge points, also provided in the side walls. Here the wall outlets were inclined downstream to provide some suction action as the spillway discharge flowed past the walls.

The most difficult seepage problem was at the bulkheads or non-overflow sections at each end of the weir, which were embedded by notching into the shale-limestone abutments as shown on Fig. 11. The problem bed here was the 18-ft Neva limestone with its lower half a network of solution cavities, generally clay filled and often decomposed to the extent of rock fragments in a matrix of soft clay as previously discussed. Early studies considered a concrete cutoff wall built in a narrow tunnel into the abutment for full height of the Neva limestone. In final design, it was decided to construct the equivalent of such a cutoff wall by grouting methods, such special grouting to be in addition to the normal grout curtain at upstream face of the bulkhead. As shown by Fig. 11, a grouting well was built in each bulkhead for drilling horizontal grout holes at least 140 ft into the abutment, washing out clay filled cavities, and refilling with grout. A series of horizontal drain holes was also provided downstream of the grout cutoff, draining into the grout well and thence into the longitudinal drain behind each chute wall. By March 1960, this work was underway. No serious difficulties were anticipated since the grout well provides for flexibility in performing additional grouting or in drilling more drain holes if experience should show such desirable. Furthermore, for the entire length of the chute walls, the lower Neva outcrop was covered by the wall backfill of sand (Fig. 10) which will serve as a filter to prevent any piping out of the clay cavity filling. To minimize possible effects of rebound opening previously grouted fissures, grouting was deferred to near end of construction and when substantially full load of the spillway structure was in place.

At the outset, possible rebound due to unloading by excavation was a matter of conjecture, although it was expected to be more in the order of inches rather than in the magnitude of feet as measured at Fort Peck[11] and Garri-

[11] "Fort Peck Dam Spillway Movement Survey," Corps of Engrs. Report, Fort Peck Dist., July, 1947.

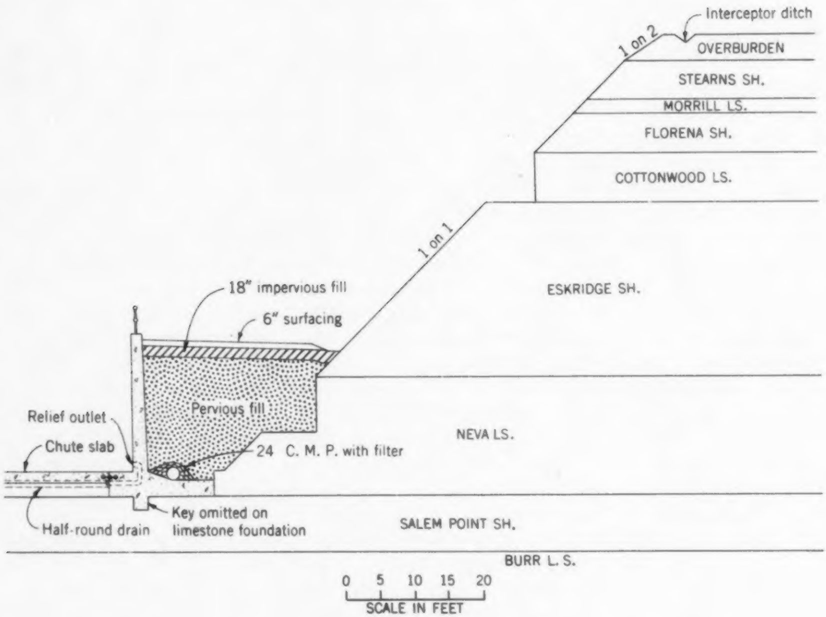

FIG. 10.—SECTION-SPILLWAY SIDEWALL

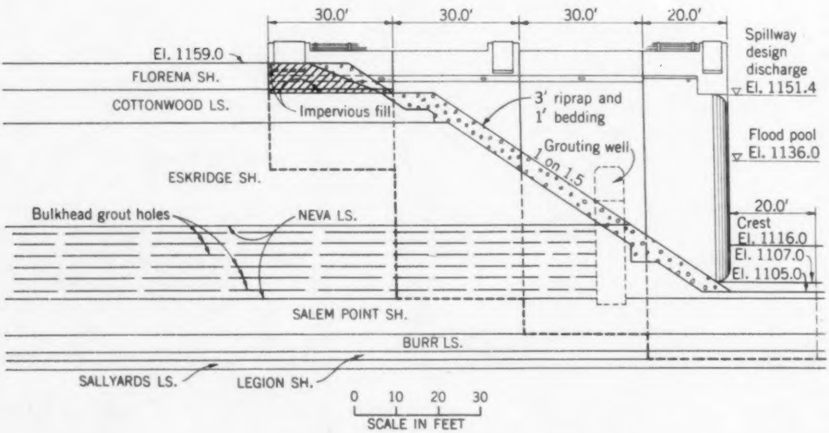

FIG. 11.—UPSTREAM ELEVATION-SPILLWAY BULKHEAD

son[12] Dams on much younger shale. Excavation of some 110 ft to base of the weir removed a load of about 8 tons per sq ft, whereas load of the weir added back was much smaller, around 2 tons per sq ft. To measure effect of this net unloading, rebound gages were installed along the weir in advance of excavation (each consisting of a pin grouted in the Sallyards limestone at bottom of a drill hole) plus 3 shallower gages upstream extending below the approach channel floor. Measurements showed the rebound quite small, around 2 in. to 3 in. during excavation unloading plus $\frac{1}{2}$ in. to $\frac{3}{4}$ in. in the next 2 yr of observation. The latter was roughly the magnitude of probable reliability since the pins proved difficult to read and were not entirely satisfactory. (A type of rebound gage developed at Oahe Dam has proven more satisfactory—readings obtained by a Bureau of Reclamation type torpedo originally developed for measuring settlement through retractable wings contacting under-side of an annular ring in the boring casing; plus utilizing a Wilson tiltmeter to measure inclination needed to correct for drift of hole from the vertical.) Principal provisions for the rebound were deferring the grouting as previously discussed and setting the chute pavement slightly below the weir surface to allow for some future differential rebound between the light slab and heavier weir.

EXCAVATION SLOPES

Slopes in composite formations, such as the alternating beds of shale and limestone here, are not very susceptible to conventional stability analyses using strengths derived from laboratory tests. While the shales generally failed in tests parallel to the bedding planes, in nature the slope would be controlled more by strength normal to the bedding. Also the harder limestones would serve to reinforce the slopes and, being generally more pervious, to contribute to a favorable orientation of seepage forces. Hence, slope studies were directed principally toward observing existing railway and highway slopes and computing strength represented by assumed safety factors of 1.0 and 1.3, then extrapolating through a slope chart for the significantly higher slopes involved in the spillway excavation. As a result, the shale-limestone slopes were established at 1 on 1 for the 90-ft maximum height downstream along the chute walls, and at an average of 1 on $1\frac{1}{4}$ for the 120-ft maximum height upstream. The lower conservatism upstream was deliberate for economy, since a modest slide in the spillway approach channel here would not seriously hamper project operation. Ample safety was desired adjacent to the weir and was obtained by widening the adjacent roadway excavation to form parking areas which resulted in a 55-ft high slope at the weir, 1 on 1 downstream and 1 on $1\frac{1}{2}$ upstream.

Since the limestones generally broke about vertical, slope studies considered berms located both at top and bottom of the major limestones. A common practice has been to place a berm at top of the limestone, excavating the limestone vertically and the shale on a slope. With seepage frequently emerging at base of the limestone, this has often resulted in eroding the shale to undercut the limestone which then fell as large blocks, sometimes aggravated by frost wedging in joints of the limestone exposed to surface water by the berm on top of the limestone. While this erosion has not effected stability

12 "Designing for Foundation Movements at Garrison Dam," by K. S. Lane, Transactions, 5th Congress on Large Dams, Vol. III, Paris, 1955.

of the slope proper, it has generally created a maintenance nuisance and sometimes a hazard. Some recent slope designs, particularly in shales of Pennsylvania and West Virginia, have attempted to reduce this maintenance problem by locating the berm on shale at bottom of the limestone. Purpose is to require far more shale to erode before undercutting the limestone; also to reduce entrance of surface water into the limestone joints by the seal of overlying shale. The latter design with berms located on shale is shown in Fig. 10 and was adopted for the more important locations in an effort to reduce maintenance.

CONCLUSIONS

Construction at Tuttle Creek Dam has clearly shown the practicality of placing the sand shell in a modern earth dam by dredging directly into the embankment, and also the high caliber compacted fill which can be produced from a mixture of shale and limestone by proper combination of breakage in blasting and manipulation on the fill. The important principle of adapting embankment zoning to fit local materials governed the embankment design which worked out quite satisfactorily in the construction. The use of material unsuitable for rolled fill in traffic compacted berms was a definite economy which technique has also been applied at several of the large dams along the Missouri River. The opportunity for an economical spillway was a controlling factor in site selection which has similarly been the situation at numerous dams in the Great Plains region where soft rocks require costly spillways, but permit economical embankments.

ACKNOWLEDGMENTS

Design and construction of Tuttle Creek Dam has been carried out by the Kansas City District, Corps of Engineers, currently under the direction of Colonel L. B. Laurion as District Engineer. Design was guided by L. G. Feil as Chief, Engineering Division, particularly assisted by R. L. Gillis as Chief, Structures Section and K. V. Taylor as Chief, Foundations and Materials Branch, who was succeeded by the senior author in the final design stage. Soils phases of the design were handled by R. J. Spiegel as Chief, Soils Section and by the junior author as Project Engineer; bedrock phases by S. G. Happ as Chief, Geology Section, succeeded by C. R. Golder in final design stage. Special mention should be accorded to B. V. Reany, Resident Engineer, and to List and Clark Co., contractor for bulk of the earthwork, particularly to their Vice President, Joe Clark, who supplied the authors with most of the data on dredge equipment.

Journal of the

SOIL MECHANICS AND FOUNDATIONS DIVISION

Proceedings of the American Society of Civil Engineers

DEWATERING THE PORT ALLEN LOCK EXCAVATION

By C. I. Mansur,[1] M. ASCE, and R. I. Kaufman,[2] M. ASCE

SYNOPSIS

Thirty-six large-diameter deep wells were installed around the top of the excavation for Port Allen Lock for the purpose of lowering the hydrostatic head in the deep stratum of pervious sand that lies beneath the lock. Specifications for the project required that the number, arrangement, and capacity of the wells and pumps be capable of reducing the hydrostatic head in the deep sands to a level 5 ft below the bottom of the excavation (about el -26 mlg) with a river stage of 45 ft mean low gulf (mlg). It was required that the ground water table in the excavation areas and behind the excavation slopes be lowered as was needed for satisfactory construction operations. After completion of the excavation to within 5 ft of grade, the water table in the foundation was to be maintained 5 ft or more below the bottom of the excavation until construction work would permit flooding the structure. Approval of the dewatering system was contingent, in part, on its proven performance. After installation of the deep well system, tests were made to determine its adequacy.

The observed test data indicated that the 30 temporary and 6 of the 8 permanent wells would be adequate for controlling the hydrostatic pressure in the deep sands beneath the main portion of the excavation for river stages up to el-45. Lowering the head in the deep sand below the bottom of the excavation for a river stage of 45 mlg would require a pumping rate of about 45,000 gpm. This corresponds to an average flow of about 1,250 gpm per well. The total well flow was about 500 gpm per ft of average drawdown. The permeability of

Note.—Discussion open until May 1, 1961. To extend the closing date one month, a written request must be filed with the Executive Secretary, ASCE. This paper is part of the copyrighted Journal of the Soil Mechanics Division, Proceedings of the American Society of Civil Engineers, Vol. 86, No. SM 6, December, 1960.

1 Vice-Pres., Fruco Constr. Co., a subsidiary of Fruin-Colnon Contracting Co., St. Louis, Mo.

2 Chf., Geology, Soils, and Materials Branch, U. S. Army Engr. Div., Lower Miss. Valley, Vicksburg, Miss.

the deep sand stratum as computed from the observed well flow and piezometric data was about 700 x 10^{-4} cm per sec. Lowering the hydrostatic head in the deep sand stratum below the bottom of the excavation had little effect on drying the excavation slopes and the bottom of the excavation. The three-stage wellpoint system installed for lowering ground water level beneath the slopes and excavation proved satisfactory for this purpose.

INTRODUCTION

Port Allen Lock is located on the west bank of the Mississippi River about 1 mi south of Port Allen, Louisiana, and across the river from Baton Rouge, Louisiana. The lock site is at the terminal of the Plaquemine-Morgan City Route of the Intracoastal Waterway. The lock is of reinforced concrete, U-frame type of construction and provides a usable chamber 84 ft wide by 1,200 ft long. It is constructed directly upon alluvial soil without bearing piles. The gates are of the horizontally framed miter type designed for a maximum lift of 45 ft. The floor of the lock chamber is at el -14 and the top of the lock walls at el-54 mean low gulf (mlg). A floating concrete guide wall is provided in the river approach to the lock; timber pile guide walls are used at the canal end. Eight permanent relief wells were installed at the canal end of the lock to provide relief of excess hydrostatic pressures that will develop in the pervious sand stratum beneath the bottom of the canal adjacent to the lock when it is placed in operation.

The excavation for Port Allen Lock encompassed a plan area of about 30 acres at the top. The excavation was 1,670 ft long and 132 ft to 177 ft wide at the bottom, 60 ft deep at the gate bays, and 55 ft deep along the chamber portion of the lock. The east end of the excavation was 1,300 ft from the west bank of the Mississippi River. The location of the excavation with respect to the Mississippi River is shown in Fig. 1. The excavation for the lock had average slopes of 1-on-5.5 with a slope of about 1-on-3 between dikes and ditches constructed on the slopes to intercept surface water. The excavation for the lock chamber extended to el -26 and to -32 for the gate bays.

Foundation soils at the lock site are generalized in Fig. 2. They consist, in order of depth below the ground surface (el-28±), of 10 ft to 40 ft of clay underlain by about 40 ft to 50 ft of alternating strata of silt and sandy silt with clay strata to about el -50 to -65. These silty soils grade into silty sands riverward from the lock site. Below el -50 to -65 there is a predominance of clay that extends to about el -72 to -130. Substratum sands having a thickness of about 70 ft to 130 ft underlie the silts and clays. Pleistocene silts and clays occur at about el -200, or 230 ft below the ground surface.

Readings from piezometers installed in the deep sand stratum in 1955 show that the hydrostatic head in this stratum reflects closely the stage of the Mississippi River. A maximum river stage of el-45 during construction would create a net head of approximately 70 ft to 75 ft beneath the excavation. This head could cause heaving of the bottom of the excavation and possibly some sand boils unless it was relieved. Readings of the piezometers indicated that the water table in the upper silts and clays has relatively little correlation with the river stage. Apparently, there is sufficient continuity of the clay strata above the sand so that the hydrostatic head in the deep sand has relatively little

effect on the water table in the upper silts. The water table in the upper silts and clays was generally within 5 ft to 15 ft of the ground surface elevation. This high water table and the pervious stratum of sand under artesian pres-

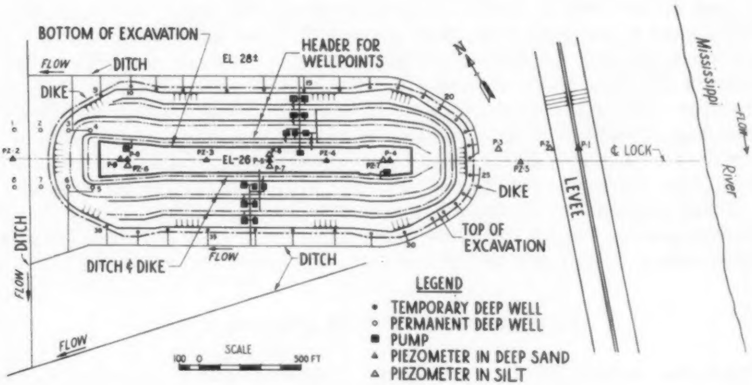

FIG. 1.—PLAN OF EXCAVATION AND DEWATERING SYSTEM

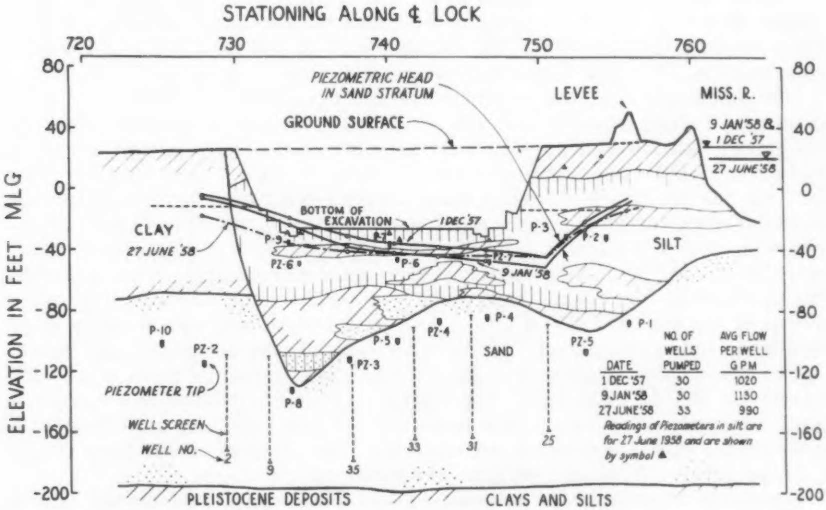

FIG. 2.—SECTION THROUGH EXCAVATION

sure beneath the excavation required that the slopes and bottom of the excavation be dewatered and the artesian pressure in the deep sand be adequately lowered.

Thirty-six large-diameter wells were installed to lower the hydrostatic head in the sands underlying the excavation. Three stages of wellpoints were installed on the excavation slopes and in the bottom of the excavation to intercept seepage and lower the ground water. After, the excavation was to grade the ground water level in the silt stratum beneath the excavation, and the hydrostatic head in the underlying deep sands had to be maintained at least 5 ft below the bottom of the excavation for any river stage up to el-45. After concrete in the base slabs and walls and the backfill were placed to el-6, and the drainage system behind the lock walls placed in operation, the head in the deep sand was allowed to rise 5 ft above the top of the completed surfaces or water surface in the area, and the ground water level in the silt stratum was permitted to rise provided this did not interfere with construction operations.

Final approval of the dewatering system was contingent, in part, on proven performance in field tests. This paper summarizes the design of the dewatering systems, tests made on the systems, and evaluation of the test data.

DEWATERING SYSTEM AND ITS DESIGN

A three-stage wellpoint system was designed to lower the ground water level in the silts and clays at least 5 ft below the bottom of the excavation. The resulting wellpoint system consisted of three stages of wellpoints on 12-ft, 10-ft, and 8-ft centers installed at el-12, -1, and -17, respectively. Each wellpoint with riser was about 25 ft long. The wellpoints were installed in a cased hole and were surrounded with filter sand. Each stage was connected to a 6-in. header pipe with two 8-in. vacuum wellpoint pumps connected to each line. Fig. 3 shows a section through the excavation slope and the location of the wellpoint system. The plan location of the header pipes is shown in Fig. 1.

The discharge from the wellpoint system was computed to insure that the spacing of wellpoints and sizes of headers and pumps were adequate. The initial ground water level in the silty soils was assumed to be at the natural ground surface of el-30. The horizontal permeability of the silt was taken as 0.5×10^{-4} cm per sec, which value was obtained from laboratory permeability tests on undisturbed samples. The vertical permeability k_v obtained in the laboratory was about 1/3 the horizontal permeability k_h of the same specimen. However, because of the numerous clay lenses in the silt stratum, it was assumed that $k_v = 1/4\, k_h$ for design. Due to the predominance of clay strata near the bottom of the silt stratum, it was considered that the silt was bounded at its base by an impervious layer. From experience, it was estimated that the effective source of seepage would approximate a line source parallel to and 250 ft from the line of wellpoints. The discharge from each stage was computed from the equation for gravity flow in the silt stratum, assuming a 20-ft vacuum in the header pipe, and using the above values. The computed flows from stages 1, 2, and 3 were 38, 50, and 55 gpm, respectively.

Discharge from the third stage of wellpoints is computed from the data of Fig. 4. The section in Fig. 4 has been transformed by dividing the horizontal dimensions by $\sqrt{k_h/k_v} = \sqrt{4}$. The transformed value of L is $\bar{L}$, and was computed from

$$\bar{L} = \frac{L}{\sqrt{k_h/k_v}} = \frac{250}{\sqrt{4}} = 125 \text{ ft}$$

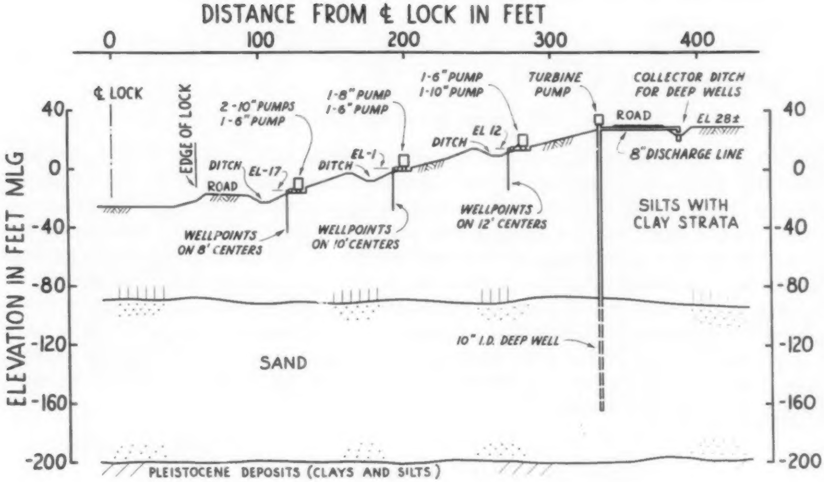

FIG. 3.—SECTION THROUGH EXCAVATION SLOPE

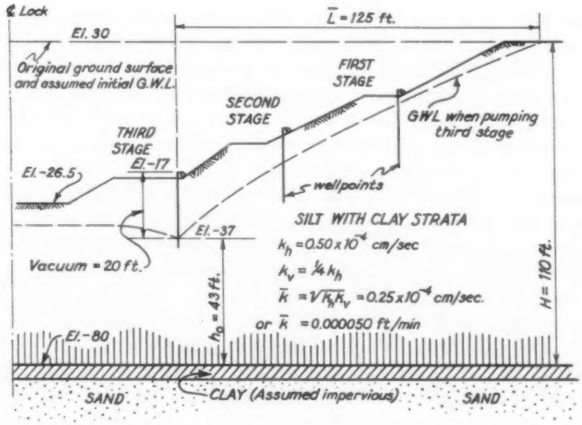

The above section has been transformed by dividing the horizontal dimensions by $\sqrt{k_h/k_v} = \sqrt{4}$. The transformed value of L is $\bar{L}$, and was computed as follows :

$$\bar{L} = \frac{L}{\sqrt{k_h/k_v}} = \frac{250}{\sqrt{4}} = 125 \text{ ft}$$

The discharge Q per ft of header was computed as follows :

$Q = \frac{\bar{k}}{2\bar{L}}(H^2 - h_o^2) = \frac{0.000050}{2 \times 125}(110^2 - 43^2)\ 7.5$ *or* $Q = 0.0154$ *gpm per ft of header = 55 gpm for the third stage wellpoint system which has a total header length of about 3550 ft.*

FIG. 4.—DISCHARGE FROM THIRD STAGE OF WELLPOINT SYSTEM

The discharge, Q, per foot of header was computed as follows:

$$Q = \frac{\bar{k}}{2\,\bar{L}}\left(H^2 - h_o^2\right) = \frac{0.000050}{2 \times 125}\left(110^2 - 43^2\right) 7.5 \text{ or}$$

$$Q = 0.0154 \text{ gpm per ft of header} = 55 \text{ gpm}$$

for the third stage wellpoint system which has a total header length of about 3550 ft. These computations were based on the assumption that the discharge from a line of closely spaced wellpoints, required to produce a given drawdown, would be the same as that from a continuous line slot. In the computations the effect of partial penetration of the wellpoints on the computed discharge was neglected. Although this procedure is not exact, it was considered sufficient in this case since the computed discharge per stage was small. To allow a margin of safety, the pumps and headers for each stage were selected to have a capacity of at least 100 gpm with minimum head loss. The wellpoint system described was considered adequate to intercept the small flows and conduct them from the excavation.

PRESSURE RELIEF SYSTEM AND ITS DESIGN

The pressure relief system consisted of 30 temporary wells located around the top of the excavation and 6 of 8 permanent wells on the banks of the (landside) canal approach to the lock. The locations of the wells are shown in Fig. 1. The temporary wells were located at the top of the excavation slope to avoid interference with construction in the excavated area. Although only about 22 temporary wells would have been required had they been located at the toe of the slope, it would have been necessary to lower header pipes and pumps at various times during excavation and raise them at intervals when structural backfill and concrete were being placed. The advantages offered by locating 30 wells at the top of the excavation were considered to outweigh those for a system of 22 wells at the toe of the slope.

The pressure relief wells consisted of 10-in. ID wood stave pipe with a riser length of about 115 ft and a screen about 70 ft long. The screen contained 3/16-by-3-in. slots, was surrounded with a 6-in. thick gravel filter, and penetrated about 65% of the pervious sand substratum. Details of a typical well are shown in Fig. 5. Each well was provided with a 10-in., impeller A, HC, Fairbanks-Morse, three-stage, deep-well turbine pump with the impeller set at elevations ranging from -50 to -60 and suction pipes extending to el -70. This pump has a rated speed of about 1,760 rpm and a safe speed of at least 2,500 rpm. The pump is capable of pumping 1,300 gpm at a static head of about 85 ft at a speed of 2,000 rpm. Each pump was driven by either a 40-horsepower diesel or 50-horsepower butane power unit. Each well had a proven capacity of about 1,200 to 1,300 gpm.

The deep-well system was designed to produce a drawdown of about 80 ft, which corresponds to a head in the deep sand about 5 ft to 7 ft below the bottom of the excavation with the Mississippi River at el-45. The coefficient of permeability of the deep sand was estimated to be 700×10^{-4} cm per sec (0.14 ft per min) from correlations[3] of in-situ permeability versus D_{10} size of the

---

[3] "Laboratory and In-Situ Permeability of Sand," by C. I. Mansur, Transactions, ASCE, Vol. 123, 1958, p. 881.

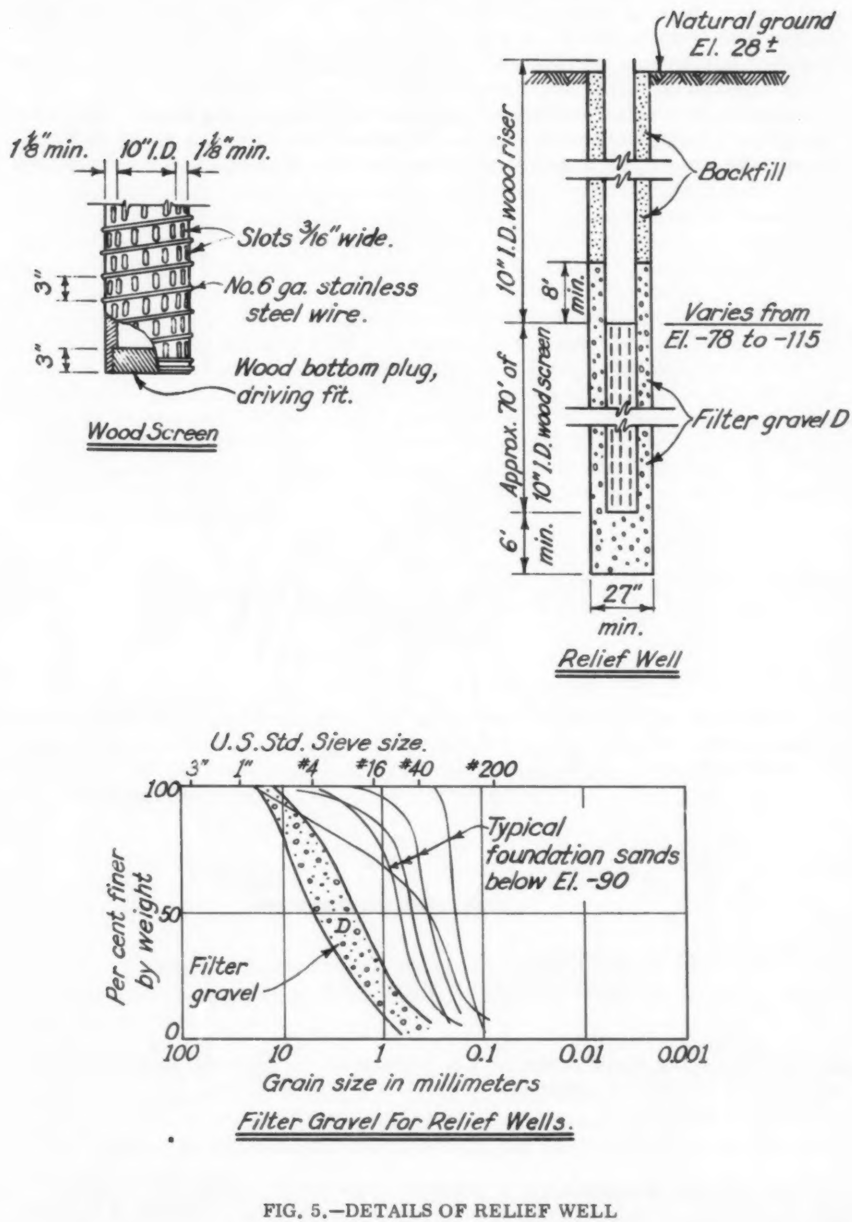

FIG. 5.—DETAILS OF RELIEF WELL

sand strata, and from pumping test data reported by the United States Geological Survey, Dept. of Interior (USGS), aquifer. The effective depth of the sand aquifer was taken as 100 ft. It was initially considered that the wells would be installed in plan on a rectangle about 600 ft by 2,050 ft, and that the near bank of the Mississippi River would simulate a line source of seepage.

Actually, the wells were installed in an oval-shaped ring about 700 ft wide and 2,050 ft long as shown in Fig. 6. A flow net was drawn, as shown in Fig. 6, to compute the required discharge from the well system. For a ring of this

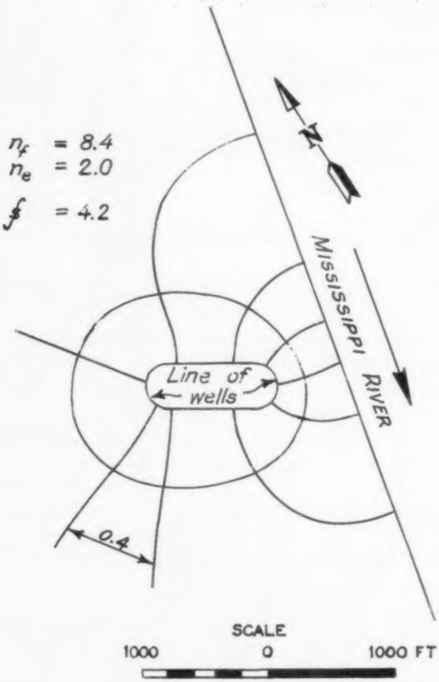

FIG. 6.—FLOW FROM PRESSURE RELIEF WELL SYSTEM COMPUTED FROM A FLOW NET

size and shape the shape factor is 4.2. Required total flow (Q) from the relief well system per foot of drawdown (H-h) was computed from

$$\frac{Q}{H-h} = k\,d\,\oint \qquad (1)$$

in which k is the permeability of pervious substratum = 700×10^{-4} cm/sec = 0.14 ft per min, d is the thickness of pervious substratum = 100 ft, $\oint$ denotes

the factor = n_f/n_e, n_f is the number of flow channels, and n_e refers to the number equipotential drops.

$$\frac{Q}{H-h} = 0.14 \times 100 \times 4.2 \times 7.5 = 441 \text{ gpm per ft of drawdown.}$$

For H-h = 80 ft the computed total discharge is Q = 441 x 80 = 35,300 gpm. It should be noted that the line of wells were simulated by a slot that fully penetrated the pervious substratum. The wells were spaced proportionally to the flow channels so that each well would intercept the same amount of flow. In the design of the well, it was considered that the screen would have a capacity of about 20 gpm per ft without excessive head loss, and that each well could produce a discharge of about 1,000 gpm. On this basis the total number of wells required for the pressure relief system was computed to be 36.

Subsequent to the initial design of the deep-well system, the drawdown along the center line of the excavation was recomputed using the equations for artesian wells and design values. The drawdown was computed at locations of selected piezometers assuming the source of seepage at the near bank of the Mississippi River, and also assuming that the source of seepage consisted of an oval-shaped ring about 1,500 ft from the ring of wells. To facilitate computations, the oval-shaped ring was replaced by an equivalent circular ring having a radius of 2,000 ft. The line source of seepage at the bank of the Mississippi River was computed from

$$\text{Drawdown} = \frac{1}{2 \pi k d} \sum_{n=1}^{n=n} Q_n \ln \frac{S_n}{r_n} = \frac{1}{2 \pi k d} \sum_{n=1}^{n=n} F_{L_n} \quad \ldots\ldots (2)$$

$$= 1.51 \sum \ln \frac{S_n}{r_n} \text{ for } Q_n = 1000 \text{ gpm and in which k is}$$

the coefficient of permeability = 700×10^{-4} cm per sec; d denotes thickness of sand stratum = 100 ft; S_n is the distance from image well n to piezometer; r_n refers to the distance from well n to piezometer, and Q_n is the flow from well n. The ring source of seepage is computed from

$$\text{Drawdown} = \frac{1}{2 \pi k d} \sum_{n=1}^{n=n} Q_n \ln \frac{R}{r_n} = \frac{1}{2 \pi k d} \sum_{n=1}^{n=n} F_{R_n} \quad \ldots\ldots (3)$$

$$= 1.51 \sum \ln \frac{R}{r_n} \text{ (for } Q_n = 1000 \text{ gpm and kd is as pre-}$$

viously given) in which R is the distance from the ring source of seepage to the piezometer.

Typical values for drawdown at piezometer P-5 at the center of the excavation are shown in Table 1. Drawdowns computed in a similar manner for other piezometer locations are listed in Table 2. Also shown in Table 2 is the head reduction at the periphery of selected wells which was computed to determine the elevation at which to set the bottom of the section pipe on the deep-well turbine pumps.

The preceding computations were made assuming that the wells fully penetrated the pervious substratum. The well penetration does not affect the drawdown along the central portion of the excavation (where the residual head would

tend to be larger than at any other point within the ring of wells), because the distance from the wells to the central portion of the excavation exceeded the radius of the zone in which the drawdown is affected by well penetration. According to P. T. Bennett and R. A. Barron,[4] this radius is about equal to the thickness of the pervious stratum, or about 100 ft at Port Allen Lock. However,

TABLE 1.—DRAWDOWN AT PIEZOMETER P-5, PORT ALLEN LOCK

Well	F_L	F_R	Well	F_L	F_R	Well	F_L	F_R	Well	F_L	F_R
2	1.48	0.55	12	2.06	1.29	21	1.18	0.76	30	1.54	0.97
3	1.58	0.68	13	2.30	1.59	22	1.13	0.61	31	1.81	1.19
4	1.68	0.80	14	2.44	1.77	23	1.13	0.60	32	2.10	1.45
5	1.70	0.81	15	2.30	1.68	24	1.13	0.60	33	2.41	1.71
6	1.60	0.68	16	1.98	1.41	25	1.14	0.60	34	2.47	1.73
7	1.49	0.55	17	1.73	1.20	26	1.18	0.72	35	2.27	1.48
9	1.64	0.79	18	1.51	1.02	27	1.22	0.74	36	2.01	1.18
10	1.78	0.96	19	1.35	0.89	28	1.31	0.80	37	1.84	0.98
11	1.90	1.10	20	1.28	0.83	29	1.39	0.87	38	1.70	0.81

TOTAL	WELLS	ΣF_{L_n}	DD^+-ft	ΣF_{R_n}	DD^+-ft
	9 - 38	51.2	77.4	32.3	48.8
	3-6 & 9-38	57.8	87.2	35.3	53.3
	2-7 & 9-38	60.8	91.8	36.4	55.0

+ For Q_n = 1000 gpm

TABLE 2.—COMPUTED DRAWDOWN AT SELECTED PIEZOMETERS AND WELLS

Group of Wells	Computed drawdown (H-h), in feet: Line source of seepage at Mississippi River					Ring source of seepage, R = 2,000 ft				
	P-4	P-5	P-8	Well 14	Well 26	P-4	P-5	P-8	Well 14	Well 26
9-38	76.6	77.4	70.5	83.2	80.8	56.1	48.8	34.6	55.4	63.9
2-7 & 9-38	85.7	91.8	96.3	98.0	87.8	58.1	55.0	51.2	61.4	63.9

Note: (1) Drawdown computed from equations in Table 1 for k = 700 x 10^{-4} cm per sec, d = 100 ft, and Q_n = 1,000 gpm per well.
(2) Drawdown at well computed assuming effective well radius = 13.5 in. = distance from center of well to outer periphery of gravel filter.
(3) To obtain drawdown when pumping wells at an average discharge Q_n other than 1,000 pgm, multiply above drawdowns by $Q_n/1000$.

as will be described, it was necessary to consider the fact that the water level in a partially penetrating well is lower than that in a fully penetrating well

[4] "Design Data for Partially Penetrating Relief Wells," by P. T. Bennett and R. A. Barron, Proceedings, Fourth Internatl. Conf. on Soil Mechanics and Foundation Engrg., Vol. II, London, 1957, pp. 282 ff.

pumped at the same discharge. As shown in Table 2, the greatest computed drawdown, assuming a fully penetrating well system, was 98 ft at well 14.

Using the procedure described by Bennett and Barron,[4] the drawdown at wells penetrating 65% of the pervious substratum was computed to be about 3 ft greater, resulting in a maximum drawdown of 101 ft. Allowing 1 ft for hydraulic head loss, the drawdown in well 14 would be 102 ft. Thus, for a river stage of 45 ft mlg, the water level in well 14 would be at about el -57. Since it was considered possible that the wells might be pumped at rates somewhat greater than 1,000 gpm, the suction pipes on the deep-well turbine pumps were set at el -70, which proved to be satisfactory.

PIEZOMETERS

Piezometers were installed in the silty foundation beneath the lock site and in the underlying deep sand stratum at the locations shown in Figs. 1 and 2 to measure the ground water level and hydrostatic head during construction. They consisted of 1-1/2-in. diam by 24-in. brass wellpoints with No. 25 slots attached to 1-1/2-in. diameter riser pipes. Piezometer screens in silt were surrounded with a sand filter about 3 in. thick.

PERFORMANCE OF DEWATERING SYSTEM

The north half of the first stage wellpoint system and eight of the deep wells were placed in operation on August 26, 1957, at which time the Mississippi River was at about el-8. This portion of the wellpoint system lowered the ground water level in the silt stratum from el-11.5 to about el-2 and the flow from it averaged about 40 gpm. On October 10, 1957, the north side of the second stage wellpoint system was placed in operation. By this date the flow from both stages one and two on the north side was 25 gpm. Pumping these two stages lowered the ground water level to about el -2. Pumping the south side of the second stage wellpoint system started on October 27, 1957. The first and second stages were pumped from that time until December 16, 1957, after which time the first stage was cut off. The total discharge from the first and second stages was about 50 gpm; the resulting ground water level was at about el -20.

On December 16, 1957, the Mississippi River was at el-24, or about 4 ft below the natural ground surface. As no seepage was observed emerging from the slope above the second stage when the first stage was not pumped, the first stage of wellpoints on the north slope was removed on January 2, 1958. The total flow from the second stage wellpoint system, after the first stage had been shut off, was about 65 gpm, and the ground water level along the second stage of wellpoints was about at el -18. Although the wellpoints in the second stage extended only to el -25, they caused a lowering of the water table in piezometers installed beneath the bottom of the excavation at el -35.

The third stage of the dewatering system was placed in operation on February 7, 1958, and the second and third stages were pumped concurrently until the end of May 1958. During this period, the Mississippi River stage ranged between el-10 and -33, and the ground water level in the silty soils beneath the bottom of the excavation was maintained at about el -30. The second and third

stages were pumped about 12 hr a day during this period at a rate of about 50 to 70 gpm. From June 1958 until March 13, 1959, only the third stage wellpoint system was pumped. The discharge from this system was about 75 gpm at Mississippi River stages of about 9 ft mlg and about 60 gpm when half of the third stage system was pumped with the Mississippi River at about el-27.

During most of this period, the ground water level in the silty soils was maintained at about el -25 to -30, but was permitted to rise gradually as construction permitted. From March 13 to June 28, 1959, only the second stage wellpoint system was pumped because construction had progressed to the extent that pumping the third stage wellpoint system was unnecessary. The entire wellpoint system had been removed by June 28, 1959.

The observed discharge from the wellpoint system was somewhat greater than computed design values cited previously. This is attributed to limitations in the equation used to estimate the required discharge from the system, and in the accuracy of estimating the distance to the effective source of seepage and permeability of the silty soils. Although the exact value of the overall permeability of the silt stratum could not be determined from the observed piezometric data and wellpoint discharge, an approximate value was obtained from observations when only the third stage of wellpoints was pumped as follows. Based on the vacuum at the pump, it was estimated that the effective vacuum in the wellpoint header was 20 ft. The ground water level that would occur without pumping was assumed equal to the stage of the Mississippi River. Using the previous values, a source of seepage of 250 ft, and the equation for gravity flow to a slot in Fig. 4, the horizontal permeability was computed for each observed discharge, assuming the horizontal permeability equal to four times the vertical permeability. For these values, the average horizontal permeability of the silt stratum was computed to be 1.3×10^{-4} cm per sec, as compared to the value of 0.50×10^{-4} cm per sec assumed in design.

Although the observed discharges were greater than those computed in design, the wellpoint system performed satisfactorily since an ample allowance was made in designing the system so that it could adequately handle flows considerably greater than those computed. The wellpoint system, as installed adequately, lowered the ground water level in the silty soils to the values required by the specifications.

TESTS ON PRESSURE RELIEF SYSTEM

On November 28, 1957, a test was started to determine the capacity of the 30 temporary deep wells, the pumps and power units, and the maximum drawdown obtainable with the deep well system. The test was performed by first adjusting the pumps to a constant speed and then observing the piezometers installed in the deep sand and measuring the flow from the relief wells at periodic intervals. The flow from the wells was measured by a pitotmeter inserted in the 8-in. discharge line from the deep-well turbine pump. To obtain sufficient back pressure to operate the pitotmeter, it was necessary to insert a 4-in. wide paddle into a slot in the top of the 8-in. discharge line from the pump. The total flow from the relief well system was checked by measuring the flow in the two collector ditches for the well discharge by means of a midget Gurley flow meter.

On November 28, 1957, each pump on the 30 temporary wells was adjusted to operate at an average speed of 1,760 rpm. On November 29, the average well flow was about 990 gpm as determined from the pitotmeter measurements. However, since the paddle inserted to operate the pitotmeter was found to create a back pressure of 7.3 ft at a flow of 1,050 gpm, and 9.2 ft at 1,200 gpm, the flow measured by the pitotmeter had to be corrected for back pressure on the pump in order to obtain the flow that occurred without a paddle in the discharge line. The correction factor was obtained from the pump characteristic curve for impeller A on the basis of a total pumping head of 80 ft without the paddle and 87.3 ft with the paddle. The correction factor amounted to about 5%. Thus, the average flow per well as measured by the pitotmeter and corrected for back pressure was 1,030 gpm. The average well flow as obtained from measurements in the collector ditches on November 29, was 1,028 gpm, which checked that measured by the pitotmeter closely. On December 3, 1957, the flow from the wells was again measured. The average flow per well obtained from the pitotmeter and corrected for back pressure was 1,010 gpm. The average flow obtained from the measurements in the collector ditch was 1,150 gpm. Based on these measurements, the average flow per well during the test was considered to be 1,020 gpm.

Readings of piezometers observed on December 1, 1957, are plotted in Fig. 2. Drawdowns observed at three selected piezometers (P-4, P-5, and P-8) during the test are plotted versus time in Fig. 7. As shown in Fig. 2, piezometers P-4 and P-8 are near the river and canal ends of the lock, respectively, and piezometer P-5 is at the center of the lock. The drawdown plotted in Fig. 7 is the difference between the Mississippi River stage and the piezometer reading. Although the drawdowns are somewhat erratic due to the effect of adjustments that had to be made to the pumps during the test, there is a tendency for the drawdown to increase with time. Thus, curves of best fit were drawn as straight lines on the semi-log plots in Fig. 7 to reflect this increase in drawdown with time in accordance with C. E. Jacob's[5] theory.

From Fig. 7, it appears that the drawdown observed after pumping the pressure relief system at a constant rate for 10 days will be about 3% greater than that at the end of the first day. If the Mississippi River were to rise to el-45 (about 15 ft above ground surface), it could be expected to remain at high stages for at least 10 days, therefore, the drawdown at the end of 10 days was used as the effective drawdown produced by the system. As shown in Fig. 7, the drawdown in piezometers P-4, P-5, and P-8, after pumping the 30 temporary wells 10 days at an average discharge of 1,020 gpm, was 68.6 ft, 65.3 ft, and 47.8 ft, respectively.

Computed drawdowns for a ring and for a line source of seepage at the Mississippi River for wells 9 through 38, pumped at a flow of 1,020 gpm per well, are plotted in Fig. 8. The drawdown observed during the pumping test is intermediate between that computed for a line source and that for a ring source. A comparison between the computed and observed drawdown in the deep sand for piezometers P-4, P-5, and P-8 is shown for this test in Table 3, under well group D. From this table, it is seen that the observed drawdowns range from 67% to 88% of the drawdown computed for a line source, and from 120% to 136%

---

[5] "Drawdown Test to Determine Effective Radius of Artesian Well," by C. E. Jacob, Transactions, ASCE, Vol. 112, 1947, p. 1047.

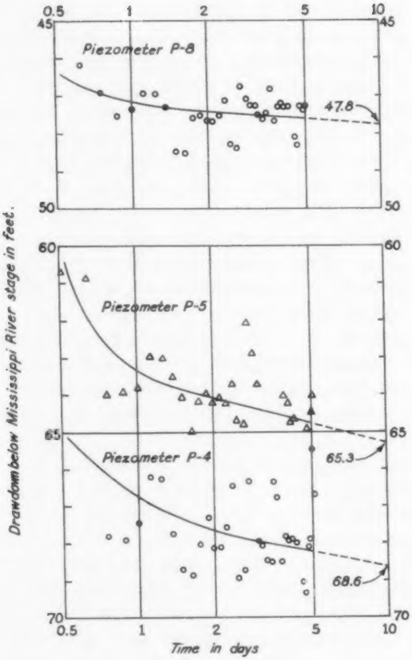

FIG. 7.—DRAWDOWN VS TIME DURING TEST FROM 28 NOV. TO 3 DEC. 1957

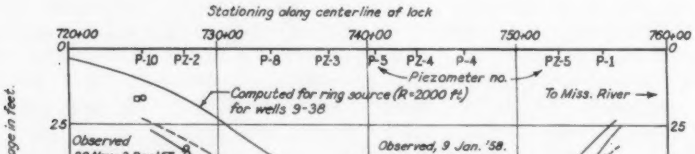

FIG. 8.—OBSERVED AND COMPUTED DRAWDOWN IN DEEP SAND

TABLE 3.—COMPUTED AND OBSERVED DRAWDOWN IN DEEP SAND FOR VARIOUS COMBINATIONS OF WELLS

Well Group	No. of wells pump-ed	Avg[a] flow per well gpm	Piezometer P-4 Drawdown in ft Obs	P-4 Computed Line	P-4 Computed Ring	P-4 Obs DD in Comp DD % Line	P-4 Obs DD in Comp DD % Ring	Piezometer P-5 Drawdown in ft Obs	P-5 Computed Line	P-5 Computed Ring	P-5 Obs DD in Comp DD % Line	P-5 Obs DD in Comp DD % Ring	Piezometer P-8 Drawdown in ft Obs	P-8 Computed Line	P-8 Computed Ring	P-8 Obs DD in Comp DD % Line	P-8 Obs DD in Comp DD % Ring
A	7	1000	16.2	19.2	15.5	84	104	13.1	17.5	11.8	75	111	6.5	12.8	5.3	51	123
B	8	1000	14.7	21.0	16.1	70	91	13.4	20.4	13.3	99	152	6.5	16.9	7.9	38	82
C	8	1000	17.6	21.4	16.2	82	109	16.3	21.3	14.2	116	173	9.8	17.7	8.3	55	118
D	30	1020	68.6[b]	78.2	57.3	88	120	65.3[b]	78.9	49.7	83	131	47.8[b]	71.8	35.2	67	136
E	10	1200	28.0	31.7	23.9	88	117	26.9	32.2	21.2	83	127	17.1	26.2	12.3	65	139
F	18	1100	48.2	54.5	43.1	88	112	42.1	50.5	33.0	83	128	24.9	38.7	16.4	64	152
Avg D, E, & F						88	116				83	129				65	143

[a] Values estimated except for flow from Group D which was measured. Drawdown computed from equations and values in Table 1.

[b] Drawdown adjusted for 10-day period, see Fig. 7.

Well Group	Wells being pumped	Date (1957)
A	13,15,16,18,21,24, and 27	21 Sep
B	13,15,16,18,21,24,27, and 37	7 Oct
C	13,15,16,18,21,27,31, and 37	30 Oct
D	9 through 38	29 Nov-) 3 Dec)
E	10,13,16,18,21,25,27,31, 33, and 34	12 Dec
F	10,13,15,16,17,18,19,21,22,24, 25,27,28,30,31,32,33, and 34	25 Dec

of that computed assuming a ring source of seepage. As seen from Table 3, the drawdown near the canal or landward end of the well system was only about 67% of that computed assuming a line source of seepage at the Mississippi River. Therefore, the flow toward this portion of the well system exceeded that computed. This is attributed, in part, to the pervious substratum having a greater thickness (130 ft) landward from the well system than the value (100 ft) used in design (Fig. 2).

Since none of the permanent wells were pumped during the tests, and since it was planned to pump six of these eight wells (wells 2 through 7) if the river stage approached el-45, it was necessary to estimate the additional drawdown that would be produced by pumping wells 2 through 7 at a discharge of 1,020 gpm per well. This was done by computing the drawdown at piezometers P-4, P-5, and P-8, assuming a line source of seepage and multiplying computed drawdowns by correction factors of 88%, 83%, and 67%, respectively (Table 4). The drawdown at the same piezometers also was computed assuming a ring source of seepage and multiplying the computed drawdown at piezometers P-4, P-5, and P-8 by correction factors of 120%, 131%, and 140%, respectively. The two drawdowns computed for a given piezometer in the preceding manner were then averaged as shown in Table 4.

Based on these computations, it was estimated that a total drawdown of 74.4 ft, 75.6 ft, and 68.3 ft would be produced at piezometers P-4, P-5, and P-8, respectively, if wells 2 through 7 in addition to wells 9 through 38 were pumped at a discharge of 1,020 gpm. The total drawdown produced by pumping this combination of 36 wells at an average discharge of 1,020 gpm is shown on Fig. 8 as an "adjusted observed drawdown." As seen on Fig. 8 and Table 4, this drawdown is somewhat less than the maximum drawdown that would be required for a Mississippi River stage at el-45. Thus, it was apparent that pumping wells 2 through 7 and 9 through 38 at a discharge of 1,020 gpm per well would not quite produce the required drawdown, should the Mississippi River rise to el-45 with the excavation to grade.

Since pumping 36 wells at a discharge of 1,020 gpm would not produce the required maximum drawdown, it was necessary to determine the maximum safe capacity of the wells, turbine pumps, and power units for computing the drawdown that could be produced by pumping the wells at a greater discharge. On January 8, 1958, tests were made on six wells to determine the increase in well discharge obtainable by increasing the speed of the pump. At the time the individual well and pump were tested, all of the remaining temporary wells were being pumped at a speed of about 1,760 rpm and a discharge of about 1,020 gpm. During this time the water table in the deep sand was at about el -35 at piezometers P-4 and P-5. Thus, the head on the pumps being tested was as high as would be required for maximum drawdown. On this date the Mississippi River was at about el-28. The results of the tests on the 6 wells indicated an average discharge of about 1,020 gpm at 1,760 rpm, which increased linearly with pump speed to 1,370 gpm at 2,150 rpm. At a speed of 2,000 rpm the discharge was about 1,230 gpm.

Later on January 8, 1958, all of the pumps in the 30 temporary wells were set at a speed of 1,970 rpm, and on January 9, the average well flow, as measured in the collector ditches, was 1,320 gpm per well. Because of the discrepancy on December 3, 1957, between well flow measured in the ditch and that measured by the pitotmeter, the well flow on January 9, 1958 was computed

from the pump speed and estimated head on the pump to serve as a check on the flow measured in the ditch. The flow computed in this manner was 1,130 gpm, which is about 15% less than the flow measured in the ditch. Because the drawdown produced in an artesian stratum increases linearly with well discharge, and since the drawdown on January 9 was about 111% of that at the end of the first day of the November 28 - December 3 test when the discharge per

TABLE 4.—ESTIMATED MAXIMUM CAPACITY OF PRESSURE RELIEF SYSTEM

Well Group	No. of wells pumped	Pump Speed rpm	Avg flow per well gpm	Piez. No.	Computed drawdown ft		Corrected[a] factor percent		Corrected computed drawdown - ft		Avg[b] corrected computed drawdown ft	Max[c] required drawdown ft
					Line	Ring	Line	Ring	Line	Ring		
9-38	30	1760	1020	P-4	78.2	57.3	88	120	68.6	68.6	68.6	82
				P-5	78.9	49.7	83	131	65.5	65.0	65.3	76
				P-8	71.8	35.2	67	136	48.0	47.8	47.9	82
9-38	30	2000	1230	P-4	94.2	69.0	88	120	82.9	82.9	82.9	82
				P-5	95.1	59.9	83	131	78.9	78.5	78.7	76
				P-8	86.5	42.5	67	136	57.9	57.7	57.8	82
2-7, & 9-38	36	1760	1020	P-4	87.6	59.6	88	120	77.1	71.6	74.4	82
				P-5	93.6	55.9	83	131	77.8	73.4	75.6	76
				P-8	98.3	52.1	67	136	65.8	70.8	68.3	82
2-7, & 9-38	36	1880	1130	P-4	97.0	66.0	88	120	85.4	79.3	82.4	82
				P-5	103.8	61.9	83	131	86.3	81.3	83.8	76
				P-8	109.0	57.7	67	136	72.9	78.4	75.7	82
2-7, & 9-38	36	2000	1230	P-4	105.8	72.0	88	120	93.8	86.3	89.7	82
				P-5	113.0	67.5	83	131	93.8	88.4	91.0	76
				P-8	118.6	62.8	67	136	79.5	85.4	82.5	82

[a] Obtained from Table 3 for well group D.
[b] Drawdown expected after pumping at indicated discharge for 10 days.
[c] Drawdown for head in deep sand lowered 5 ft below bottom of excavation with excavation to grade and Mississippi River at el 45.

well was 1,020 gpm, it is believed that on January 9, the discharge per well was 1.11 times 1,020 gpm or 1,130 gpm, which agrees with the value computed from the pump rating curves.

The drawdown produced in the deep sand during this test is shown in Fig. 8. Since this drawdown was not great enough, the drawdown that would be produced if wells 2 through 7 were also pumped at a rate of 1,130 gpm was computed using the procedure described above. The results of these computations are

shown in Table 4 and indicate that drawdowns of 82.4 ft, 83.8 ft, and 75.7 ft would be produced at piezometers P-4, P-5, and P-8, respectively, if the 36 wells were pumped at a rate of 1,130 gpm. As seen from Table 4, the drawdown at piezometer P-4 (canal end gate bay) did not meet the required maximum drawdown by about 6 ft, even though the drawdown beneath the remainder of the excavation was adequate.

From the preceding, it was concluded that it would be necessary to pump all 36 wells at a discharge in excess of 1,130 gpm or else pump the river end wells at about 1,130 gpm and the canal end wells in excess of 1,130 gpm to obtain the maximum required drawdown. It was estimated from the pump rating curves that if the pumps were operated at a speed of about 2,000 rpm, a discharge of about 1,230 gpm could be produced from each well for the lowest water level required. The drawdowns obtainable by pumping the 30 temporary wells at a discharge of 1,230 gpm were computed and are shown in Table 4.

From Table 4 it is apparent that pumping the 30 temporary wells at this discharge would produce the required maximum drawdown in the deep sand beneath the river end half of the excavation. However, since these 30 wells could not satisfactorily lower the ground water level the maximum amount required at the canal end gate bay for a Mississippi River stage of el-45, it was necessary to determine the additional drawdown that could be produced by pumping permanent wells 2 through 7 at a discharge of 1,230 gpm. This was accomplished by computing the drawdown at piezometers P-4, P-5, and P-8, for both a line source and ring source of seepage, multiplying the computed values by the appropriate correction factors (ratio of observed to computed drawdown for well group D, table 3), and averaging the results for each piezometer. These computations are summarized in Table 4. The resulting total drawdown is shown in Fig. 8 as the observed drawdown adjusted for wells 2 through 7 and 9 through 38 pumped at an average discharge of 1,230 gpm. From Table 4 and Fig. 8, it is apparent that pumping these 36 wells at an average discharge of 1,230 gpm (pump speed equal 2,000 rpm) will produce a drawdown slightly greater than the required maximum drawdown for the Mississippi River at el-45.

From the results of these pumping tests, it was concluded that the deep well system was adequate to relieve hydrostatic pressures in the deep sand stratum during construction of Port Allen Lock, but that it would be necessary to pump 6 of the 8 permanent wells and the 30 temporary wells at a discharge of up to 1,230 gpm to produce the required drawdown for a Mississippi River stage of 45 ft mlg.

PERFORMANCE OF PRESSURE RELIEF SYSTEM

Piezometers were observed at frequent intervals during construction to determine whether the pressure relief system was being operated in accordance with specified requirements. Flow from the system was measured about monthly and at more frequent intervals during high river stages to check on the performance of the system. Piezometric data for selected dates during construction are plotted in Fig. 2. In general, the pressure relief well system lowered the hydrostatic head in the deep sand stratum to required values. This was accomplished by altering the number of wells pumped and the pump speed at various times, with the number of wells pumped being increased during high river stages.

The Mississippi River reached a maximum stage of about el-28 in January 1958. During this stage, the drawdown at the center of the excavation as measured in piezometer P-5 was 70 ft. Thirty wells were pumped at a discharge of about 34,000 gpm to produce this drawdown. In August 1958, the river again rose to el-28, and 27 wells were pumped at a discharge of 27,900 gpm to produce a drawdown of 56 ft. The piezometric levels corresponding to these drawdowns were below those required by the specifications, as were the piezometric

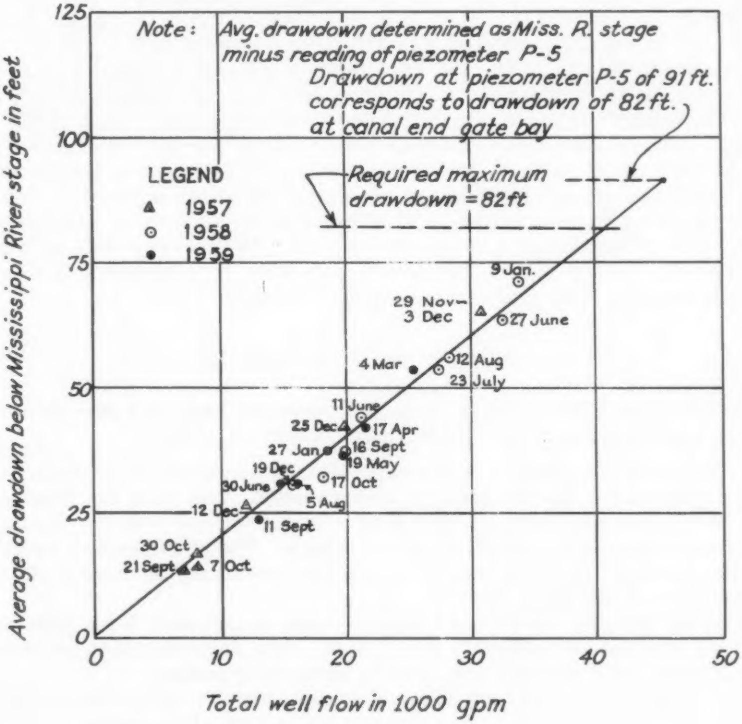

FIG. 9.—OBSERVED DISCHARGE FROM PRESSURE RELIEF SYSTEM VS AVERAGE DRAWDOWN IN DEEP SAND

levels in the other piezometers in the deep sand. As of November 1959, most of the concrete in the lock structure had been placed, and the sand backfill behind the lock walls had been placed to about el-12. As of that time, the pressure relief system had performed entirely satisfactorily.

Piezometric data obtained from August 25, 1957, to December 3, 1957, indicated that the ground water level in the silt stratum was not greatly affected by lowering the hydrostatic head in the deep sand stratum. The water table in the silt stratum fell slowly (2.5 ft to 4 ft per month) until parts of the second stage wellpoint system were operated. This rate of fall was about equal to that

observed in the 1955 low water season before any wells had been installed. The fact that lowering the head in the deep sand caused little to no significant lowering of ground water in the silt is attributed to the silt containing numerous clay lenses and strata and the predominance of clay strata in the lower portion of the silt stratum.

The discharge from the pressure relief system, observed during the pumping tests and subsequent construction plotted in Fig. 9, versus the average drawdown in the deep sand stratum observed at piezometer P-5. As seen from this figure, the discharge was about 500 gpm per ft of average drawdown. Had the Mississippi River risen to el-45 when the excavation was to grade, it would have been necessary to produce a maximum drawdown of 82 ft at the gate bays (piezometers P-4 and P-8) and 76 ft beneath the lock chamber (piezometer P-5). To lower the pressure in the deep sand stratum beneath the center of the excavation, 76 ft would have required a total discharge of about 38,000 gpm (Fig. 9). To produce the required drawdown (82 ft) beneath the canal end gate bay by pumping 36 wells at the same discharge would result in a drawdown of about 91 ft beneath the center of the excavation, as shown in Table 4. For this drawdown the required discharge from Fig. 9 is 45,000 gpm or 1,250 gpm per well. This value compares favorably with the 1,230 gpm per well in Table 4. The pressure relief system has adequate capacity to intercept this flow and pump it from the deep sand stratum beneath the excavation.

SUMMARY AND CONCLUSIONS

On the basis of the pumping tests, analyses, and observed performance of the dewatering system, the following conclusions are noted.

1. The deep well system would satisfactorily reduce the hydrostatic pressure in the deep sands underlying the excavation. Lowering the hydrostatic head in the deep sand stratum did not have an appreciable effect on drying the excavation slopes and bottom of the excavation. The 30 temporary wells and 6 of the 8 permanent wells were adequate for controlling the head in the deep sands for river stages up to el-45.
2. A well flow of about 44,000 to 45,000 gpm is indicated for a river stage of el-45 with the excavation to final grade. This corresponds to an average flow of about 1,230 gpm per well with 36 wells being pumped.
3. The observed drawdown in the deep sand stratum was intermediate between that computed for a group of artesian wells with a line source at the near bank of the Mississippi River and for a ring source of seepage having a radius of 2,000 ft. In general, the flow intercepted by the landward portion of the pressure relief system is greater than that computed assuming a line source of seepage at the Mississippi River. This is attributed, in part, to the greater thickness of the pervious sand stratum landward from the dewatering system.
4. The average permeability of the deep sand stratum is about 700×10^{-4} cm per sec.
5. The three-stage wellpoint system installed on the slopes satisfactorily lowered the ground water level in the slopes and in the bottom of the excavation. The maximum discharge per stage of this system was about 120 gpm. Although the exact value of the permeability of the silt stratum could not be determined from the piezometric and wellpoint discharge data, it is believed that the overall horizontal permeability of the silt stratum is about 1.3×10^{-4} cm per sec.

6. The observed wellpoint discharges were slightly greater than those computed in design, however, the wellpoint system performed satisfactorily since ample allowance was made in designing the system so that it could adequately handle flows considerably greater than those computed in design.

ACKNOWLEDGMENTS

The Port Allen Lock was designed by the United States Army Corps of Engineer Division, Lower Mississippi Valley, assisted by the Corps of Engineer Waterways Experiment Station, Vicksburg, Mississippi. It was constructed under the supervision of the New Orleans District, Corps of Engineers. The pumping tests on the dewatering system were performed by representatives of the Independent Wellpoint Corporation, the Lower Mississippi Valley Division, and the New Orleans District.

Journal of the
SOIL MECHANICS AND FOUNDATIONS DIVISION
Proceedings of the American Society of Civil Engineers

STRESS CONDITIONS IN TRIAXIAL COMPRESSION

By A. Balla[1]

SYNOPSIS

A new solution is developed for the stress conditions in a cylindrical test specimen with any length-diameter ratio and subjected to axial and radial external loads. The influence of end restraint, exerted by stiff loading plates with and degree of roughness, is considered by introduction of a simplified roughness function. Numerical solutions are presented for a test specimen with a length-diameter ratio of 2.0 and for maximum roughness of the loading plates.

SOLUTION OF STRESS CONDITIONS IN TRIAXIAL COMPRESSION

Triaxial Compression Test as One of the Problems of the Theory of Elasticity.—Among the tests executed in soil mechanics laboratories, a rather important place is taken by the investigations used to determine the shearing strength of the soil. The shearing strength of the soil was formerly determined by a shearing test, but recently the triaxial compression test is more and more gaining ground and plays an increasingly important role. From the theoretical point of view as well as in respect of the practical application of the results obtained in the laboratory, a very interesting problem arises; that is, what stresses and deformations occur in the test specimen during the test? The present paper deals with this problem. In full knowledge of the stress specimen applied in the triaxial test, two questions, of considerable importance from the experimental point of view, require elucidation: How is the result of the test affected by the slenderness of the specimen and how by the roughness of the loading plate?

Note.—Discussion open until May 1, 1961. To extend the closing date one month, a written request must be filed with the Executive Secretary, ASCE. This paper is part of the copyrighted Journal of the Soil Mechanics Division, Proceedings of the American Society of Civil Engineers, Vol. 86, No. SM 6, December, 1960.

1 Asst. Prof., Tech. Univ., Budapest, Hungary.

As an introduction to our considerations we wish to examine the boundary conditions induced by the shape of the test specimen, by the manner of the transmission of the external load, and by the deformations.

The test specimen used in a triaxial compression test is of cylindrical form with its axis in a vertical position. The top and bottom surfaces of the test specimen communicate with a rigid, rough loading plate. The vertical external loading force is applied upon the upper loading plate in the middle of the latter; that is, in the center line of the test specimen, while at the bottom surface there arises a reacting force of identical value, but of opposed sense.

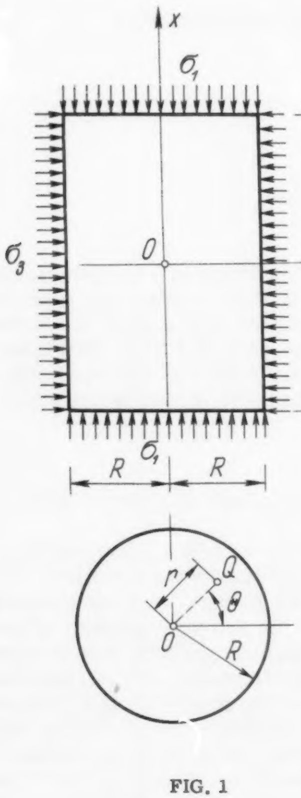

FIG. 1

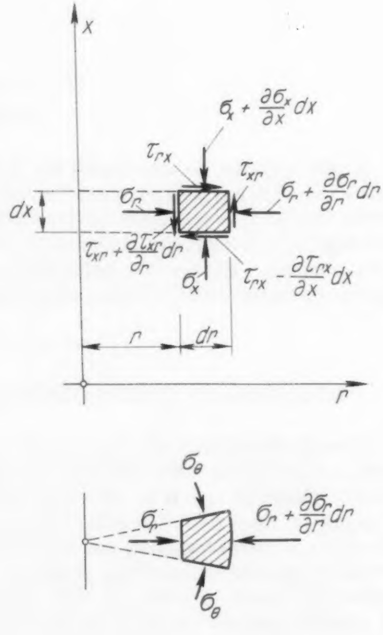

FIG. 2

On the lateral surface of the test specimen there acts an evenly distributed horizontal and radial lateral pressure. As manifested by the shape of the test specmen and by the character of the loads, the stress conditions are in axial symmetry (Fig. 1). Tangential stresses do not act on the mantle surface of the specimen. Because of the rigidity of the loading plates, the top and bottom surfaces of the test specimen are displaced under the influence of the load paralleling them; they are not deformed. The lateral surface of the test specimen can undergo arbitrary deformations.

Thus the solution of the stress conditions must satisfy all boundary conditions.

The problem will be discussed on the basis of the theory of elasticity in a cylindrical coordinate system (Fig. 1).

Basic Relationships of the Theory of Elasticity.—The starting point for the theory of elasticity is shown in Fig. 2. In case of axial symmetry and disregarding the dead weight, the stresses acting upon the elementary particles of the specimen satisfy the following equations of equilibrium:

$$\frac{\partial \sigma_r}{\partial r} + \frac{\partial \tau}{\partial x} + \frac{\sigma_r - \sigma_\theta}{r} = 0 \quad \ldots\ldots\ldots\ldots\ldots \quad (1)$$

and

$$\frac{\partial \tau}{\partial r} + \frac{\partial \sigma_x}{\partial x} + \frac{\tau}{r} = 0 \quad \ldots\ldots\ldots\ldots\ldots\ldots \quad (2)$$

in which σ_x, σ_r and σ_θ are the normal stresses acting in point Q; τ is the shearing stress acting in point Q; and x, r, and θ denote the cylindrical coordinates determining the location in the test specimen of the arbitrary point Q.

The geometrical equations are

$$\epsilon_x = \frac{\partial \xi}{\partial x} \quad \ldots\ldots\ldots\ldots\ldots\ldots\ldots \quad (3a)$$

$$\epsilon_r = \frac{\partial \rho}{\partial r} \quad \ldots\ldots\ldots\ldots\ldots\ldots\ldots \quad (3b)$$

$$\epsilon_\theta = \frac{\rho}{r} \quad \ldots\ldots\ldots\ldots\ldots\ldots\ldots\ldots \quad (3c)$$

and

$$\gamma = \frac{\partial \xi}{\partial r} + \frac{\partial \rho}{\partial x} \quad \ldots\ldots\ldots\ldots\ldots\ldots \quad (3d)$$

in which ϵ_x, ϵ_r, and ϵ_θ are the specific longitudinal variations occurring in point Q; ξ and ρ are the displacement of point Q in the x and r directions; and γ is the angular displacement occurring in point Q.

The solution must also satisfy the so-called equations of compatibility.

In the case of axially symmetrical stress conditions a so-called stress function can be noted. The stresses deduced from the stress function must satisfy the equations of equilibrium as well as the equations of compatibility relative to the compatibility of the deformations.

The stress function satisfying the equations of equilibrium and compatibility, ϕ, satisfies the following differential equation:

$$\left(\frac{\partial^2}{\partial x^2} + \frac{\partial^2}{\partial r^2} + \frac{1}{r}\frac{\partial}{\partial r}\right)\left(\frac{\partial^2}{\partial x^2} + \frac{\partial^2}{\partial r^2} + \frac{1}{r}\frac{\partial}{\partial r}\right)\phi = \nabla^2 \nabla^2 \phi = 0 \quad \ldots\ldots \quad (4)$$

in which ∇^2 is the differential operator.

The stress and deformation components can be expressed by the stress functions

$$\sigma_r = \frac{\partial}{\partial x}\left[\mu \nabla^2 \phi - \frac{\partial^2 \phi}{\partial r^2}\right] \quad \ldots\ldots\ldots\ldots\ldots \quad (5)$$

$$\sigma_x = \frac{\partial}{\partial x}\left[(2-\mu)\nabla^2\phi - \frac{\partial^2\phi}{\partial x^2}\right] \qquad (6)$$

$$\sigma_\theta = \frac{\partial}{\partial x}\left[\mu\nabla^2\phi - \frac{1}{r}\frac{\partial^2\phi}{\partial r^2}\right] \qquad (7)$$

$$\tau = \frac{\partial}{\partial r}\left[(1-\mu)\nabla^2\phi - \frac{\partial^2\phi}{\partial x^2}\right] \qquad (8)$$

$$\xi = \frac{1+\mu}{E}\left[2(1-\mu)\nabla^2\phi - \frac{\partial^2\phi}{\partial x^2}\right] \qquad (9)$$

and

$$\rho = -\frac{1+\mu}{E}\frac{\partial^2\phi}{\partial x\,\partial r} \qquad (10)$$

in which μ is Poisson's ratio and E is the modulus of elasticity.

The Stress Function Constituting the Solution of the Problem.—The solutions of the partial differential equation of the fourth degree (Eq. 4) can be constituted by certain polynomes as well as by the products of Bessel's function and expressions consisting of sine or cosine functions. The total solution is their sum.

On account of the conditions postulated by symmetry, x can figure in the polynomes with an uneven exponent and r with an even exponent, the polynomes, however, can be of any degree.

To express the stress function which constitutes the solution is, consequently, synonymous with the following problem: Polynomes of what degree must be added so as to obtain an adequate number of unknown coefficients in order to satisfy the boundary conditions and, at the same time, not to obtain too intricate a relationship?

On the basis of such considerations, taking certain symmetry conditions already into account and using suitable symbols, we shall start from the following stress function:

$$\begin{aligned}\phi = \sigma_1 \frac{1}{30}\frac{1}{1+\mu}&\left[5(1-2\mu)x^3 + 15\mu x r^2\right]\\ &+\left[2x^3 - 3xr^2\right]F + \left[x^3 + xr^2\right]G\\ &+\left[8x^5 - 40x^3r^2 + 15xr^4\right]C + \left[2x^5 - x^3r^2 - 3xr^4\right]D\\ &+\left[A\,J_0\left(ik\frac{r}{R}\right) + B\,r\,J_1\left(ik\frac{r}{R}\right)\right]\sin\frac{k}{R}x \qquad (11)\end{aligned}$$

in which F, G, C, D, A, R, and B are coefficients; J_0 (ir) is Bessel's function of the zero order with imaginary argument; R denotes the radius of the cylindrical test specimen; and J_1 (ir) is Bessel's function of the first order with imaginary argument.

In the stress function

$$J_0\left(ik\frac{r}{R}\right) = 1 + \frac{\left(\frac{k}{2R}r\right)^2}{1!^2} + \frac{\left(\frac{k}{2R}r\right)^4}{2!^2} + \ldots \qquad (12)$$

and

$$J_1\left(ik\,\frac{r}{R}\right) = i\,\frac{k}{2R}\,r\left[1 + \frac{\left(\frac{k}{2R}\,r\right)^2}{1\cdot2\cdot1} + \frac{\left(\frac{k}{2R}\,r\right)^4}{1\cdot2\cdot3\cdot1\cdot2} + \ldots\right] \ldots \quad (13)$$

It should be emphasized that the solution in Eq. 11 is not an exclusive one; adding polynomes

$$\phi_7 = a_7\,x^7 + b_7\,x^5\,r^2 + C_7\,x^3\,r^4 + d_7\,x\,r^6 \quad \ldots\ldots\ldots \quad (14a)$$

and

$$\phi_9 = a_9\,x^9 + b_9\,x^7\,r^2 + C_9\,x^5\,r^4 + d_9\,x^3\,r^6 + e_9\,x\,r^8 \quad \ldots \quad (14b)$$

or other polynomes of a similar form, in which, however, the coefficients must be in the relationships as indicated in Eq. 4, further stress functions are obtained, which are more involved than Eq. 11. In these equations a_n, b_n and so on are coefficients of Fournier's series.

Stress and Deformation Components.—By means of Eqs. 5 through 10, the expressions of stresses and deformations can be deduced from the stress function, Eq. 11:

$$\sigma_r = 6\,F + (10\,\mu - 2)\,G + 60\left(4\,x^2 - 3\,r^2\right)C + \left[6\,(1 + 18\,\mu)\,x^2 + 18(2 - 3\,\mu)\,r^2\right]D - \left\{A\left[J_0\left(ik\,\frac{r}{R}\right) - \frac{R}{k}\,\frac{1}{r}\,\frac{1}{i}\,J_1\left(ik\,\frac{r}{R}\right)\right] + i\,B\left[(1 - 2\,\mu)\,\frac{R}{k}\,J_0\left(ik\,\frac{r}{R}\right) + r\,\frac{1}{i}\,J_1\left(ik\,\frac{r}{R}\right)\right]\right\}\left(\frac{k}{R}\right)^3 \cos\frac{k}{R}\,x \quad \ldots \quad (15)$$

$$\sigma_x = \sigma_1 - 12\,F + (14 - 10\,\mu)\,G - 240\left[2\,x^2 - r^2\right]C + \left[(96 - 108\,\mu)\,x^2 - (102 - 54\,\mu)\,r^2\right]D + \left\{A\,J_0\left(ik\,\frac{r}{R}\right) + i\,B\left[2\,(2 - \mu)\,\frac{R}{k}\,J_0\left(ik\,\frac{r}{R}\right) + r\,\frac{1}{i}\,J_1\left(ik\,\frac{r}{R}\right)\right]\right\}\left(\frac{k}{R}\right)^3 \cos\frac{k}{R}\,x \quad \ldots \quad (16)$$

$$\sigma_\theta = 6\,F + (10\,\mu - 2)\,G + 60\left[4\,x^2 - r^2\right]C + \left[6\,(1 + 18\,\mu)\,x^2 + 6\,(2 - 9\,\mu)\,r^2\right]D - \left\{A\,\frac{R}{k}\,\frac{1}{r}\,\frac{1}{i}\,J_1\left(ik\,\frac{r}{R}\right) + i\,B\,(1 - 2\,\mu)\,\frac{R}{k}\,J_0\left(i\,k\,\frac{r}{R}\right)\right\}\left(\frac{k}{R}\right)^3 \cos\frac{k}{R}\,x \quad \ldots\ldots\ldots\ldots\ldots \quad (17)$$

$$\tau = 480\,C\,x\,r - (96 - 108\,\mu)\,D\,x\,r + \left\{A\,\frac{1}{i}\,J_1\left(ik\,\frac{r}{R}\right) + i\,B\left[2(1 - \mu)\,\frac{R}{k}\,\frac{1}{i}\,J_1\left(ik\,\frac{r}{R}\right) + r\,J_0\left(ik\,\frac{r}{R}\right)\right]\right\}\left(\frac{k}{R}\right)^3 \sin\frac{k}{R}\,x \quad \ldots\ldots \quad (18)$$

$$\frac{1}{1+\mu} E\xi = \left[\frac{1}{1+\mu}\sigma_1 - 12 F + (14 - 20\mu) G\right] x - 80\left[2x^3 - 3xr^2\right] C$$

$$+ \left[(32 - 72\mu) x^3 - (102 - 108\mu) x r^2\right] D + \left\{A J_0\left(ik\frac{r}{R}\right)\right.$$

$$\left. + i B\left[4(1-\mu)\frac{R}{k} J_0\left(ik\frac{r}{R}\right) + r\frac{1}{i} J_1\left(ik\frac{r}{R}\right)\right]\right\}\left(\frac{k}{R}\right)^2 \sin\frac{k}{R} x \quad \ldots \quad (19)$$

and

$$\frac{1}{1+\mu} E\rho = \frac{\mu}{1+\mu}\sigma_1 r + (6F - 2G) r + 60\left[4x^2 r - r^3\right] C$$

$$+ 6\left[x^2 r + 2r^3\right] D$$

$$- \left\{A\frac{1}{i} J_1\left(ik\frac{r}{R}\right) + i B r J_0\left(ik\frac{r}{R}\right)\right\}\left(\frac{k}{R}\right)^2 \cos\frac{k}{R} x \quad \ldots\ldots\ldots \quad (20)$$

Determination of the Constants on the Basis of Boundary Conditions.—In the stress function, Eq. 11, as well as in the expressions of stresses and deformations Eqs. 15 through 20, there are seven constants: A, B, C, D, F, G, and k. The values of these constants are determined on the basis of the boundary conditions.

First Boundary Condition.—The top and bottom surfaces of the cylinder remain plane even after deformation and are displaced parallel with themselves; that is, at point $x = H$ the value of ξ is independent of r. This is possible only if in Eq. 19 the multiplication factors of the members containing r are equal to zero:

$$\left[240\,C - (102 - 108\,\mu)\,D\right] x\,r^2 = 0 \quad \ldots\ldots\ldots\ldots \quad (21a)$$

and

$$\sin\frac{k}{R} x = 0 \quad \ldots\ldots\ldots\ldots\ldots\ldots\ldots \quad (21b)$$

From Eqs. 21

$$C = \frac{1}{40}(17 - 18\,\mu)\,D \quad \ldots\ldots\ldots\ldots\ldots\ldots \quad (22a)$$

and

$$k\frac{H}{R} = n\,\pi \quad \ldots\ldots\ldots\ldots\ldots\ldots\ldots\ldots\ldots \quad (22b)$$

in which H is the half height of the specimen and n = 1, 2, 3. . . etc. are arbitrary positive integers.

It follows that the products of the multiplication of Bessel's functions by sine or cosine occur infinitely often, and all their coefficients are different

A_n, B_n. Substituting Eqs. 22 and 23, Eqs. 15 through 20 take the following form:

$$\sigma_r = 6\,F + (10\,\mu - 2)\,G + \left[108\,x^2 - \frac{1}{2}(81 - 54\,\mu)\,r^2\right]D$$

$$- \sum_{n=1}^{\infty} \Big\{ A_n \left[J_0\left(i\,n\,\pi\,\frac{R}{H}\frac{r}{R}\right) - \frac{H}{n\,\pi}\,\frac{1}{r}\,\frac{1}{i}\,J_1\left(i\,n\,\pi\,\frac{R}{H}\,\frac{r}{R}\right)\right]$$

$$+ i\,B_n\left[(1-2\,\mu)\,\frac{H}{n\,\pi}\,J_0\left(i\,n\,\pi\,\frac{R}{H}\frac{r}{R}\right) + r\,\frac{1}{i}\,J_1\left(i\,n\,\pi\,\frac{R}{H}\frac{r}{R}\right)\right]\Big\}$$

$$\left(\frac{n\,\pi}{H}\right)^3 \cos n\,\pi\,\frac{x}{H} \quad \ldots\ldots\ldots\ldots \quad (23)$$

$$\sigma_x = \sigma_1 - 12\,F + (14 - 10\,\mu)\,G - 54\left[2(1-\mu)\,x^2 + \mu\,r^2\right]D$$

$$+ \sum_{n=1}^{\infty} \Big\{ A_n\,J_0\left(i\,n\,\pi\,\frac{R}{H}\frac{r}{R}\right)$$

$$+ i\,B_n\left[2(2-\mu)\,\frac{H}{n\,\pi}\,J_0\left(i\,n\,\pi\frac{R}{H}\frac{r}{R}\right) + r\,\frac{1}{i}\,J_1\left(i\,n\,\pi\,\frac{R}{H}\,\frac{r}{R}\right)\right]\Big\}$$

$$\left(\frac{n\,\pi}{H}\right)^3 \cos n\,\pi\,\frac{x}{H} \quad \ldots\ldots\ldots\ldots \quad (24)$$

$$\sigma_\theta = 6\,F + (10\,\mu - 2)\,G + 27\left[4\,x^2\,\frac{1}{2}\,(1 + 2\,\mu)\,r^2\right]D - \sum_{n=1}^{\infty}\Big\{A_n\,\frac{H}{n\,\pi}\,\frac{1}{r}\,\frac{1}{i}\,J_1$$

$$\left(i\,n\,\pi\,\frac{R}{H}\,\frac{r}{R}\right) + i\,B_n\,(1-2\,\mu)\,\frac{H}{n\,\pi}\,J_0\left(i\,n\,\pi\,\frac{R}{H}\frac{r}{R}\right)\Big\}\left(\frac{n\pi}{H}\right)^3 \cos n\,\pi\frac{x}{H} \ldots \quad (25)$$

$$\tau = 108\,(1 - \mu)\,D\,x\,r + \sum_{n=1}^{\infty}\Big\{A_n\,\frac{1}{i}\,J_1\left(i\,n\,\pi\,\frac{R}{H}\frac{r}{R}\right)$$

$$+ i\,B_n\left[2(1-\mu)\,\frac{H}{n\,\pi}\,\frac{1}{i}\,J_1\left(i\,n\,\pi\frac{R}{H}\frac{r}{R}\right) + r\,J_0\left(i\,n\,\pi\,\frac{R}{H}\frac{r}{R}\right)\right]\Big\}$$

$$\left(\frac{n\,\pi}{H}\right)^3 \sin n\,\pi\,\frac{x}{H} \quad \ldots\ldots\ldots\ldots \quad (26)$$

$$\frac{1}{1+\mu}\,E\xi = \frac{1}{1+\mu}\,\sigma_1\,x - 12\,F\,x + (14 - 20\,\mu)\,G\,x - 36\,D\,x^3$$

$$+ \sum_{n=1}^{\infty}\Big\{A_n\,J_0\left(i\,n\,\pi\,\frac{R}{H}\frac{r}{R}\right) + i\,B_n\left[4(1-\mu)\,\frac{H}{n\,\pi}\,J_0\left(i\,n\,\pi\,\frac{R}{H}\frac{r}{R}\right)\right.$$

$$\left. + r\,\frac{1}{i}J_1\left(i\,n\,\pi\frac{R}{H}\,\frac{r}{R}\right)\right]\Big\}\left(\frac{n\,\pi}{H}\right)^2 \sin n\,\pi\,\frac{x}{H} \quad \ldots\ldots\ldots\ldots \quad (27)$$

and

$$\frac{1}{1+\mu}\,E\,\rho = -\frac{\mu}{1+\mu}\,\sigma_1\,r + 6\,F\,r - 2\,G\,r + 27\left[4\,(1-\mu)\,x^2\,r\right.$$

$$\left.-\frac{1}{2}\,(1-2\,\mu)\,r^3\right]D - \sum_{n=1}^{\infty}\left\{A_n\,\frac{1}{i}\,J_1\left(i\,n\,\pi\,\frac{R}{H}\,\frac{r}{R}\right)\right.$$

$$\left.+\,i\,B_n\,r\,J_0\left(i\,n\,\pi\,\frac{R}{H}\,\frac{r}{R}\right)\right\}\left(\frac{n\,\pi}{H}\right)^2\cos n\,\pi\,\frac{x}{H} \;\ldots\ldots\ldots\ldots\ldots\ldots \quad (28)$$

Second Boundary Condition.—The horizontal radial stress at the mantle surface is constant and equal to σ_3.

In case of $r = R$,

$$(\sigma_r)_{r=R} = \sigma_3 \;\ldots\ldots\ldots\ldots\ldots\ldots\ldots \quad (29)$$

On the basis of this condition, with application of Fourier's series, we obtain

$$x^2 = \frac{a_o}{2} + \sum_{n=1}^{\infty} a_n \cos n\,\pi\,\frac{x}{H} \;\ldots\ldots\ldots\ldots\ldots\ldots \quad (30a)$$

$$\frac{D}{2}\,(81 - 54\,\mu)\,R^2 - 36\,D\,H^2 - 6\,F - (10\,\mu - 2)\,G + \sigma_3 = 0 \;\ldots\ldots \quad (30b)$$

and

$$\left(\frac{H}{n\,\pi}\right)^3\frac{2\,H}{n\,\pi}\,108\,D\cos n\,\pi = \frac{n\,\pi}{2\,H}\left\{A_n\left[J_0\left(i n \pi\,\frac{R}{H}\right)\right.\right.$$

$$\left.-\frac{1}{n\pi}\,\frac{H}{R}\,\frac{1}{i}\,J_1\left(i n \pi\,\frac{R}{H}\right)\right] + i\,B_n\,R\left[(1-2\,\mu)\,\frac{1}{n\pi}\,\frac{H}{R}\,J_0\left(i n \pi\,\frac{R}{H}\right)\right.$$

$$\left.\left.+\frac{1}{i}\,J_1\left(i n \pi\,\frac{R}{H}\right)\right]\right\} \;\ldots\ldots\ldots\ldots \quad (30c)$$

Third Boundary Condition.—The value of the tangential stresses at the mantle surface is zero. At point $r = R$

$$\tau_{r=R} = 0 \;\ldots\ldots\ldots\ldots\ldots\ldots\ldots \quad (31)$$

$$x = \sum_{n=1}^{\infty} b_n \sin n\,\pi\,\frac{x}{H} \;\ldots\ldots\ldots\ldots\ldots \quad (32)$$

and

$$\left(\frac{H}{n\,\pi}\right)^3\frac{2\,H}{n\,\pi}\,108\,D\cos n\,\pi = \frac{1}{1=\mu}\,\frac{1}{R}\left\{A_n\,\frac{1}{i}J_1\left(i n \pi\,\frac{R}{H}\right)\right.$$

$$\left.+\,i\,B_n\,R\left[2\,(1-\mu)\,\frac{1}{n\,\pi}\,\frac{H}{R}\,\frac{1}{i}\,J_1\left(i\,n\,\pi\,\frac{R}{H}\right) + J_0\left(i n \pi\,\frac{R}{H}\right)\right]\right. \;\ldots \quad (33)$$

Comparing Eq. 33 with Eq. 30c we obtain the relationship between A_n and B_n:

$$i\,B_n\,R = \frac{(1-\mu)\,\dfrac{i\,J_0\,(i\,n\,\pi\,R/H)}{J_1\,(i\,n\,\pi\,R/H)} - (3-\mu)\,\dfrac{1}{n\pi}\,\dfrac{H}{R}}{(1-\mu)\left[\left(\dfrac{2}{n\pi}\dfrac{H}{R}\right)^2 - 1\right] + \left(1+3\,\mu - 2\,\mu^2\right)\dfrac{1}{n\pi R}\dfrac{H}{R}\,\dfrac{i\,J_0\,(i n\pi R/H)}{J_1\,(i n\pi R/H)}}\,A_n \quad . . \quad (34)$$

With simplified notation:

$$i\,B_n\,R = U_n\,A_n \quad . . . . \quad (35)$$

Substituting this expression into Eq. 33 and introducing the notation

$$V_n = 1 - U_n\left[2\,(1-\mu)\,\frac{1}{n\,\pi}\,\frac{H}{R} + \frac{i\,J_0\,(i\,n\,\pi\,R/H)}{J_1\,(i\,n\,\pi\,R/H)}\right] \quad . . . . \quad (36)$$

we obtain

$$A_n = \frac{216}{\pi}\,(1-\mu)\left(\frac{H}{n\,\pi}\right)^3 H\,R\,\frac{\cos n\,\pi}{\frac{1}{i}\,J_1\,(i n\pi\,R/H)\;n\,V_n}\;D \quad . . \quad (37)$$

Fourth Boundary Condition.—The external force acting upon the loading plate and the resultant of the vertical stresses transmitted from the plate to the test specimen are equal; that is, there exists an equilibrium:

$$\int_0^{2\pi}\int_0^{R} \sigma_{x_{\,x=H}}\; r\,dr\,d\theta - P = \int_0^{2\pi}\int_0^{R} \sigma_{x_{\,x=H}}\; r\,dr\,d\theta - R^2\,\pi\,\sigma_1 = 0 \quad . . . . \quad (38)$$

in which $\sigma_1 = P/R^2 n$, the average stress acting upon the loading plate.

We then obtain:

$$\int_0^{2\pi}\int_0^{R} \sigma_{x_{\,x=H}}\; r\,dr\,d\theta = R^2\,\pi\,\sigma_1 + \pi\,R^2\left\{- 12\,F + (14 - 10\,\mu)\,G\right.$$

$$\left. - 54\left[2(1-\mu)\,H^2 + \mu\,\frac{R}{2}^2\right] D + 2\,\frac{216}{\pi^2}\,(1-\mu)\,H^2 D \sum_{n=1}^{\infty}\frac{\cos^2 n\,\pi}{n^2}\right. \quad . . \quad (39)$$

and

$$- 12\,F + (14 - 10\,\mu)\,G - \left[108\,(1-\mu)\,H^2 + 27\,\mu\,R^2\right] D$$

$$+ 72\,(1-\mu)\,H^2\,D = 0 \quad . . . . \quad (40)$$

From Eqs. 30 and 40, the values of F and G can be expressed as

$$F = \frac{\left[(567 - 729\,\mu) - \left(432 + 72\,\mu - 360\,\mu^2\right)(H/R)^2\right] R^2\,D + (14 - 10\,\mu)\,\sigma_3}{60\,(1+\mu)} \quad . . \quad (41)$$

$$G = \frac{\left[(81 - 27\mu) - 36(1+\mu)\ (H/R)^2\right] R^2 D + 2\sigma_3}{10(1+\mu)} \quad \ldots\ldots \quad (42)$$

in which σ_3 is the lateral pressure acting upon the mantle surface of the cylinder.

Thus the seven original unknowns can be expressed by a single coefficient, D.

Consideration of the Roughness of the Loading Plate.—In order to determine the constant D which appears in the equations which constitute the solution of the stress conditions, a certain boundary condition must be introduced or an assumption must be accepted. In contradiction with the conditions discussed previously, the condition which is going to be applied here is theoretically not a close-limit condition but a disputable one.

This constant should, in the writer's opinion, be applied for the characterization of the roughness of the loading plate as it is evident that it exerts some influence on the stresses and deformations, an influence that has been disregarded up to now.

The assumption to be applied here must, in any case, be regarded as just an approximation because we have no knowledge of experimental results concerning conditions of roughness on the loading plate and the relative displacements occurring on it and because, on the other hand, the introduction of more exact values would present mathematical difficulties. Therefore, one must endeavor to operate with an assumption that is mathematically simple, but nevertheless reflects actual conditions to a satisfactory extent.

Let the roughness of the loading plate be characterized by the coefficient of the surface friction f. From the point of view of the theoretical solution, it is not essential whether the numerical value of the coefficient of surface friction is known or not; it is sufficient to stipulate that the numerical value of the coefficient of the surface friction should very from $f = 0$ to $f = f_{max}$.

The assumption on which we wish to determine the constant D is this: The radial horizontal displacements of the peripheral points situated at the end—surface of the test specimen change inversely with the coefficient of the surface friction which is characteristic of the roughness of the loading plate (that is, they change with the ratio of the radial integral—resultant—of the shear stresses and normal stresses), and as a first approximation, one can take this change to be linear. If the loading plate is perfectly smooth and frictionless ($f = 0$), then the displacement attains its maximum value$\left(\rho_{H,R} = \rho_{H,R\,max}\right)$; if the coefficient of the surface friction attains its maximum value, the constraint will also be greatest, and this will manifest itself through the fact that the points of the periphery will execute no outward movement and will remain in their place $\left(\rho_{HR} = 0\right)$.

This assumption is in accordance with the observations made in the course of the tests. In this case:

$$f = f_{max}\left[1 - \frac{\rho_{HR}}{\rho_{HR\,max}}\right] \quad \ldots\ldots\ldots\ldots \quad (43)$$

Let us introduce the factor

$$\psi = \frac{f}{f_{max}} = 1 - \frac{\rho_{HR}}{\rho_{HR\,max}} \quad \ldots\ldots\ldots\ldots \quad (44)$$

and let us determine the value of $\rho_{H,R\,max}$. If the loading place is perfectly smooth, the vertical and radial directions represent everywhere chief stress directions and $\sigma_x = \sigma_1$, $\sigma_r = \sigma_\theta = \sigma_3$, and $\tau = 0$.

In this case

$$E\,\rho_{H,R\,max} = -\mu\,\sigma_1 R + (1-\mu)\,\sigma_3 R \quad \ldots\ldots \quad (45)$$

Substituting values x = H and r = R into Eq. 28:

$$\begin{aligned} E\,\rho_{H,R} &= \mu\,\sigma_1 R + (1-\mu)\,\sigma_3 R \\ &+ D R^3 \frac{1}{2} \Big\{ 27(3-5\mu) - 72\left(1-\mu^2\right)(H/R)^2 \\ &+ 216\left(1-\mu^2\right)(H/R)^2 - 27\left(1-\mu-2\mu^2\right) \\ &- \frac{432}{\pi^2}\left(1-\mu^2\right)(H/R)^2 - \sum_{n=1}^{\infty} \frac{\cos^2 n\pi}{n^2}\,\frac{1}{V_n}\left[1 - U_n \frac{i J_0(i n\pi R/H)}{J_1(i n\pi R/H)}\right] \end{aligned} \quad \ldots \quad (46)$$

Let us now introduce the notation

$$K = \sum_{n=1}^{\infty} \frac{\cos^2 n\pi}{n^2}\,\frac{1}{V_n}\left[1 - U_n \frac{i J_0(i n\pi R/H)}{J_1(i n\pi R/H)}\right] \quad \ldots\ldots\ldots\ldots \quad (47)$$

Substituting Eqs. 45 and 46 into Eq. 43 and considering the notations quoted in Eqs. 44 and 47, the following final result is obtained:

$$D = \psi\,\frac{1}{9}\,\frac{\frac{\mu}{1-\mu}\,\sigma_1 - \sigma_3}{3(1-\mu) + 8(1+\mu)\left(1 - \frac{3}{\pi^2}K\right)(H/R)^2}\,\frac{1}{R^2} \quad \ldots\ldots \quad (48)$$

Thus all constants in the equations are determined.

Stress and Deformations.—The value of D having been determined (Eq. 48) the stresses and deformations are as follows:

$$\begin{aligned} \sigma_x = \sigma_1 &- \left(\frac{\mu}{1-\mu}\,\sigma_1 - \sigma_3\right)\psi\,\frac{1}{3(1-\mu) + 8(1+\mu)\left(1 - \frac{3K}{\pi^2}\right)\left(\frac{H}{R}\right)^2} \Bigg\{ -3\mu \\ &- 4(1-\mu)\left(\frac{H}{R}\right)^2 + 12(1-\mu)\left(\frac{H}{R}\right)^3\left(\frac{x}{H}\right)^2 + 6\mu\left(\frac{r}{R}\right)^2 \\ &- \frac{24}{\pi}(1-\mu)\frac{H}{R}\sum_{n=1}^{\infty} \frac{\cos n\pi}{n V_n}\cdot\frac{1}{\frac{1}{i} J_1(i n\pi R/H)} \\ &\left[\left(1 - U_n\, 2(2-\mu)\,\frac{1}{n\pi}\frac{H}{R}\right) J_0\left(i n\pi \frac{R}{H}\frac{r}{R}\right)\right. \\ &\left. - U_n \frac{r}{R}\,\frac{1}{i}\,J_1\left(i n\pi \frac{R}{H}\frac{r}{R}\right)\right] \cos n\pi \frac{x}{H} \Bigg\} \end{aligned} \quad \ldots\ldots\ldots\ldots \quad (49)$$

$$\sigma_r = \sigma_3 + \left(\frac{\mu}{1-\mu}\,\sigma_1 - \sigma_3\right)\,\psi\,\frac{1}{3\,(1-\mu) + 8\,(1+\mu)\,\left(1 - \frac{3\,K}{\pi^2}\right)\left(\frac{H}{R}\right)^2}$$

$$\left\{\frac{3}{2}\,(3-2\,\mu) \;\; -4\,\left(\frac{H}{R}\right)^2 + 12\left(\frac{H}{R}\right)^2\left(\frac{x}{H}\right)^2 - \frac{3}{2}\;\;(3-2\,\mu)\,\left(\frac{r}{R}\right)^2\right.$$

$$-\,\frac{24}{\pi}\,(1-\mu)\,\frac{H}{R}\sum_{n=1}^{\infty}\,\frac{\cos n\,\pi}{n\,V_n}\;\;\frac{1}{\frac{1}{i}\,J_1\left(i\,n\,\pi\,\frac{R}{H}\,\frac{r}{R}\right)}$$

$$\left[\left(1 - U_n\,(1-2\,\mu)\,\frac{1}{n\,\pi}\,\frac{H}{R}\right)\,J_0\left(i\,n\,\pi\,\frac{R}{H}\,\frac{r}{R}\right)\right.$$

$$\left.\left. -\left(\frac{1}{n\,\pi}\,\frac{H}{R}\,\frac{R}{r} + U_n\,\frac{r}{R}\right)\,\frac{1}{i}\,J_1\left(i\,n\,\pi\,\frac{R}{H}\,\frac{r}{R}\right)\right]\;\cos n\,\pi\,\frac{x}{H}\right\}\;\ldots\ldots\ldots \quad (50)$$

$$\sigma_\theta = \sigma_3 + \left(\frac{\mu}{1-\mu}\,\sigma_1 - \sigma_3\right)\psi\;\frac{1}{3\,(1-\mu) + 8\,(1+\mu)\;\left(1 - \frac{3\,K}{\pi^2}\right)\left(\frac{H}{R}\right)^2}\;\left\{\frac{3}{2}\,(3-2\,\mu)\right.$$

$$-4\left(\frac{H}{R}\right)^2 + 12\left(\frac{H}{R}\right)^2\left(\frac{x}{H}\right)^2 - \frac{3}{2}\,(1+2\,\mu)\,\left(\frac{r}{R}\right)^2 - \frac{24}{\pi}\,(1-\mu)\,\frac{H}{R}\;\sum_{n=1}^{\infty}\frac{\cos n\,\pi}{n\,V_n}$$

$$\frac{1}{\frac{1}{i}\,J_1\left(i n \pi\,\frac{R}{H}\,\frac{r}{R}\right)}\;\left[-\,U_n\,(1-2\,\mu)\,\frac{1}{n\pi}\,\frac{H}{R}\,J_0\left(i n \pi\,\frac{R}{H}\frac{r}{R}\right)\right.$$

$$\left.\left. +\,\frac{1}{n\pi}\,\frac{H}{R}\,\frac{R}{r}\frac{1}{i}\,J_1\left(i\,n\,\pi\,\frac{R}{H}\,\frac{r}{R}\right)\right]\cos n\,\pi\,\frac{x}{H}\right\}\;\ldots\ldots\ldots\ldots\ldots\ldots \quad (51)$$

$$\tau = \left(\frac{\mu}{1-\mu}\sigma_1 - \sigma_3\right)\psi\,\frac{1}{3\,(1-\mu) + 8\,(1+\mu)\left(1 - \frac{3K}{\pi^2}\right)\left(\frac{H}{R}\right)^2}\;\left\{12(1-\mu)\,\frac{H}{R}\,\frac{x}{H}\,\frac{r}{R}\right.$$

$$-\,\frac{24}{\pi}\,(1-\mu)\,\frac{H}{R}\sum_{n=1}^{\infty}\,\frac{\cos n\pi}{n\,V_n}\;\;\frac{1}{\frac{1}{i}\,J_1\,(i n \pi\;R/H)}\;\left[U_n\,\frac{r}{R}\,J_0\;\left(i\,n\,\pi\,\frac{R}{H}\,\frac{r}{R}\right)\right.$$

$$\left.\left. -\left(1 - U_n\,2\,(1-\mu)\,\frac{1}{n\pi}\,\frac{H}{R}\right)\;\frac{1}{i}\,J_1\left(i\,n\,\pi\frac{R}{H}\,\frac{r}{R}\right)\right]\;\sin n\,\pi\,\frac{x}{H}\right\}\;\ldots\ldots\ldots \quad (52)$$

$$E\,\xi\,\frac{1}{H} = \frac{x}{H}\,\sigma_1 - 4\,\mu\,\frac{x}{H}\,\sigma_3 - (1+\mu)\,\left(\frac{\mu}{1-\mu}\;\sigma_1 - \sigma_3\right)$$

$$\psi\,\frac{1}{3\,(1-\mu) + 8\,(1+\mu)\,\left(1 - \frac{3\,K}{\pi^2}\right)\left(\frac{H}{R}\right)^2}\;\left\{6\,\mu\,\frac{1-\mu}{1+\mu}\;\frac{x}{H}\; - \frac{182}{45}\,\left(\frac{H}{R}\right)^2\left(\frac{x}{H}\right)\right.$$

$$+ 4\,\left(\frac{H}{R}\right)^2\left(\frac{x}{H}\right)^3 - \frac{24}{\pi}\,(1-\mu)\,\frac{H}{R}\;\sum_{n=1}^{\infty}\frac{\cos n\,\pi}{n\,V_n}\;\frac{1}{\frac{1}{i}\;J_1\,(i\,n\,\pi\;R/H)}\;\;\frac{1}{n\,\pi}$$

$$\left[\left(1 - U_n\,4\,(1-\mu)\,\frac{1}{n\pi}\;\frac{H}{R}\right)\,J_0\left(i\,n\,\pi\;\frac{R}{H}\,\frac{r}{R}\right)\right.$$

$$\left.\left. - U_n\,\frac{r}{R}\,\frac{1}{i}\;J_1\left(i\,n\,\pi\,\frac{R}{H}\;\frac{r}{R}\right)\right]\;\sin n\,\pi\;\frac{x}{H}\right\} \quad \ldots\ldots\ldots\ldots\ldots\ldots\ldots \quad (53)$$

$$E\,\rho\,\frac{1}{R} = -\,\mu\,\frac{r}{R}\,\sigma_1 + (1-\mu)\,\frac{r}{R}\;\sigma_3 - \;\frac{\mu}{1-\mu}\,\sigma_1 - \sigma_3$$

$$\psi\;\frac{1}{3\,(1-\mu) + 8\,(1+\mu)\left(1 - \frac{3\,K}{\pi^2}\right)\left(\frac{H}{R}\right)^2}$$

$$\left\{-\,\frac{3}{2}\;\;(3 - 5\,\mu)\;\frac{r}{R}\; + 4\left(1 - \mu^2\right)\,\left(\frac{H}{R}\right)^2\frac{r}{R}\; - 12\;\left(1-\mu^2\right)\left(\frac{H}{R}\right)^2\;\left(\frac{x}{H}\right)^2\left(\frac{r}{R}\right)\right.$$

$$+ \frac{3}{2}\;\left(1 - \mu - 2\;\mu^2\right)\,\left(\frac{r}{R}\right)^3 - \frac{24}{\pi}\,(1-\mu)\;\frac{H}{R}\;\,(1+\mu)\;\frac{H}{R}\sum_{n=1}^{\infty}\;\frac{\cos n\,\pi}{n\,V_n}$$

$$\frac{1}{\frac{1}{i}\;J_1\;(i\,n\;\pi\,R/H\,)}\;\frac{1}{n\,\pi}\;\left[U_n\;\frac{r}{R}\;J_0\left(i\;n\;\pi\;\frac{R}{r}\;\frac{r}{R}\right)\right.$$

$$\left.\left. -\,\frac{1}{i}J_1\left(i\;n\;\pi\;\frac{R}{H}\;\frac{r}{R}\right)\right]\;\;\cos n\;\pi\;\frac{x}{H}\right\} \quad \ldots\ldots\ldots\ldots\ldots\ldots\ldots \quad (54)$$

In Eqs. 34, 35, 36, and 37, the following abbreviations have been used:

$$U_n = \frac{(3-\mu)\,\frac{1}{n\,\pi}\;\frac{H}{R} - (1-\mu)\;\frac{i\,J_0\;(i\;n\;\pi\;R/H)}{J_1\;(i\;n\;\pi\;R/H)}}{(1-\mu)\;\left[4\left(\frac{1}{n\,\pi}\right)^2\left(\frac{H}{R}\right)^2 - 1\right] + \left(1 + 3\;\mu - 2\;\mu^2\right)\frac{1}{n\pi}\;\frac{H}{R}\;\frac{i\;J_0\;(i\,n\;\pi\;R/H)}{J_1\;(i\,n\;\pi\;R/H)}} \quad (55)$$

$$V_n = 1 - U_n \left[2(1-\mu) \frac{1}{n\pi} \frac{H}{R} + \frac{i\, J_0\,(i\, n\, \pi\; R/H)}{J_1\,(i\, n\, \pi\; R/H)} \right] \ldots\ldots\ldots\ldots\ldots \quad (56)$$

and

$$K = \sum_{n=1}^{\infty} \frac{1}{n^2} \frac{1}{V_n} \left[1 - U_n \frac{i\, J_0\,(i\, n\, \pi\; R/H)}{J_1\,(i\, n\, \pi\; R/H)} \right] \ldots\ldots\ldots\ldots\ldots \quad (57)$$

In order to simplify the computations, let us introduce some additional abbreviations.

$$Q = \frac{1}{3\,(1-\mu) + 8\,(1+\mu) \left(1 - \frac{3K}{\pi^2}\right) \left(\frac{H}{R}\right)^2} \ldots\ldots\ldots\ldots\ldots \quad (58)$$

$$F_{\sigma x} = \frac{\cos n\pi}{n\, V_n} \frac{1}{\frac{1}{i} J_1\,(i\, n\, \pi\; R/H)} \left[\left(1 - U_n\, 2\,(2-\mu) \frac{1}{n\pi} \frac{H}{R}\right) J_0 \left(i n \pi \frac{R}{H} \frac{r}{R}\right) \right.$$

$$\left. U_n \frac{r}{R} \frac{1}{i} J_1 \left(i\, n\, \pi \frac{R}{H} \frac{r}{R}\right) \right] \ldots\ldots\ldots\ldots\ldots \quad (59)$$

$$F_{\sigma r} = \frac{\cos n\pi}{n\, V_n} \frac{1}{\frac{1}{i} J_1\,(i\, n\, \pi\, R/H)} \left[\left(1 - U_n\,(1 - 2\mu) \frac{1}{n\pi} \frac{H}{R}\right) J_0 \left(i n \pi\, \frac{R}{H} \frac{r}{R}\right) \right.$$

$$\left. - \left(\frac{1}{n\pi} \frac{H}{R} \frac{R}{r} + U_n \frac{r}{R}\right) \frac{1}{i} J_1 \left(i\, n\, \pi\, \frac{R}{H} \frac{r}{R}\right) \right] \ldots\ldots\ldots \quad (60)$$

$$F_{\sigma \theta} = \frac{\cos n\pi}{n\, V_n} \frac{1}{\frac{1}{i} J_1\,(i\, n\, \pi\; R/H)} \left[- U_n\,(1 - 2\,\mu) \frac{1}{n\pi} \frac{H}{R} J_0 \left(i\, n\, \pi\, \frac{R}{H} \frac{r}{R}\right) \right.$$

$$\left. + \frac{1}{n\pi} \frac{H}{R} \frac{R}{r} \frac{1}{i} J_1 \left(i\, n\, \pi\, \frac{R}{H} \frac{r}{R}\right) \right] \ldots\ldots\ldots\ldots \quad (61)$$

$$F_{\tau} = \frac{\cos n\pi}{n\, V_n} \frac{1}{\frac{1}{i} J_1\,(i n \pi R/H)} \left[U_n \frac{r}{R} J_0 \left(i\, n\, \pi \frac{R}{H} \frac{r}{R}\right) \right.$$

$$\left. - \left(1 - U_n\, 2\,(1-\mu) \frac{1}{n\pi} \frac{H}{R}\right) \frac{1}{i} J_1 \left(i\, n\, \pi \frac{R}{H} \frac{r}{R}\right) \right] \ldots \quad (62)$$

$$F_{\xi} = \frac{\cos n\pi}{n^2\, V_n} \frac{1}{\frac{1}{i} J_1\,(i\, n\, \pi R/H)} \left[\left(1 - U_n\, 4\,(1-\mu) \frac{1}{n\pi} \frac{H}{R}\right) J_0 \left(i n \pi \frac{R}{H} \frac{r}{R}\right) \right.$$

$$\left. - U_n \frac{r}{R} \frac{1}{i} J_1 \left(i\, n\, \pi \frac{R}{H} \frac{r}{R}\right) \right] \ldots\ldots\ldots\ldots\ldots \quad (63)$$

$$F_\rho = \frac{\cos n\pi}{n^2 V_n} \cdot \frac{1}{\frac{1}{i} J_1 (i n \pi R/H)} \left[U_n \frac{r}{R} J_0 \left(i n \pi \frac{R}{H} \frac{r}{R} \right) \right.$$

$$\left. - \frac{1}{i} J_1 \left(i n \pi \frac{R}{H} \frac{r}{R} \right) \right] \quad \ldots\ldots\ldots\ldots\ldots\ldots\ldots \quad (64)$$

$$\phi_{\sigma x} = Q \left[-3\mu - 4(1-\mu)\left(\frac{H}{R}\right)^2 + 12(1-\mu)\left(\frac{H}{R}\right)^2 \left(\frac{x}{H}\right)^2 + 6\mu \left(\frac{r}{R}\right)^2 \right.$$

$$\left. - \frac{24}{\pi}(1-\mu)\frac{H}{R} \sum_{n=1}^{\infty} F_{\sigma x} \cos n\pi \frac{x}{H} \right] \quad \ldots\ldots\ldots \quad (65)$$

$$\phi_{\sigma r} = Q \left[\frac{3}{2}(3-2\mu) - 4\left(\frac{H}{R}\right)^2 + 12\left(\frac{H}{R}\right)^2 \left(\frac{x}{H}\right)^2 - \frac{3}{2}(3-2\mu)\left(\frac{r}{R}\right)^2 \right.$$

$$\left. - \frac{24}{\pi}(1-\mu)\frac{H}{R} \sum_{n=1}^{\infty} F_{\sigma r} \cos n\pi \frac{x}{H} \right] \quad \ldots\ldots\ldots \quad (66)$$

$$\phi_{\sigma\theta} = Q \left[\frac{3}{2}(3-2\mu) - 4\left(\frac{H}{R}\right)^2 + 12\left(\frac{H}{R}\right)^2 \left(\frac{x}{H}\right)^2 - \frac{3}{2}(1+2\mu)\left(\frac{r}{R}\right)^2 \right.$$

$$\left. - \frac{24}{\pi}(1-\mu)\frac{H}{R} \sum_{n=1}^{\infty} F_{\sigma\theta} \cos n\pi \frac{x}{H} \right] \quad \ldots\ldots\ldots \quad (67)$$

$$\phi_\tau = Q \left[12(1-\mu)\frac{H}{R}\frac{x}{H}\frac{r}{R} - \frac{24}{\pi}(1-\mu)\frac{H}{R} \sum_{n=1}^{\infty} F_\tau \sin n\pi \frac{x}{H} \right] \quad \ldots \quad (68)$$

$$\phi_\xi = Q \left[-3\mu\frac{x}{H} - 4(1-\mu)\left(\frac{H}{R}\right)^2 \frac{x}{H} + 4\left(\frac{H}{R}\right)^2 \left(\frac{x}{H}\right)^3 \right.$$

$$\left. - \frac{24}{\pi^2}(1-\mu)\frac{H}{R} \sum_{n=1}^{\infty} F_\xi \sin n\pi \frac{x}{H} \right] \ldots \quad (69)$$

and

$$\phi_\rho = Q \left[-\frac{3}{2}(3-5\mu)\frac{r}{R} + 4\left(1-\mu^2\right)\left(\frac{H}{R}\right)^2 \frac{r}{R} - 12\left(1-\mu^2\right)\left(\frac{H}{R}\right)\left(\frac{x}{H}\right)^2 \frac{r}{R} \right.$$

$$\left. + \frac{3}{2}(1-\mu-2\mu)\left(\frac{r}{R}\right)^3 \quad \frac{24}{\pi^2}\left(1-\mu^2\right)\left(\frac{H}{R}\right)^2 \sum_{n=1}^{\infty} F_\rho \cos n\pi \frac{x}{H} \right] \ldots\ldots \quad (70)$$

By applying these abbreviations, the formulas can be written in a simplified form,

$$\sigma_x = \sigma_1 \left[1 - \psi \frac{\mu}{1-\mu} \phi_{\sigma x} \right] + \sigma_3 \psi \phi_{\sigma x} \quad \ldots\ldots\ldots \quad (71)$$

$$\sigma_r = \sigma_1 \psi \frac{\mu}{1-\mu} \phi_{\sigma r} + \sigma_3 \left[1 - \psi \phi_{\sigma r}\right] \qquad (72)$$

$$\sigma_\theta = \sigma_1 \psi \frac{\mu}{1-\mu} \phi_{\sigma\theta} + \sigma_3 \left[1 - \psi \phi_{\sigma\theta}\right] \qquad (73)$$

$$\tau = \sigma_1 \psi \frac{\mu}{1-\mu} \phi_\tau - \sigma_3 \psi \phi_\tau \qquad (74)$$

$$\xi = \frac{H}{E} \left\{ \sigma_1 \left[\frac{x}{H} - \psi \mu \frac{\mu}{1-\mu} \phi_\xi\right] - \sigma_3 \left[4 \mu \frac{x}{H} - \psi (1-\mu) \phi_\xi\right] \right\} \qquad (75)$$

and

$$\rho = -\frac{R}{E} \left\{ \sigma_1 \left[\mu \frac{r}{R} + \psi \frac{\mu}{1-\mu} \phi_\rho\right] - \sigma_3 \left[(1-\mu) \frac{r}{R} + \psi \phi_\rho\right] \right\} \qquad (76)$$

PRACTICAL APPLICATION OF THE STRESS CONDITIONS IN TRIAXIAL COMPRESSION IN THE FIELD OF SOIL MECHANICS

Applicability of the Theory of Elasticity.—In the first part of this paper, the discussion concerning stress conditions in triaxial compression was based on the theory of elasticity. It should be emphasized that the author regards the first as the more important part of this paper, that is the part containing the theoretically close-limit solution of the problem of stress conditions is the more important part. There exist, however, several practical applications of this solution.

Among the practical applications, one of the possibilities lies in the field of soil mechanics. As mentioned previously, it is by means of triaxial compression tests that the shearing strength of soils is determined. Of course the question arises as to whether the results obtained in this manner are applicable to soils. The theoretical relationships obtained herein, as well as the numerical results to be discussed are, strictly speaking, valid for elastic materials only.

When investigating stress conditions in triaxial compression for a soil mechanics test, it is less important to obtain numerically accurate values, than to get acquainted with the character of stress distribution and deformation, compute their approximate order of magnitude, and obtain an idea of the influence of the various factors.

By founding our discussion of the problem in question on such considerations, the results obtained can be applied also to soil mechanics, because the character of the distribution of stresses actually occurring will, presumably, be similar to that obtained on a theoretical basis. The theoretical part of the science of soil mechanics is relying largely on the theory of elasticity. Therefore, in the given case, the application of the theory of elasticity is justified at least as much as in the case of other soil mechanics problems.

Calculation of the Stress Conditions of a Cylinder with a Slenderness of H/R = 2.—The height to diameter ration (slenderness) of test specimens used in soil mechanics laboratories is usually H/R = 2.

The absolute dimensions of the cylinder are of no significance, because Eqs. 49 through 54 show that the stresses depend only on the slenderness factor H/R, and not on the absolute dimensions. The value of Poisson's ratio has been chosen as a good average in $\mu = 1/3$. Finally the case of maximum roughness ($\psi = 1$) is discussed from the point of view of the roughness of the loading plate.

TABLE 1

n	r/R = 0	0.2	0.4	0.6	0.8	1.0
	$J_0\left(i\,n\,\pi\frac{R}{H}\frac{r}{R}\right)$					
1	1	1.0248	1.1011	1.2347	1.4355	1.7188
2	1	1.1011	1.4355	2.106	3.324	5.478
3	1	1.2347	2.106	4.247	9.275	21.09
4	1	1.4355	3.324	9.275	27.90	87.10
5	1	1.7188	5.478	21.09	87.10	373.0
6	1	2.106	9.275	49.12	278.3	1633
	$\frac{1}{i}J_1\left(i\,n\,\pi\frac{R}{H}\frac{r}{R}\right)$					
1	0	0.1590	0.3299	0.5255	0.7608	1.0538
2	0	0.3299	0.7608	1.4279	2.547	4.491
3	0	0.5255	1.4279	3.382	7.921	18.69
4	0	0.7608	2.547	7.921	24.94	79.84
5	0	1.0538	4.491	18.69	79.84	348.4
6	0	1.4279	7.921	44.54	259.2	1544

TABLE 2

n	$n\,\pi\frac{R}{H}$	$J_0\left(i\,n\,\pi\frac{R}{H}\right)$	$\frac{1}{i}J_1\left(i\,n\,\pi\frac{R}{H}\right)$	$\frac{i\,J_0(i\,n\,\pi\,R/H)}{J_1(i\,n\,\pi\,R/H)}$	U_n	V_n
1	1.5708	1.7188	1.0538	1.6310	+0.2700	+0.3303
2	3.1416	5.478	4.491	1.2197	+0.1215	+0.8002
3	4.7124	21.09	18.69	1.1279	+1.5364	-1.1676
4	6.2832	87.10	79.84	1.0910	+1.0430	-0.3593
5	7.8540	373.0	348.4	1.0706	+0.9810	-0.2180
6	9.4248	1633	1544	1.0578	+0.9660	-0.1585

With regard to axial symmetry, it is sufficient to examine one single vertical section and, within its limits, a quarter of the whole section of the test specimen. In the chosen quarter of the plane section thirty-six points are marked out and computed in connection with the values of the stresses. The first task consists in determination of the numerical values of Bessel's functions (Table 1). It is followed by that of the values of the auxiliary quantities U_n and V_n (Table 2), which depend on the value of n used in the computation (Eqs. 55

TABLE 3

$\frac{x}{H}$	$\Sigma F \cos n\pi \frac{x}{H}$ / $\Sigma F \sin n\pi \frac{x}{H}$	r/R					
		0	0.2	0.4	0.6	0.8	1.0
1.0	$\Sigma F_{\sigma x} \cos n\pi \frac{x}{H}$	+ 1.337	+ 1.355	+ 1.415	+ 1.555	+ 1.924	+ 4.868
	$\Sigma F_{\sigma r} \cos n\pi \frac{x}{H}$	+ 1.326	+ 1.363	+ 1.457	+ 1.662	+ 2.100	+ 3.142
	$\Sigma F_{\sigma \theta} \cos n\pi \frac{x}{H}$	+ 1.326	+ 1.338	+ 1.382	+ 1.456	+ 1.545	+ 1.594
	$\Sigma F_{\tau} \sin n\pi \frac{x}{H}$	0	0	0	0	0	0
0.8	$\Sigma F_{\sigma x} \cos n\pi \frac{x}{H}$	+ 1.029	+ 1.028	+ 1.061	+ 1.080	+ 0.998	+ 0.580
	$\Sigma F_{\sigma r} \cos n\pi \frac{x}{H}$	+ 1.054	+ 1.084	+ 1.161	+ 1.314	+ 1.471	+ 1.445
	$\Sigma F_{\sigma \theta} \cos n\pi \frac{x}{H}$	+ 1.054	+ 1.065	+ 1.105	+ 1.182	+ 1.318	+ 1.572
	$\Sigma F_{\tau} \sin n\pi \frac{x}{H}$	0	+ 0.152	+ 0.319	+ 0.534	+ 0.818	+ 1.256
0.6	$\Sigma F_{\sigma x} \cos n\pi \frac{x}{H}$	+ 0.273	+ 0.266	+ 0.227	+ 0.150	+ 0.025	- 0.200
	$\Sigma F_{\sigma \Gamma} \cos n\pi \frac{x}{H}$	+ 0.342	+ 0.342	+ 0.329	+ 0.304	- 0.241	+ 0.126
	$\Sigma F_{\sigma \theta} \cos n\pi \frac{x}{H}$	+ 0.342	+ 0.342	+ 0.342	+ 0.340	+ 0.330	+ 0.255
	$\Sigma F_{\tau} \sin n\pi \frac{x}{H}$	0	+ 0.209	+ 0.419	+ 0.625	+ 0.848	+ 0.942
0.4	$\Sigma F_{\sigma x} \cos n\pi \frac{x}{H}$	- 0.477	- 0.482	- 0.505	- 0.538	- 0.571	- 0.585
	$\Sigma F_{\sigma \Gamma} \cos n\pi \frac{x}{H}$	- 0.452	- 0.468	- 0.511	- 0.585	- 0.688	- 0.816
	$\Sigma F_{\sigma \theta} \cos n\pi \frac{x}{H}$	- 0.452	- 0.457	- 0.478	- 0.518	- 0.574	- 0-645
	$\Sigma F_{\tau} \sin n\pi \frac{x}{H}$	0	+ 0.159	+ 0.307	+ 0.448	+ 0.568	+ 0.628
0.2	$\Sigma F_{\sigma x} \cos n\pi \frac{x}{H}$	- 0.949	- 0.948	- 0.947	- 0.936	- 0.902	- 0.840
	$\Sigma F_{\sigma \Gamma} \cos n\pi \frac{x}{H}$	- 1.006	- 1.026	- 1.079	- 1.155	- 1.256	- 1.382
	$\Sigma F_{\sigma \theta} \cos n\pi \frac{x}{H}$	- 1.006	- 1.015	- 1.044	- 1.092	- 1.158	- 1.242
	$\Sigma F_{\tau} \sin n\pi \frac{x}{H}$	0	+ 0.070	+ 0.149	+ 0.214	+ 0.280	+ 0.314
0	$\Sigma F_{\sigma x} \cos n\pi \frac{x}{H}$	- 1.103	- 1.099	- 1.89	- 1.067	- 1.022	- 0.953
	$\Sigma F_{\sigma \Gamma} \cos n\pi \frac{x}{H}$	- 1.198	- 1.214	- 1.263	- 1.340	- 1.443	- 1.570
	$\Sigma F_{\sigma \theta} \cos n\pi \frac{x}{H}$	- 1.198	- 1.208	- 1.238	- 1.291	- 1.369	- 1.482
	$\Sigma F_{\tau} \sin n\pi \frac{x}{H}$	0	0	0	0	0	0

and 56), after this the value of the constants K and Q (Eqs. 57 and 58) will be computed.

The next step is the computation of functions $F_{\sigma x}$, $F_{\sigma r}$, $F_{\sigma\theta}$ and F_{τ} and, this done, the determination of the numerical values of expressions like $\sum_{n=1}^{\infty} F_{\sigma x} \cos n\pi \frac{x}{H}$, and so. The results are indicated in Table 3.

After the substitution of the numerical values, the expressions $\phi_{\sigma x}$, $\phi_{\sigma r}$, $\phi_{\sigma\theta}$ and ϕ_{τ} used in Eqs. 65 through 70 assume the form.

TABLE 4

$\frac{x}{H}$	ϕ_σ / ϕ_τ	r/R: 0	0.2	0.4	0.6	0.8	1.0
1.0	$\phi_{\sigma x}$	+ 0.3769	+ 0.3711	+ 0.3503	+ 0.2927	+ 0.1132	- 1.530
	$\phi_{\sigma r}$	+ 1.2344	+ 1.2053	+ 1.1281	+ 0.9716	+ 0.6662	0
	$\phi_{\sigma\theta}$	+ 1.2344	+ 1.2219	+ 1.1799	+ 1.1096	+ 1.0194	+ 0.9409
	ϕ_τ	0	+ 0.1796	+ 0.3592	+ 0.5388	+ 0.7184	+ 0.8979
0.8	$\phi_{\sigma x}$	- 0.0936	- 0.0942	- 0.0939	- 0.0823	- 0.0041	+ 0.2743
	$\phi_{\sigma r}$	+ 0.4200	+ 0.3950	+ 0.3275	+ 0.2007	+ 0.0560	0
	$\phi_{\sigma\theta}$	+ 0.4200	+ 0.4081	+ 0.3685	+ 0.2964	+ 0.1793	- 0.0164
	ϕ_τ	0	+ 0.0568	+ 0.1050	+ 0.1258	+ 0.1071	0
0.6	$\phi_{\sigma x}$	- 0.1642	- 0.1557	- 0.1200	- 0.0535	+ 0.0493	+ 0.2183
	ϕ_{σ}	+ 0.0728	+ 0.0649	+ 0.0488	+ 0.0238	+ 0.0049	0
	$\phi_{\sigma\theta}$	+ 0.0728	+ 0.0672	+ 0.0504	+ 0.0235	- 0.0101	- 0.0178
	ϕ_τ	0	- 0.0118	- 0.0240	- 0.0340	- 0.0366	0
0.4	$\phi_{\sigma x}$	- 0.0948	- 0.0874	- 0.0608	- 0.0195	+ 0.0220	+ 0.0792
	$\phi_{\sigma r}$	- 0.0121	- 0.0109	- 0.0098	- 0.0070	- 0.0029	0
	$\phi_{\sigma\theta}$	- 0.0121	- 0.0149	- 0.0197	- 0.0249	- 0.0322	- 0.0421
	ϕ_τ	0	- 0.0191	- 0.0318	- 0.0406	- 0.0374	0
0.2	$\phi_{\sigma x}$	- 0.0405	- 0.0365	- 0.0236	- 0.0075	+ 0.0045	+ 0.0093
	$\phi_{\sigma r}$	- 0.0188	- 0.0152	- 0.0086	- 0.0043	- 0.0015	0
	$\phi_{\sigma\theta}$	- 0.0188	- 0.0192	- 0.0195	- 0.0201	- 0.0217	- 0.0242
	ϕ_τ	0	- 0.0041	- 0.0134	- 0.0175	- 0.0163	0
0	$\phi_{\sigma x}$	- 0.0242	- 0.0220	- 0.0142	- 0.0044	+ 0.0011	+ 0.0025
	$\phi_{\sigma r}$	- 0.0167	- 0.0154	- 0.0110	- 0.0063	- 0.0024	0
	$\phi_{\sigma\theta}$	- 0.0167	- 0.0167	- 0.0163	- 0.0141	- 0.0088	+ 0.0052
	ϕ_τ	0	0	0	0	0	0

$$\phi_{\sigma x} = -0.6547 + 1.7958\left(\frac{x}{H}\right)^2 + 0.1122\left(\frac{r}{R}\right)^2 - 0.5716 \sum_{n=1}^{\infty} F_{\sigma x} \cos n\pi \frac{x}{H}$$

$$\phi_{\sigma r} = -0.7015 + 2.6938\left(\frac{x}{H}\right)^2 - 0.1964\left(\frac{r}{R}\right)^2 - 0.5716 \sum_{n=1}^{\infty} F_{\sigma r} \cos n\pi \frac{x}{H}$$

$$\phi_{\sigma\theta} = -0.7015 + 2.6938\left(\frac{x}{H}\right)^2 - 0.1403\left(\frac{r}{R}\right)^2 - 0.5716 \sum_{n=1}^{\infty} F_{\sigma\theta} \cos n\pi \frac{x}{H}$$

and

$$\phi_{\tau} = 0.8979 \frac{x}{H}\frac{r}{R} - 0.5716 \sum_{n=1}^{\infty} F_{\tau} \sin n\pi \frac{x}{H}$$

Table 4 shows the computations that have been completed for the points indicated.

In case of $\mu = 1/3$ and $\psi = 1$, Eqs. 71 through 76 can be written in the form

$$\sigma_x = \left[1 - 0.5\,\phi_{\sigma x}\right]\sigma_1 + \phi_{\sigma x}\,\sigma_3$$

$$\sigma_r = 0.5\,\phi_{\sigma r}\,\sigma_1 + \left[1 - \phi_{\sigma r}\right]\sigma_3$$

$$\sigma_\theta = 0.5\,\phi_{\sigma\theta}\,\sigma_1 + \left[1 - \phi_{\sigma\theta}\right]\sigma_3$$

and

$$\tau = 0.5\,\phi_\tau\,\sigma_1 - \phi_\tau\,\sigma_3$$

Using the values indicated in Table 4, the stresses acting at the examined points of the specimen can be expressed as functions of external loading stresses σ_1 and σ_3 (Table 5). The table gives a good cross section and permits, by means of the given numerical values, a quick computation of the values of the stresses at any point of the test specimen and under any external loading stress.

The infinite series figuring in the expressions generally converge quickly enough, so that in using a mechanical computer the stress values were computed with the desired accuracy almost everywhere.

As an exception, the value of $\sum_{n=1}^{\infty} F_{\sigma x} \cos n\pi \frac{x}{H}$ at points x = H and r = R must be mentioned. Here the infinite series converges rather slowly and, therefore, the computation could not be executed with the desirable accuracy and we had to apply a certain approximation. If an electronic computer had been used, this fault could have been avoided. As a consequence of the approximation, the numerical value of σ_x should be regarded as approximate at points x = H and r = R. As an example, the stress conditions of a cylinder charged by stresses $\sigma_1 = 4$ and $\sigma_3 = 1$ are demonstrated.

TABLE 5

$\frac{x}{H}$	σ / τ	r/R = 0	0.2	0.4	0.6	0.8	1.0
1.0	σ_x	$+0.812\sigma_1 +0.377\sigma_3$	$+0.815\sigma_1 +0.371\sigma_3$	$+0.825\sigma_1 +0.350\sigma_3$	$+0.854\sigma_1 +0.293\sigma_3$	$+0.943\sigma_1 +0.113\sigma_3$	$+1.765\sigma_1 -1.530\sigma_3$
	σ_Γ	$+0.617\sigma_1 -0.234\sigma_3$	$+0.603\sigma_1 -0.205\sigma_3$	$+0.564\sigma_1 -0.128\sigma_3$	$+0.486\sigma_1 +0.028\sigma_3$	$+0.333\sigma_1 +0.334\sigma_3$	$+1.000\sigma_3$
	σ_θ	$+0.617\sigma_1 -0.234\sigma_3$	$+0.611\sigma_1 -0.222\sigma_3$	$+0.590\sigma_1 -0.180\sigma_3$	$+0.555\sigma_1 -0.110\sigma_3$	$+0.510\sigma_1 -0.019\sigma_3$	$+0.470\sigma_1 +0.059\sigma_3$
	τ	0	$+0.090\sigma_1 -0.180\sigma_3$	$+0.180\sigma_1 -0.360\sigma_3$	$+0.270\sigma_1 -0.540\sigma_3$	$+0.360\sigma_1 -0.720\sigma_3$	$+0.450\sigma_1 -0.900\sigma_3$
0.8	σ_x	$+1.047\sigma_1 -0.094\sigma_3$	$+1.047\sigma_1 -0.094\sigma_3$	$+1.047\sigma_1 -0.094\sigma_3$	$+1.041\sigma_1 -0.082\sigma_3$	$+1.002\sigma_1 -0.004\sigma_3$	$+0.863\sigma_1 +0.274\sigma_3$
	σ_Γ	$+0.210\sigma_1 +0.580\sigma_3$	$+0.198\sigma_1 -0.605\sigma_3$	$+0.164\sigma_1 +0.672\sigma_3$	$+0.100\sigma_1 +0.799\sigma_3$	$+0.028\sigma_1 +0.944\sigma_3$	$+1.000\sigma_3$
	σ_θ	$+0.210\sigma_1 +0.580\sigma_3$	$+0.204\sigma_1 +0.592\sigma_3$	$+0.184\sigma_1 +0.632\sigma_3$	$+0.148\sigma_1 +0.704\sigma_3$	$+0.090\sigma_1 +0.821\sigma_3$	$-0.008\sigma_1 +1.016\sigma_3$
	τ	0	$+0.018\sigma_1 -0.056\sigma_3$	$+0.052\sigma_1 -0.104\sigma_3$	$+0.063\sigma_1 -0.126\sigma_3$	$+0.054\sigma_1 -0.108\sigma_3$	0
0.6	σ_x	$+1.082\sigma_1 -0.164\sigma_3$	$+1.078\sigma_1 -0.156\sigma_3$	$+1.060\sigma_1 -0.120\sigma_3$	$+1.027\sigma_1 -0.054\sigma_3$	$+0.975\sigma_1 +0.049\sigma_3$	$+0.891\sigma_1 +0.218\sigma_3$
	σ_Γ	$+0.036\sigma_1 +0.927\sigma_3$	$+0.032\sigma_1 +0.935\sigma_3$	$+0.024\sigma_1 +0.951\sigma_3$	$+0.012\sigma_1 +0.976\sigma_3$	$+0.002\sigma_1 +0.995\sigma_3$	$+1.000\sigma_3$
	σ_θ	$+0.036\sigma_1 +0.927\sigma_3$	$+0.034\sigma_1 +0.933\sigma_3$	$+0.025\sigma_1 +0.950\sigma_3$	$+0.012\sigma_1 +0.976\sigma_3$	$-0.005\sigma_1 +1.010\sigma_3$	$-0.009\sigma_1 +1.018\sigma_3$
	τ	0	$-0.006\sigma_1 +0.012\sigma_3$	$-0.012\sigma_1 +0.024\sigma_3$	$-0.017\sigma_1 +0.034\sigma_3$	$-0.018\sigma_1 +0.036\sigma_3$	0
0.4	σ_x	$+1.047\sigma_1 -0.095\sigma_3$	$+1.044\sigma_1 -0.087\sigma_3$	$+1.030\sigma_1 -0.061\sigma_3$	$+1.010\sigma_1 -0.020\sigma_3$	$+0.989\sigma_1 +0.022\sigma_3$	$+0.960\sigma_1 +0.079\sigma_3$
	σ_Γ	$-0.006\sigma_1 +1.012\sigma_3$	$-0.006\sigma_1 -1.011\sigma_3$	$-0.005\sigma_1 +1.010\sigma_3$	$-0.004\sigma_1 +1.007\sigma_3$	$-0.002\sigma_1 +1.003\sigma_3$	$+1.000\sigma_3$
	σ_θ	$-0.006\sigma_1 +1.012\sigma_3$	$-0.007\sigma_1 +1.015\sigma_3$	$-0.010\sigma_1 +1.020\sigma_3$	$-0.012\sigma_1 +1.025\sigma_3$	$-0.016\sigma_1 +1.032\sigma_3$	$-0.021\sigma_1 +1.042\sigma_3$
	τ	0	$-0.009\sigma_1 +0.018\sigma_3$	$-0.016\sigma_1 +0.032\sigma_3$	$-0.020\sigma_1 +0.040\sigma_3$	$-0.019\sigma_1 +0.038\sigma_3$	0
0.2	σ_x	$+1.020\sigma_1 -0.040\sigma_3$	$+1.018\sigma_1 -0.036\sigma_3$	$+1.012\sigma_1 -0.024\sigma_3$	$+1.004\sigma_1 -0.008\sigma_3$	$+0.998\sigma_1 +0.004\sigma_3$	$+0.995\sigma_1 +0.009\sigma_3$
	σ_Γ	$-0.009\sigma_1 +1.019\sigma_3$	$-0.008\sigma_1 +1.015\sigma_3$	$-0.004\sigma_1 +1.009\sigma_3$	$-0.002\sigma_1 +1.004\sigma_3$	$-0.001\sigma_1 +1.002\sigma_3$	$+1.000\sigma_3$
	σ_θ	$-0.009\sigma_1 +1.019\sigma_3$	$-0.010\sigma_1 +1.019\sigma_3$	$-0.010\sigma_1 +1.020\sigma_3$	$-0.010\sigma_1 +1.020\sigma_3$	$-0.011\sigma_1 +1.022\sigma_3$	$-0.012\sigma_1 +1.024\sigma_3$
	τ	0	$-0.002\sigma_1 +0.004\sigma_3$	$-0.007\sigma_1 +0.014\sigma_3$	$-0.009\sigma_1 +0.018\sigma_3$	$-0.008\sigma_1 +0.016\sigma_3$	0
0	σ_x	$+1.012\sigma_1 -0.024\sigma_3$	$+1.011\sigma_1 -0.022\sigma_3$	$+1.007\sigma_1 -0.014\sigma_3$	$+1.002\sigma_1 +0.004\sigma_3$	$+0.999\sigma_1 +0.001\sigma_3$	$+0.999\sigma_1 +0.002\sigma_3$
	σ_Γ	$-0.008\sigma_1 +1.017\sigma_3$	$-0.008\sigma_1 +1.015\sigma_3$	$-0.006\sigma_1 +1.011\sigma_3$	$-0.003\sigma_1 +1.006\sigma_3$	$-0.001\sigma_1 +1.002\sigma_3$	$+1.000\sigma_3$
	σ_θ	$-0.008\sigma_1 +1.017\sigma_3$	$-0.008\sigma_1 +1.017\sigma_3$	$-0.008\sigma_1 +1.016\sigma_3$	$-0.007\sigma_1 +1.014\sigma_3$	$-0.004\sigma_1 +1.009\sigma_3$	$+0.003\sigma_1 +0.995\sigma_3$
	τ	0	0	0	0	0	0

It must be pointed out that the dimension of the external loading stresses can be arbitrary while the stresses occurring in the interior of the test specimen must, naturally, be understood in the same dimension.

TABLE 6

$\frac{x}{H}$	σ / τ	r/R: 0	0.2	0.4	0.6	0.8	1.0
1.0	σ_x	3.623	3.629	3.650	3.707	3.885	5.530
	σ	2.234	2.205	2.128	1.972	1.662	1.000
	σ_θ	2.234	2.222	2.180	2.110	2.019	1.941
	τ	0	0.180	0.360	0.540	0.720	0.900
0.8	σ_x	4.094	4.094	4.094	4.082	4.004	3.726
	σ_r	1.420	1.395	1.327	1.201	1.056	1.000
	σ_θ	1.420	1.408	1.368	1.296	1.179	0.984
	τ	0	0.057	0.105	0.126	0.107	0
0.6	σ_x	4.164	4.156	4.120	4.053	3.951	3.782
	σ_r	1.073	1.065	1.049	1.024	1.005	1.000
	σ_θ	1.073	1.067	1.050	1.023	0.990	0.982
	τ	0	-0.012	-0.024	-0.034	-0.037	0
0.4	σ_x	4.095	4.087	4.061	4.019	3.978	3.921
	σ_r	0.988	0.989	0.990	0.993	0.997	1.000
	σ_θ	0.988	0.985	0.980	0.975	0.968	0.958
	τ	0	-0.019	-0.032	-0.041	-0.037	0
0.2	σ_x	4.040	4.036	4.024	4.007	3.996	3.991
	σ_r	0.981	0.985	0.991	0.996	0.999	1.000
	σ_θ	0.981	0.981	0.981	0.980	0.978	0.976
	τ	0	-0.004	-0.013	-0.017	-0.016	0
0	σ_x	4.024	4.022	4.014	4.004	3.999	3.998
	σ_r	0.983	0.985	0.989	0.994	0.998	1.000
	σ_θ	0.983	0.983	0.984	0.986	0.991	1.005
	τ	0	0	0	0	0	0

The stress condition of the test specimen is characterized by the intensity of the tangential stresses.

$$\tau_0 = \sqrt{\frac{1}{6}\left[(\sigma_x - \sigma_r)^2 + (\sigma_r - \sigma_\theta)^2 + (\sigma_\theta - \sigma_x)^2\right] + \tau^2} \quad \ldots (77)$$

The so-called octahedral shearing stress and the intensity of the tangential stresses assume the following relationship:

$$\tau_n = \sqrt{\frac{2}{3}}\,\tau_0 \quad \ldots\ldots\ldots\ldots\ldots\ldots \quad (78)$$

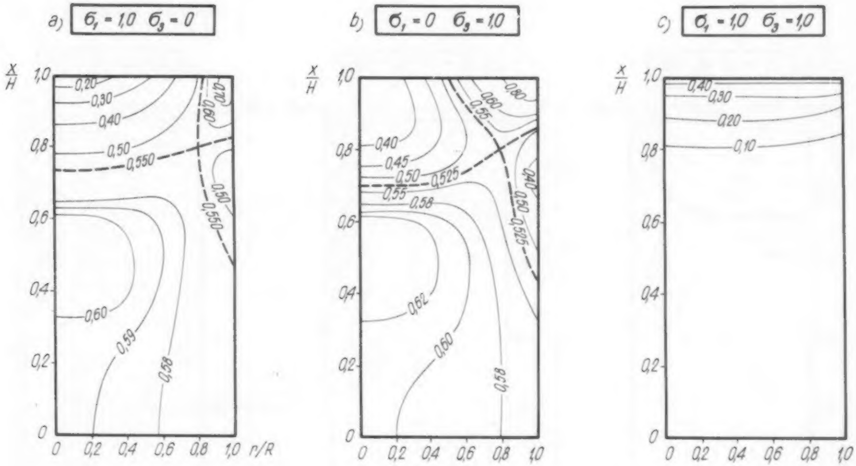

FIG. 3

TABLE 7

x/H	r/R					
	0	0.2	0.4	0.6	0.8	1.0
(a) $\sigma_1 = 1;\ \sigma_3 = 0$						
1.0	0.113	0.150	0.230	0.334	0.501	1.018
0.8	0.485	0.491	0.508	0.535	0.549	0.500
0.6	0.605	0.602	0.598	0.586	0.564	0.533
0.4	0.608	0.606	0.604	0.589	0.572	0.555
0.2	0.594	0.592	0.588	0.582	0.580	0.580
0	0.591	0.590	0.586	0.570	0.578	0.576
(b) $\sigma_1 = 0;\ \sigma_3 = 1$						
1.0	0.353	0.382	0.463	0.581	0.741	1.454
0.8	0.390	0.405	0.443	0.500	0.526	0.424
0.6	0.630	0.629	0.618	0.595	0.550	0.457
0.4	0.638	0.634	0.621	0.600	0.574	0.544
0.2	0.610	0.606	0.600	0.586	0.580	0.578
0	0.600	0.599	0.593	0.585	0.580	0.574
(c) $\sigma_1 = 1;\ \sigma_3 = 1$						
1.0	0.465	0.466	0.470	0.472	0.463	0.592
0.8	0.095	0.093	0.091	0.083	0.070	0.077
0.6	0.026	0.026	0.023	0.019	0.022	0.060
0.4	0.030	0.029	0.027	0.023	0.019	0.018
0.2	0.017	0.015	0.013	0.011	0.010	0.006
0	0.012	0.011	0.008	0.004	0	0

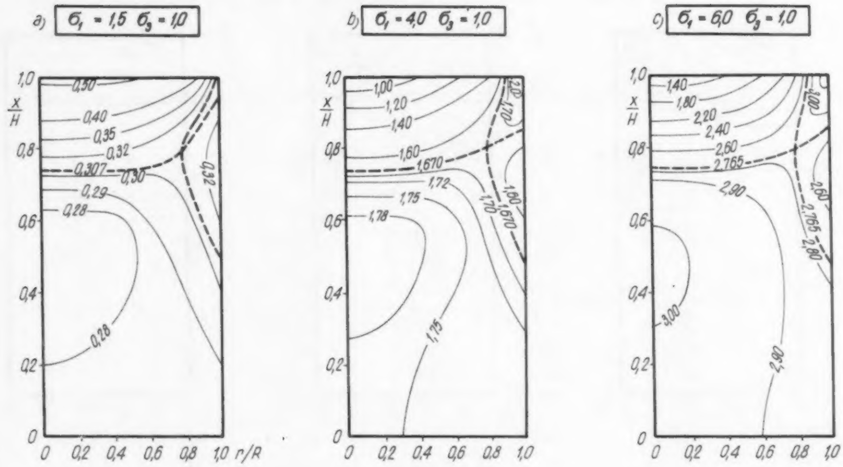

FIG. 4

TABLE 8

x/H	r/R 0	0.2	0.4	0.6	0.8	1.0
(a) σ_1 = 1.5; σ_3 = 1						
1.0	0.524	0.519	0.511	0.500	0.462	0.297
0.8	0.336	0.333	0.327	0.314	0.307	0.327
0.6	0.275	0.276	0.278	0.284	0.295	0.319
0.4	0.273	0.274	0.278	0.283	0.289	0.297
0.2	0.280	0.281	0.283	0.286	0.288	0.288
0	0.283	0.283	0.284	0.286	0.288	0.289
(b) σ_1 = 4; σ_3 = 1						
1.0	0.800	0.844	0.935	1.105	1.391	2.560
0.8	1.535	1.555	1.588	1.635	1.670	1.578
0.6	1.784	1.784	1.780	1.752	1.710	1.610
0.4	1.795	1.790	1.776	1.750	1.730	1.700
0.2	1.768	1.760	1.750	1.740	1.738	1.732
0	1.755	1.758	1.748	1.740	1.730	1.731
(c) σ_1 = 6; σ_3 = 1						
1.0	1.025	1.120	1.355	1.731	2.360	4.590
0.8	2.510	2.533	2.620	2.710	2.766	2.572
0.6	2.995	2.990	2.961	2.923	2.836	2.650
0.4	3.020	3.011	2.974	2.932	2.881	2.820
0.2	2.954	2.945	2.931	2.910	2.893	2.890
0	2.930	2.928	2.921	2.900	2.890	2.890

The reduced stress differs from the intensity of the tangential stresses only by a constant factor:

$$\sigma_{red} = \sqrt{3}\,\tau_o \quad \ldots\ldots\ldots\ldots\ldots\ldots \quad (79)$$

Thus the intensity of the tangential stresses τ_o for various loads have been computed.

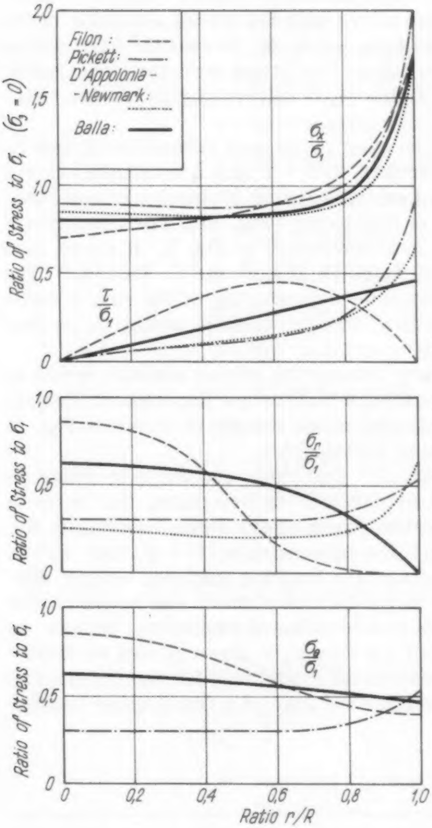

FIG. 5

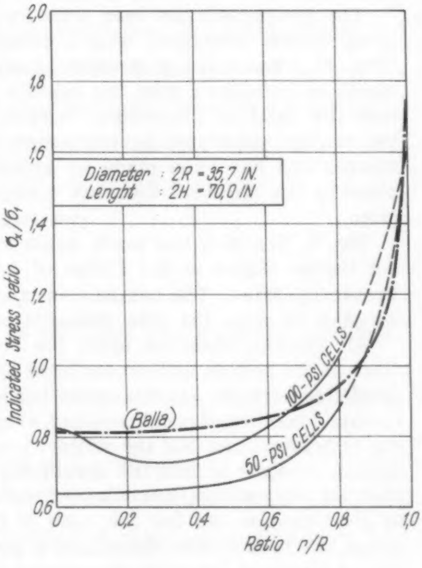

FIG. 6

The case $\sigma_1 = 1$; $\sigma_3 = 0$ represents that of unaxial compression (Fig. 3(a) and Table 7(a)). In the case of $\sigma_1 = 0$; $\sigma_3 = 1$ only a uniformly distributed radial stress acts upon the test specimen (Fig. 3(b), Table 7(b)) in which $\sigma_1 = 1$; $\sigma_3 = 1$, apart from the surroundings of the top surface ($x > 0, 8\ H$), the intensity of the tangential stresses is rather small in the test specimen (Fig. 3(c), Table 7(c)).

In the case of $\sigma_3 = 1$; and $\sigma_1 = 1, 5, 4,$ and 6 respectively, the increase of the intensity of the tangential stresses can well be observed (Fig. 4 and Table 8). It shouldbe pointed out that the case of $\sigma_1 = 2$, and $\sigma_3 = 1$ represents a special case.

At every pointof the test specimen $\sigma_x = \sigma_1$; $\sigma_r = \sigma_\theta = \sigma_3$ and $\tau = 0$. That is, in which $\psi = 1$ and the ratio of the two external stresses $\sigma_1/\sigma_3 = 2$, the chief stress directions andthe values of the individual stresses are constant at every point of the specimen.

Comparison with the Existing Theoretical and Experimental Results.—Many research workers have concerned themselves with the stress condition of the cylindrical test specimens. E. D'Appolonia and N. M. Newmark[2] have solved the stress conditions of the cylinder by taking the lattice structure as a basis. The comparison of the two methods is all the more interesting as the two solutions follow entirely different lines.

The comparison has been made for the case of uniaxial compression test by using a test specimen with a slenderness $H/R = 1$ and a roughness $\psi = 1$ (Fig. 5). The value of stresses, based on the work of D'Appolonia and Newmark, is compared with the results of this paper (Fig. 5). The comparison with the existing theoretical results are shown also in Fig. 5. It shows also the results presented by the paper of L. N. G. Filon[3] and G. Pickett.[4] The comparison has been made by side-by-side reproducing of the values computed by the different theories concerning stress condition acting on the end plate.

Mr. J. Hvorslev has made some very interesting stress measurements in the United States at the Corps of Engineers Waterways Experiment Station, Vicksburg, Miss. The comparison made with these results is shown in Fig. 6. As shall be seen, the coincidence is quite satisfactory.

All existing theories apply the boundary condition, according to which no point of the bottom and top surfaces is displaced in its own plane, that is, constraint is perfect. On the other hand, this paper offers some opportunity for the consideration of roughness and, even in the extreme case ($\psi = 1$), the writer has only stipulated that the outward points of the limiting surfaces are not displaced. In spite of this, the agreement is good, from which it can be concluded that our supposition, introduced for the cosideration of roughness, proves to be good enough. As for the case of full constraint, it gives almost no divergence, whereas on the other hand it presents an opportunity for the consideration of different degrees of roughness and, for the case of a frictionless loading

---

2 "A Method for Solution of the Restrained Cylinder under Axial Compression," by E. D'Appolonia and N. M. Newmark, Proceedings, First U. S. Natl. Conf. of Applied Mechanics, Amer. Soc. of Mech. Engrs., 1951, pp. 217-226.

3 "The Elastic Equilibrium of Circular Cylinders under Certain Practical Systems of Load," by L. N. G. Filon, Philosophical Transactions, Royal Soc., Series A, Vol. 198, London, 1902, pp. 147-233.

4 "Application of the Fourier Method to the Solution of Certain Boundary Problems in the Theory of Elasticity," by G. Pickett, Journal of Applied Mechanics, Amer. Soc. Mech. Engrg., Vol. II, 1944, pp. A-176-189.

5 Discussion by J. Hvorslev, Proceedings of the Fourth Internatl. Conf. on Soil Mechanics and Foundation Engrg., Vol. III, 1957, p. 105.

plate ($\psi = 0$), the formulas lead us back to the known specific case $\sigma_x = \sigma 1$; $\sigma_r = \sigma_\theta = \tau = 0$.

APPENDIX : NOTATION

---

x, r, θ : the cylindrical coordinates determining the place of arbitrary point Q of the test specimen,

$\sigma_x, \sigma_r, \sigma_\theta$: the normal stresses acting in point Q,

τ : the shearing stress acting in point Q,

$\epsilon_x, \epsilon_r, \epsilon_\theta$: the specific longitudinal variations occurring in point Q,

γ : the angular displacement occurring in point Q,

ξ, ρ : the displacement of point Q in the directions x and r,

H : the half-height of the cylindrical test specimen,

R : the radius of the cylindrical test specimen,

E : the modulus of elasticity,

μ : Poisson's ratio,

ϕ : the stress function,

$J_0(ir)$: Bessel's function of the zero order with imaginary argument,

$J_1(ir)$: Bessel's function of the first order with imaginary argument,

A_n, B_n, C, D, F, G, k : coefficients figuring in the solution,

f : the coefficient of the surface friction,

f_{max} : maximum of the coefficient of the surface friction,

$\psi = \frac{f}{f_{max}}$: ratio,

P : external loading strength transmitted on the upper loading plate,

$\sigma_1 = \frac{P}{R^2 \pi}$: average stress acting upon the loading plate,

σ_3 : lateral pressure acting upon the mantle surface of the cylinder,

∇^2 : differential operator,

a_n, b_n : coefficients of Fourier's series

n : 1, 2, 3, 4 . . . etc. arbitrary positive integers,

$F_{\sigma x}$, $F_{\sigma r}$, $F_{\sigma\theta}$, F_{τ}, F_{ξ}, F_{ρ} : expressions conditional on n and r/R,

$\phi_{\sigma x}$, $\phi_{\sigma r}$, $\phi_{\sigma\theta}$, ϕ_{τ}, ϕ_{ξ}, ϕ_{ρ} : expressions conditional on x/H and r/R,

τ_o : reduced shearing stress, intensity of stresses,

κ : soil characteristic expressing the plastic state.

Journal of the

SOIL MECHANICS AND FOUNDATIONS DIVISION

Proceedings of the American Society of Civil Engineers

DISCUSSION

STATISTICAL STUDY OF SOIL SAMPLING[a]

Closure by Thomas H. Thornburn and Wesley R. Larsen

THOMAS H. THORNBURN,[1] F. ASCE, AND WESLEY R. LARSEN,[2] M. ASCE.—The authors are indebted to Mr. Focht, Jr. for raising a very interesting and important point of discussion. There is no doubt that a portion of the variation in index properties among samples taken from a given soil horizon is attributable to variations inherent in the testing technique. However, the fact that this is not a major portion of the variation can be shown by a comparison of the writers' data with that quoted in the discussion.

The values given in the table in the summary indicate the precision with which the mean value of a given index property can be determined for an entire population on the basis of tests made on only five samples taken from that population. Furthermore, the percentages given there are not stated in terms of the mean value but rather are ranges in liquid limit, plasticity index or clay content all of which are expressed as percentage values. As an example, let us suppose that the average liquid limit value of five samples taken from similar soil horizons is 40%. The summary table then indicates that there is a 95% probability that the population mean liquid limit of that particular soil horizon will be between 33.5% and 46.5% (40.0 ± 6.5%).

In order to examine the range of individual values which make up the sample means, one must refer to Columns 4 and 5, Table 1. If the ranges between maximum and minimum liquid limit values are expressed as percentages of their respective means they are found to vary from 24% to 52%. These values are significantly greater than the 10% of scatter which appears to be attributable to testing technique. The degree of dispersion of individual values from the mean of a normally distributed population is given statistically by the standard deviation or the coefficient of variation (the standard deviation expressed as a percentage of the mean). For the soils tested, these statistics are given in Columns 7 and 8, Table 1. The range of all possible liquid limit values for a particular soil horizon may be estimated, with 95% probability, as the mean liquid limit (based on 10 samples) ± 2.26 times the standard deviationation (or coefficient of variation). If the coefficient of variation is used the ranges for the soil horizons tested in this study become

sample mean liquid limit ± 15.8 to 35.7%.

Thus, it may be seen that the probable range of variation of individual test values from the mean liquid limit value of a given soil horizon is not of the

---

[a] October, 1959, by Thomas H. Thornburn and Wesley R. Larsen.

[1] Prof., Civ. Engrg., Univ. of Illinois, Urbana, Ill.

[2] Liaison Engr., Federal Elec. Corp., Industrial Park, Paramus, N. J.

order of ± 5% but is more likely to have a magnitude 3 to 7 times as great. Nevertheless, the importance of variations due to sample preparation and testing technique should not be overlooked. Additional statestical studies of these variations are needed for the guidance of the engineer.

MAJOR POWER STATION FOUNDATION IN BROKEN LIMESTONE[a]

Closure by W. F. Swiger and H. M. Estes

W. F. SWIGER,[1] F. ASCE.—Foundation conditions in areas underlain by limestone which has been subjected to extensive solution are probably the most difficult faced by the engineer, yet surprisingly little has been published dealing with foundations for structures under these conditions. Mr. Peck's discussion is most welcome since it points up the wide variations and conditions which may occur within a very short distance and why completely different methods of founding were required for various portions of a single structure.

---

[a] October, 1959, by W. F. Swiger and H. M. Estes.
[1] Cons. Engr., Stone & Webster Engineering Corp., Boston, Mass.

LINEARLY VARIABLE LOAD DISTRIBUTION ON A RECTANGULAR FOUNDATION[a]

Closure by Aris C. Stamatopoulos

ARIS C. STAMATOPOULOS,[1] M. ASCE.—Mr. Ambraseys developed interesting equations and graphs which contribute to the solution of stress distribution under a linearly variable unit load. In particular, the graph giving the variation of vertical stress under the unloaded corner of the rectangular foundation (Fig. 1) gives a full picture of the effect of the ratio of the two sides of the rectangle on the variation of the vertical stress.

[a] December, 1959, by Aris C. Stamatopoulos.

[1] Soil and Foundations Engr., Athens, Greece.

SOIL STRUCTURE AND THE STEP-STRAIN PHENOMENON[a]

Discussion by John L. McRae

JOHN L. McRAE,[35] M. ASCE.—Although the writer is not entirely in accord with the authors' hypothesis, he believes that they have made a definite contribution regarding the possible mechanics of soil structure for a composite soil. Such an imaginative approach to this highly complex problem will surely helf to stimulate progress toward a rational theory of compacted soil structure. Certainly, a sound theory of compacted soil structure is greatly needed for very practical reasons related primarily to the need for fabricating and testing laboratory specimens from which data on shear, consolidation, permeability, and so forth, are obtained for design purposes. Soil structure has a major influence on these test measurements, and knowledge in this area is needed so that it will be possible to prepare and intelligently use the test results from laboratory specimens that are truly representative of field conditions with regard to stress-strain as well as to permeability characteristics. The metallurgist knows how, through proper manipulations, to produce metals of varying degrees of hardness and ductility, and he can control these factors very closely so as to meet rigid specifications which give the engineer the material that is best suited to a particular need. It is neither practical nor desirable that the soil technician try to reach a degree of precision in controlling the quality of compacted soils that the metallurgist has reached in controlling metals. However, it is believed desirable that the soils engineers and technicians take greater cognizance of the fact that there is much room for study and advancement in the general direction of closer control over the stress-strain and permeability characteristics of compacted soils through control of conditions and methods at the time of compaction. If a given soil is used in constructing a certain portion of an earth dam, it is desirable that this soil be placed so that it has a high strain at the yield point and can withstand large differential settlements without rupture and also have a low permeability value. On the other hand, if this same soil is used for highway or airport construction, small deflections are the controlling factor and high permeability is desired for best drainage. These are two opposite requirements for the same soil depending on the type of structure. More and better knowledge of the structure of compacted soils would permit the most intelligent use of the soil for the particular application.

The writer was very much interested to learn that the authors have independently arrived at a postulation regarding the particle arrangement and mechanics of shear for a composite soil that has a great deal in common with

---

[a] April, 1960, by D. H. Trollope and C. K. Chan.

[35] Engr. Chf., Bituminous and Chemical Section, Flexible Pavement Branch, Soils Div., U. S. Army Engr. Waterways Experiment Station, Vicksburg, Miss.

a postulation which was advanced as a result of studies conducted by the Soils Division of the Waterways Experiment Station[36] for composite soils that were compacted on the wet side of the optimum water content. The similarity of the postulations is mainly restricted to that for samples compacted on the wet side of the optimum water content. It is desired to point out that other postulations were also advanced, in the report of the studies of the Waterways Experiment Station, regarding the structure of samples compacted on the dry side of the optimum water content; also, differences in structure were recognized for different methods of compaction. This earlier work is referenced here for the benefit of those having a primary interest in the studies of compacted soil structure because it is believed very important to keep in mind the need for a comprehensive theory that takes into consideration the differences in structure caused by variations in water content on a given soil type and the variations due to different methods of compaction as well as differences due to soil type.

36 "The California Bearing Ratio Test as Applied to the Design of Flexible Pavements for Airports," Technical Memorandum No. 213-1, U. S. Army Engineer Waterways Experiment Station, CE, Vicksburg, Miss., July, 1945.

COMPUTER ANALYSIS OF SLOPE STABILITY[a]

Discussion by A. L. Little, N. R. Morgenstern, and V. E. Price

A. L. LITTLE,[7] N. R. MORGENSTERN,[8] A.M. ASCE, AND V. E. PRICE.[9]—Mr. Horn has made an interesting contribution to the literature on the application of electronic computers to slope stability analysis.

As the writers have been successfully operating a comprehensive program for the English Electric DEUCE computer for the last two years it may be of use if they describe their experience with it. Reference should be made to an article by the writers for more detailed information.[10] However, considerable development has taken place since then, some details of which are given subsequently.

The program will analyze slopes or dams constructed from any number, up to 128, of different types of soil, the section of the dam and the boundaries of each type of soil being specified by up to 256 points and up to 256 straight lines. Each type of soil is specified in the usual terms by shear parameters and densities, in addition pore pressures can be specified by a pore pressure ratio in the way described by Mr. Horn or alternatively by reference to a piezometric surface. The program will also allow for external water pressure if desired.

The program was devised to evaluate the factor of safety for each individual circular arc trace, specified in terms of its center and the depth of its horizontal tangent. The method of analysis that has been adopted is that given by Bishop (1955).[11] The method used by Mr. Horn explicitly ignores the effect of the internal forces between the slices and for a typical case gives values of the factor of safety approximately 10% to 15% lower than those given by Bishop's method.

The two methods also differ in their definitions of the factor of safety. The factor of safety with respect to shear strength, that is, the ratio of the available shear strength of the soil to that required to maintain equilibrium, has been used in the DEUCE computer program. Unlike the definition adopted by Mr. Horn, this definition is applicable to both circular and non-circular sliding surfaces. For methods of analysis that consider the internal forces, the two definitions only give the same numerical value when the factor of safety is unity.

---

[a] June, 1960, by John A. Horn.

[7] Assoc., Messrs. Binnie, Deacon and Gourley, Cons. Engrs., London, England.

[8] Lecturer, Civ. Eng., Imperial College of Science and Technology, London, England.

[9] Manager, London Computing Service, English Electric Co. Ltd., London, England.

[10] "The Use of an Electronic Computer for Slope Stability Analysis," by A. L. Little and V. E. Price, Géotechnique, Vol. 8, 1958, p. 113.

[11] "The Use of the Slip Circle in the Stability Analysis of Slopes," by A. W. Bishop, Géotechnique, Vol. 5, 1955, p. 7.

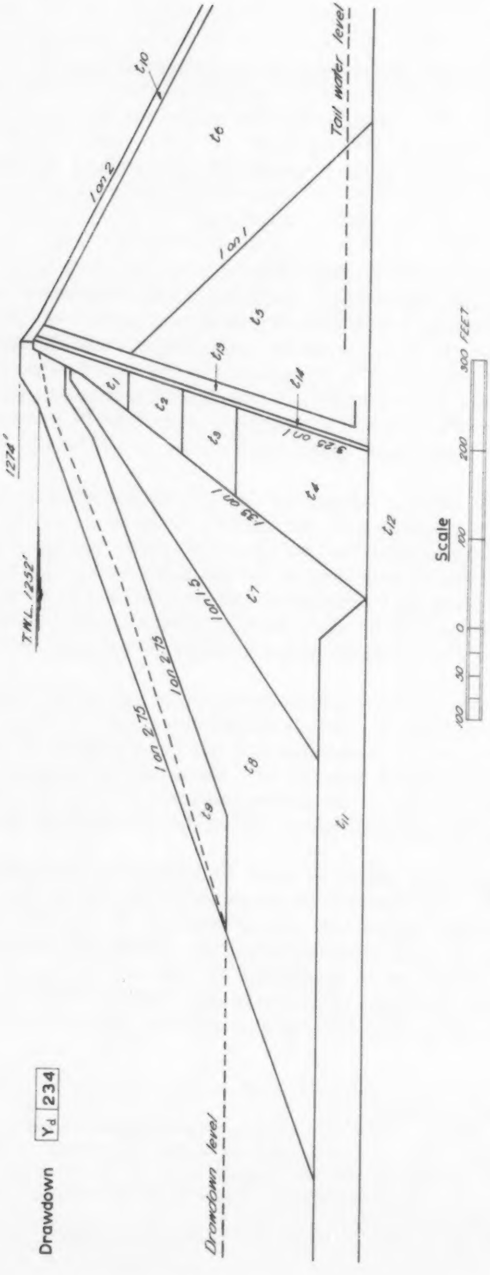

FIG. 17.—STABILITY ANALYSIS BY ELECTRONIC COMPUTER, COMPOSIT SECTION

At any early stage it was realized that it [illegible]e desirable if the computer could be made to find automatically the circle with the lowest factor of safety. However, with a fairly complicated structure it is well known that there may be more than one local minimum in the values of the factor of safety. Thus, if the computer were programmed to search for a minimum, it might produce only a local minimum value and not the absolute minimum unless some preliminary overall survey were made to determine the region in which the lowest value occurred. It was felt that this would be uneconomical, and this conclusion has recently been re-affirmed. With a much faster computer, such as the recently announced English Electric KDF9, there would be a strong argument for automatically searching for the minimum factor safety. Indeed, it may be found possible for the computer to modify certain specified

TABLE 1.—SOIL DATA

Material (1)	Type (2)	γ wet (3)	γ sat (4)	C' (5)	ϕ' (6)	Tan ϕ' (7)	r_u (8)
Clay	1	135	135	450	22	0.404	-1.00
Clay	2	135	135	450	22	0.404	0.52
Clay	3	135	135	450	22	0.404	0.61
Clay	4	135	135	450	22	0.404	0.68
Random	5	133	133	450	28	0.532	0.10
Sandstone	6	131	134	0	36	0.727	0
Sandstone	7	134	134	0	36	0.727	-1.00
Free draining gravel fill	8	135	145	0	40	0.839	-2.00
Free draining cobbles and rip-rap	9	130	145	0	40	0.839	0
Gravel fill	10	135	145	0	40	0.839	0
Alluvium	11	137	145	0	40	0.839	-2.00
Bedrock	12	-	-	-	-	-	-
Gravel drain	13	130	145	0	40	0.839	0
Filters	14	131	134	0	36	0.727	0
TOTALS		1736	1800	2250	424	8.524	-4.09

minor details in the design of the dam so that the minimum factor of safety would reach some required value.

To date about forty five different sections have been analyzed, chiefly for earth dams but including some natural slopes involving 158 computer runs on 12 jobs and a total of more than 15,000 "circles."

Fig. 17 shows a dam section which has been recently analyzed. This illustrates the various features of the program. In Table 1, pore water pressures have been specified for soil types 2, 3, 4, 5, 6, 9, 10, 13, and 14 as a fraction, r_u, of the total pressure at the point. For soil types 1, 7, the pore pressure is specified in terms of a piezometric line shown by a broken line. In the latter case, the computer computes the pore water pressure as the pressure due to a column of water extending to the piezometric line from the point on

the slip surface under consideration. Where the slip surface dips below the drawdown level, the pore water pressure is computed as an excess above this drawdown level. For soil types 8 and 11 the pore pressure has been specified as being zero in excess of the drawdown level.

It has been found best to divide the dam at a number of horizontal levels and analyze a group of circles tangential to each level. The computer takes about 5 sec to analyze one circle for a cross section of moderate complexity and up to a quarter of a minute for a large and complicated one. Work has now been started on a new program based on experience gained in analyzing non-circular traces. The new program will effect some speeding up but its main value will be in simplifying the preparation of information for presentation to the computer operator. It will also be possible to introduce additional complexities such as negative pore pressures and seismic forces into the analysis.

It has been found that the lowest factor of safety of the upstream slope is not necessarily obtained with the drawdown at its lowest level. With the existing program, it has been necessary to specify different drawdown levels and to analyze a number of circles for each level. When the program is re-written, it will be arranged so that the computer will automatically examine selected groups of circles for different (specified) drawdown levels and find the most dangerous level.

Experience has also shown the need to provide for "perched" piezometric levels. In the past it has been necessary to adopt zoning to deal with this condition. However, the re-written program will be able to include a separate piezometric surface for each type of soil (if necessary) in a single analysis.

Also under consideration is the use of analytical formulas for the integrals involved in the computation, such as are used by Mr. Horn, instead of the numerical integration employed in the "slices method" which is used in the existing program. For dams of very simple geometry the use of analytical formulas considerably speeds up the computation but in complicated cases there is less gain and in fact a stage of complexity can be reached when the analytical method is slower than the numerical integration method.

One of the particular benefits of using the computer for analysis is the large number of alternative designs which can be examined. In the past it has been possible to consider very few different cross sections for earth dams and there has been a tendency to stop the investigation as soon as one with satisfactory factors of safety has been obtained and no further search for a more economical design has been made. This will no longer be necessary and it will be possible, once a design which is satisfactory from the safety point of view has been established, to make adjustments to obtain a more economical design. On a recent job for which the computer has been used, about 20 different designs have been considered. Although some of the differences have been slight, the scale of the job is so large, that the cost has been reduced by some millions of pounds.

A further application of the program has been the determination of a set of stability coefficients to allow the ready computation of the factor of safety of most simple slopes in terms of effective stress. It is expected that these results will be published shortly.[12]

---

12 "Stability Coefficients for Earth Slopes," by A. W. Bishop and N. R. Morgenstern. (To appear in Géotechnique).

FUNDAMENTAL ASPECTS OF THIXOTROPY IN SOILS[a]

Discussion by P. L. Newland and B. H. Allely, and Anatol A. Eremin

P. L. NEWLAND[3] and B. H. ALLELY.[4]—Mr. Mitchell makes reference to a paper by the writers (24) describing experiments which showed that a sensitivity was developed during consolidation of a clay, and he suggests that thixotropy may be responsible for this behavior. Before accepting this conclusion, the following points extracted from the paper should be taken into account:—

1. The duration of increments was, with one exception, less than 30 hr.
2. Increments were terminated when primary consolidation was completed.
3. Shear tests were made on the central portion of the sample where consolidation was last to be completed.
4. The larger the consolidating pressure used (and consequently the larger the associated shear deformation or remoulding at particle contacts), the larger the sensitivity developed.
5. Sensitivities up to 3.9 were developed.
6. In a test not quoted in the paper, the sensitivity developed in a sample allowed to stand without undergoing consolidation amounted to 1.5 in 4 days.

The preceding points considered together suggest that thixotropy, defined as a phenomenon dependent solely on a lapse of time for its manifestation, is not the agency responsible for the sensitivity developed during consolidation. However, the author may dismiss the point by classing the clay as "rheopectic: that is, gentle motion accelerated the thixotropic hardening." With the possible exception of point 4 and apart from the fact that normal rheopexy has not been observed with this clay, this would be difficult to refute without quibbling over definitions. But if now rheopexy is included under the general heading of thixotropy, any hypothesis advanced to explain the mechanism underlying the latter must also afford an explanation of the former. The author in his hypothesis certainly makes no attempt to do this and it is difficult to see how in fact it could be done without considerable special pleading; for example, that above a certain intensity, remoulding forces tend to disperse, whereas below this intensity they tend to aid flocculation. In the writers' opinion, the sensitivity developed during consolidation is more akin to that developed during electro-osmosis where consolidation is induced by removal of water.

The author's interpretation of the work of P.R. Day, quoted as "Perhaps the most significant datum available thus far relating to the fundamentals of

---

[a] June, 1960, by J. J. Mitchell.
[3] Soil Physicist, Soil Mechanics Lab., D.S.I.R., Auckland, New Zealand.
[4] Soil Physicist, Soil Mechanics Lab., D.S.I.R., Auckland, New Zealand.

thixotropy . . ." will now be discussed. The writers do not have a copy of this report to hand at the time of writing so that they are not in a position to check on the way Day's measurements were carried out. However, the results as presented by the author may be interpreted in two ways. Firstly, it may be that the shear strengths of the clays increased due to thixotropic hardening. As a consequence, their resistance to consolidation increased (by virtue of an increase in their true cohesion as contended by the writers) (24) so that the externally applied pore water tension could be increased gradually as the clays aged without causing any consolidation of the clays. If this were the order of things, then the author's interpretation that the increased tension led to an increase in effective stress, which in turn led to an increase in strength, confuses cause with effect.

On the other hand, and this is suspected to be the correct order of events because the use of a simple tensiometer is mentioned, water tended to be drawn into the sample with the passage of time and equilibrium was established at higher and higher tensions, possibly due to increased osmotic pressure differences in line with factor 3 cited by the author under the heading "Thixotropy in Concentrated Suspensions." This in turn may simply be interpreted as an increase in the net repulsive force between particles with time so that again contrary to the author's claim, there is no evidence for a net increase in the effective stress which could contribute to any gain in strength. Furthermore, the gradual increase in repulsive force will act counter to the postulated decrease in these forces due to removal of the externally applied energy of remoulding.

An alternative conclusion is that the pore water tension arises from a tendency of the pore phase to shrink, for example, an increase in adsorptive forces, cited by the author as factor 4, is accompanied by an increase in the density of the adsorbed phase. Under these conditions, the pore tension may, via the air-water interfaces, cause an increase in the effective stress. However, the change in density and hence total shrinkage of the soil-water mass can only be extremely small. (Such a phenomenon is distinct from syneresis and it follows that, if this is the only source of pore tension, a sample of the hardened clay should not swell and soften when totally immersed in water.) Thus, taking account of the relatively large compressibility of the soil, the change in effective stress would be small and in any case it would be virtually impossible to measure the tensions involved since the relatively small flow of water which would allow the tension to decrease to zero once and for all could not be prevented in the ordinary methods of measuring soil-water tension.

Similar caution is also necessary in concluding that the changes in pore water tension during ageing are associated with changes in the free energy of the system.

The association between flocculation and dispersion of suspensions of clays and indeed of other materials and their thixotropic behavior has been observed by H. Van Olphen (32), and R. Houwink (33). The writers (34) have made similar observations on a clay which is not mineralogically unusual. This clay can be seen to flocculate readily in suspension but when treated with an appropriate amount of sodium hydroxide it is to all intents dispersed although it ultimately flocculates if left long enough. In paste form, there is not as clear evidence for either flocculation or dispersion, but the untreated clay possesses no measurable thixotropy (develops too rapidly?), whereas when treated its thixotropic behavior is extremely marked. In fact, sensitivities

based on strengths are developed which are greater than 10, that is, much greater than anything higherto reported. Such a clay offers considerable promise as a material for research into the fundamentals of thixotropy.

The experimental results presented by the author are primarily concerned with the low water contents associated with compacted clays. Here the differences between aged and remoulded strengths at failure are barely significant but differences in stresses at axial strains rather less than those required for failure are taken as evidence of thixotropic behavior. This change in rigidity is attributed in part at least to a spontaneous change from a "dispersed" to a "flocculated" state involving a change in orientation of particles. This conclusion is based not on direct observation but on inference from the results of other workers who have presented data purporting to demonstrate that soils compacted dry of optimum possess a "flocculated" structure whereas the same soils compacted wet of optimum possess either a "flocculated" or a "dispersed" structure depending on the method of compaction. (Whether static compaction can be considered to be a non-shear strain inducing method so far as particle contacts are concerned is open to doubt.)

All the facts could be equally well explained by postulating that thixotropic materials are such that spontaneous time-dependent changes in interparticle bonds occur which are reversible by remoulding. They lead to an increase in strength of the clay. In suspensions and perhaps thin pastes where the mobility of the particles is relatively high, the associated forces lead to flocculation which is manifested in the fluffy appearance of the sediment and in the emergence of a clear supernatant liquid after a lapse of time. There is no necessity to suppose, however, that at lower water contents there is any spontaneous orientation of the particles although increases in interparticle bonds leading to increased strength or rigidity may occur. In fact, it is difficult to believe that the forces involved are sufficiently large to overcome the shear resistance of the remoulded, let alone the partially hardened, soil to allow of such re-orientation.

ADDITIONAL REFERENCES

24. "A Study of the Sensitivity Resulting from Consolidation of a Remoulded Clay," by P. L. Newland and B. H. Allely, Proc. 4th Internatl. Conf., S.M.F.E., Vol. 1, 1957, p. 83.

32. "Forces Between Suspended Bentonite Particles," by H. Van Olphen, Clays and Clay Minerals, Proceedings, 4th Natl. Conf. on Clays and Clay Minerals, Publication 456, Natl. Acad. Sc. Natl. Res. Council, 1956.

33. "Elasticity, Plasticity and the Structure of Matter," by R. Houwink, Dover Publications, 2nd Ed., 1958.

34. "Some Effects of Sodium Hydroxide on the Strength Properties of a Clay," by B. H. Allely and P. L. Newland, being prepared for publication.

ANATOL A. EREMIN,[5] M. ASCE.—Mr. Mitchell's statement in his conclusion . . . "while thixotropy effect may cause appreciable increase in strength in terms of total stresses, they may cause little effect in terms of effective stresses . . ." requires some clarification.

---

[5] Assoc. Bridge Engr. Bridge Dept., Div. of Calif. State Highways, Sacramento, Calif.

During construction of highway fills and sea walls it has been observed that thixotropic effect resulted in increased stability of soil. Therefore, the economic advantage of considering thixotropic effect is obvious.

Furthermore, Mr. Mitchell stated that the chemical effect on thixotropic soils is minor. That is true; in practice application of chemicals in connection of thixotropic effects in soil may be found not quite economic. However, in analysis of physical and thixotropic properties of soils application of chemicals have important significance. Likewise, observing the graphs in Fig. 11 the effect of Na CL on thixotropic changes in soils is quite noticeable.

It is interesting to note that the thixotropic effect in bentonite as shown by graphs in Fig. 3(a) is similar to that as shown in the silty clay soils termed "Beamharnois," on the same Fig. 3(a).

Possibly, similar effect of thixotropy may be obtained in the montmorilonite soils. Confirmation of this thixotropic effect in montmorilonite may be found to be of considerable interest.

FOUNDATION VIBRATIONS[a]

Discussion by D. F. Coates

D. F. COATES.[3]—The author is to be congratulated for adding another excellent piece of applied research to the field of foundation engineering. If he could comment on some of the following practical aspects it would be of great assistance:

1. The proper testing of the subgrade medium remains the difficult part of analyzing and designing a foundation that includes dynamic forces. This aspect is made particularly difficult by the medium being non-linear. In these circumstances (unless it were possible to determine analytically the non-linear parameters) it is important that the test of the material should be at the same stress level as would occur in the prototype situation.

This might be achieved by vibration testing although the reservations must be retained that the full depth of the strata is probably not being tested by, in effect, the model, and it is questionable whether a technique that measures the propagation of Rayleigh waves is suitable for a prototype whose behavior is most significantly affected by the propagation of compression waves. In addition, seismic methods generally (except for some of the later work close-in to the blasts at the Nevada and Eniwetok Proving Grounds) measure velocities at low levels of stress and consequently do not give appropriate information for the prototype foundation.

For these reasons the writer feels that a static load test is more likely to be the practical method of obtaining the appropriate information. A small test still has the limitation of not testing the full depth of the subgrade; however, it is possible to vary the elevation of these tests quite easily. Recent work (16) and (37) (which indicates that cycling a stress increment around the working stress level can produce a modulus of deformation very close to that obtained by dynamic methods) suggests that it would be worth trying static testing methods again in a research program pointed towards predicting natural frequencies and amplitude magnifications. Does the author think that these problems are likely to be solved by this type of static testing?

2. Under the heading "Use of the Theoretical Procedures," the author states that the magnification effects at resonance during starting and stopping are examined. The computations are based on correlations established for steady-state conditions. If the starting and stopping of the machinery were at a slow rate it would be reasonable to use the steady-state relations; however, in normal circumstances would this apply? Possibly some guidance could be suggested on a maximum rate of change of frequency for which these relations would apply.

---

[a] August, 1960, by F. E. Richart, Jr.

[3] D. F. Coates, Ltd., Cons. Engrs., Ottawa, Ont., Canada.

3. Does the author believe that these correlations of dimensionless parameters could be used for transient or impact cases—such as drop hammers? Theoretically the natural frequency of vibration of the system is the principal parameter to be determined. Then the rise time, duration, and so forth of the blow, if known, permits the dynamic load factor to be computed. However, some work by Barkan (38) indicated that a foundation system could have a different natural frequency under vibrating conditions than under impact conditions. This might possibly just have been due to the non-linear nature of the subgrade and the different stress levels involved in the different tests.

4. Has the author considered establishing the empirical correlations with E rather than G? For the two most important cases—vertical oscillation and rocking oscillation—E can be considered to be the material property directly involved with such factors as $\left(1 - \mu^2\right)$ only influencing the answer slightly. Furthermore, in some tests such as triaxial and plate-load tests E or $E/\left(1 - \mu^2\right)$ are more easily determined than G and μ. In Fig. 8 a few trial computations indicate that if the frequency factor used E instead of G the curves for $\mu = 0$ and $\mu = 0.25$ would practically collapse onto one line and the curve for $\mu = 0.5$ would be within 10% of this combined curve. It is appreciated that a final answer on this question would probably require more paper work on the part of the author, however, any comments would be of interest.

5. Under "Example B" should "Fig. 10" read "Fig. 9"?

6. Under "Example A" should not the radius of gyration of a rectangular prism for an axis through a center line in the base be $1/3\left(h^2 + a^2\right)$, that is $1/12\left(h^2 + 4\,a^2\right)$ plus the transfer factor of $(h/2)^2$?

In conclusion the writer would like to re-emphasize his high regard for the author's present and past work.

ADDITIONAL BIBLIOGRAPHY

16. "Dynamic Triaxial Tests on Sand," by W. L. Shannon, G. Yamane, and R. J. Dietrich, Proceedings, 1st Pan American Conf. on Soil Mech. and Foundation Engrg., Mexico City, Mexico, September, 1959.

37. "Effect of Consolidation Pressure on Elastic and Strength Properties of Clay," by S. Wilson and R. Dietrich, ASCE Research Conference on Shear Strength of Cohesive Soils, 1960.

38. "Soil Mechanics, Foundations and Earth Structures," by G. Tschebotarioff, McGraw-Hill Book Co., Inc., New York, N.Y., 1951, p. 585.

PILE DRIVING ANALYSIS BY THE WAVE EQUATION[a]

Discussion by L. O. Soderberg and Marvin Gates

L. O. SODERBERG,[8] M. ASCE.—Mr. Smith has proposed a method of analyzing pile driving that goes far beyond a "pile driving formula." He offers a rational approach for studying many of the subtleties of piles that have been treated empirically in the past.

As a great deal of numerical manipulation is required to attain a solution, any simplification of these procedures will help to make the method more useful. By treating the problem as one of finite differences, significant simplifications can be attained with no loss of accuracy.

Mr. Smith can treat a tapered pile with a large variety of end conditions. His basic assumption is essentially one dimensional wave propagation where small variations in the pile cross sectional area are permitted. The partial differential equation describing this phenomenon[9] is

$$E\,dx\left(A_x \frac{\partial^2 u}{\partial x^2} + \frac{\partial A}{\partial x}\frac{\partial u}{\partial x}\right) - R = \rho\, A_x \frac{\partial^2 u}{\partial t^2}\, dx \quad \ldots\ldots\ldots(30)$$

in which A_x represents the cross sectional area of the pile at point x, u is the displacement of the pile at point x, R is the total skin friction acting on element dx, and ρ is the mass density of the pile.

Eq. 30 can be approximated directly by the technique of finite differences.[7]

$$D_m = 2\, d_m\,(1 - \phi) + \phi\, d_{m+1}\left(1 + \frac{A_{m+1} - A_{m-1}}{4\, A_m}\right)$$
$$+ \phi\, d_{m-1}\left(1 - \frac{A_{m+1} - A_{m-1}}{4\, A_m}\right) - \phi\,\frac{R\,l}{A_m E} - d_m^{*} \quad \ldots\ldots(31)$$

This notation is Mr. Smith's with the exception that

$$\phi = \frac{E\,\Delta\, t^2}{\rho\, l^2} \quad \ldots\ldots\ldots\ldots\ldots\ldots\ldots(32)$$

If the cross sectional area of the pile is constant Eq. 31 is exactly Eq. 9 with the constants that determine ϕ factored out. If the areas vary, these two equations become slightly different approximations. The value of ϕ is constant for

---

[a] August, 1960, by E. A. Smith.

[8] Research Engr., Raymond International Inc., New York, N. Y.

[9] "Theory of Elasticity," by Timoshenko and Goodier, McGraw-Hill Book Co., Inc. New York, N.Y. 1951, p. 439.

any given problem and the numerical work is greatly simplified if ϕ is computed only once during the problem and not at each step.

The approach proposed here is to reason directly from Eq. 31. This is to apply the end conditions to this equation by means of displacements and changes in displacement (strains) and thus manipulate only one basic relationship instead of the author's five (Eqs. 4 through 8).

The use of this single relationship is best illustrated by working the author's example as given in Fig. 12.

TABLE 1

EQ. 36. $D_m = 1.99\, d_m + .01\, d_{m+1} - d^*_m$

EQ. 35. $D_m = 1.80\, d_m + .07\, d_{m-1} + .13\, d_{m+1} - d^*_m$

EQ. 34. $D_m = d_m\left[1.77 - 3.85\,(d_m - d^*_m)\right] + .15\, d_{m-1} - d^*_m$

EQ. 33. $D_m = 1.64\, d_m + .18\, d_{m+1} + .18\, d_{m-1} - d^*_m$

Time	W1	W2	W3	W4	W5	W6	W7	W8	W9	W10	W11	W12
10	328	184	110	045	011	001	0	0	0	0	0	0
9	301	153	080	027	004	0	0	0	0	0	0	0
8	273	122	054	014	001	0	0	0	0	0	0	0
7	243	092	033	006	0	0	0	0	0	0	0	0
6	212	065	018	002	0	0	0	0	0	0	0	0
5	179	041	008	001	0	0	0	0	D_m	0	0	0
4	145	023	003	0	0	0	0	d_{m-1}	d_m	d_{m+1}	0	0
3	110	010	001	0	0	0	0	0	d^*_m	0	0	0
2	074	003	0	0	0	0	0	0	0	0	0	0
1	037	0	0	0	0	0	0	0	0	0	0	0
0	0	0	0	0	0	0	0	0	0	0	0	0

Displacements in .001 in/per time unit = 1/4000 sec.

With the values given for Δ t, l, E and ρ the value for ϕ is .18. As the main body of the pile has a constant cross section and has no skin friction Eq. 31 becomes Eq. 33 as shown in Table 1 for the main portion of the pile.

$$D_m = 1.64\, d_m + .18\, d_{m+1} + .18\, d_{m-1} - d^*_m \quad \ldots\ldots\ldots (33)$$

It is not immediately obvious that this relationship holds for the first pile section, W3, Mr. Smith uses the spring constant for a full section of pile between the pile cap, W2, and the first pile section, which is the approximation implied in Eq. 33.

At a boundary, such as the pile tip, there is an imaginary point outside the boundary whose displacement appears in Eq. 31. This imaginary displacement can be computed from the known strain at the boundary. This strain is known through the force at the boundary and Young's Modulus for steel, E. At the tip of this pile, for displacements less than .10 in., the imaginary point, d_{m+1}, will be replaced by

$$d_m\left(1 - \frac{K'_p\, l}{E\, A}\left(1 + \frac{J\left(d_m - d^*_m\right)}{12\, \Delta\, t}\right)\right)$$

in Eq. 31 R is 0 and the point resistance of the pile is included in the preceding relationship.

In this case the point of the pile has an added weight of 100 lb. This situation can be handled in a variety of ways. One would be to increase the cross sectional area of the last section to compensate for this weight. Mr. Smith chose to change the mass of the last section without changing its length or area. This is equivalent to changing the density for this section, or in terms of Eq. 31, ϕ is .15 for this section. With these considerations the basic relationship becomes Eq. 34 for the tip section.

$$D_m = d_m\ 1.77 - 3.85\left(d_m - d_m^*\right) + .15\ d_{m-1} - d_m^* \ldots\ldots (34)$$

The hammer and pile cap sections could easily be approximated by elastic sections of length l. The capblock forces would then be entered at the boundaries as strain as explained for the pile tip. However, Mr. Smith preferred to consider these sections as rigid bodies and the displacement relationships are easily obtained from the rules for capblock forces and motion that he has indicated. Eq. 35 and Eq. 36 are valid for capblock compression and are again shown in Table 1.

$$D_m = 1.80\ d_m + .07\ d_{m-1} + .13\ d_{m+1} - d_m^* \ldots\ldots\ldots (35)$$

and

$$D_m = 1.99\ d_m + .01\ d_{m+1} - d_m^* \ldots\ldots\ldots\ldots (36)$$

The first ten time intervals of Mr. Smith's illustrative problem are shown in Table 1. This computation treats only displacements and the initial conditions must be entered as such. At time 0 all displacements are 0, and at time 1 all displacements are still 0 with the exception of the hammer. The hammer has moved a distance equal to its initial velocity times one time interval. Next, the relationships Eq. 33 through Eq. 36 are used working up from left to right one time interval at a step.

The numerical work is essentially a weighted averaging process. As one be seen from Table 1 the points on Fig. 12 are produced accurately with a slide rule.

The relationships developed here are for capblock compression and point displacement up to .10 in. For capblock restitution and displacements in excess of .10 in. new relationships for the hammer, pile cap, and pile tip must be used.

These simplifications of Mr. Smith's basic method have been used successfully both in hand computations and on a small scale digital computer and have been found to reduce the computational work by as much as a factor of 4.

MARVIN GATES,[10] M. ASCE.—The application to pile driving of the wave equation, developed almost one hundred years ago by St. Venant[11] and later by Boussinesq,[12] is proposed by Mr. Smith in this paper as well as in several

---

[a] August, 1960, by E. A. L. Smith.
[10] Chf. Engr. and Counsel, Macari Bros. Const. Co., Windsor, Conn.
[11] Journal de Liouville, Tome XII, 1867, p. 237.
[12] Application des Potentiels, 1885, pp. 508-545.

others of his writings.[13,14,15,16] Mr. Smith is deserving of the Society's appreciation for his untiring efforts to acquaint the profession with a tool which, though little used now, may become the ultimate rationale in the area of pile driving analysis.

D. V. Issacs[17] first proposed the application to pile driving of the wave equation; followed by W. H. Glanville[18] et al., seven years later in 1938. A. E. Cummings in 1940[19] and again in 1941[20] reported on the works of the aforementioned investigators but made little contribution of his own to the furtherence of either the theory or its applications to pile driving. Ten years elapsed when the wave equation was once again proposed to the profession by Mr. Smith,[13] and ever since he has continued untiringly to update his writings.

However, in all of Mr. Smith's efforts, he implies that the wave equation can be used to solve for the bearing capacity as well as the driving stresses. This sweeping application was objected to by this writer as well as others.[21] Mr. Smith subsequently replied to these objections.[22,23] Recently[24] Mr. Smith announced the publication of this paper and an improvement on his earlier article. At the same time, specific reference was again made to bearing capacity.

It is important to note that the investigators preceding Mr. Smith unanimously cautioned against the use of the wave equation as a means of determining bearing capacity. Rather, all concurred that its application should be restricted to finding the driving stresses in piles. Some investigators went so far as to limit its application to certain types of piles under particular conditions of driving. In view of these facts, it is suggested that Mr. Smith make a definitive statement concerning the limits of application of his presentation. This is necessary to remove the haze precipitated by certain apparently conflicting statements concerning the use of this method. Mr. Smith's qualification of his previous references to bearing capacity, by mentioning in this paper soils which may either relax or set-up is no clarification at all. Because again, by implication, the wave equation will give the true bearing capacity for piles driven in soils which return to their natural state after, or remain unchanged during the pile driving operation.

There are many objections to the use of a dynamic formula in general and the wave equation in particular, to determine the bearing capacity of piles. It is sufficient here, to avoid repetition, to cite several authorities in substantiation of this statement.[25] In an important treatise on this subject[26] the

---

13 Fundamentals of Electronic Calculations, IBM, 1950, pp. 10-21.
14 "Impact and Longitudinal Wave Transmission," Transactions ASME, August, 1955.
15 "The Wave Equation Applied to Pile Driving," Raymond Conc. Pile Co., 1957.
16 "What Happens When Hammer Hits Pile," ENR, September 5, 1957, pp. 46-48.
17 Journal, Institution of Australian Engineers, Vol. 3, 1931, p. 305.
18 "An Investigation of the Stresses in Reinforced Concrete Piles During Driving," by W. H. Glanville, G. Grime, E. N. Fox, and W. W. Davies, Building Research Technical Paper No. 20, London, England, 1938.
19 Journal, Boston Society of Civil Engineers, 1940.
20 Proceedings, ASCE, 1941.
21 Engineering News Record, December 19, 1957, pp. 6-7.
22 Engineering News Record, April 24, 1958, pp. 8-12.
23 Engineering News Record, June 19, 1958, pp. 10-14.
24 Engineering News Record, September 22, 1960, p. 32.
25 Soil Mechanics Series No. 17, No. 348, Harvard University, Cambridge, Mass. 1941 to 1942.
26 Pile Foundations and Pile Structures, ASCE Manual No. 27.

question of the application to bearing capacity of dynamic type formulas is deftly summed up as follows:

> It is true that some of the (dynamic) formulas at times give results approximately correct. This is because they empirically apply to certain piles and conditions of driving.

The principal objection to the use of any dynamic formula is, of course, the attempt to equate an instantaneous (about 0.02 sec) kinetic load to a long term static load. On the other hand, static formulas lack general applicability on account of the wealth of data relating to the physical properties of the soil which is required.

However, empirical equations are frequently employed when the number of variables and their inter-relationships are not all known. Chellis[27] lists several empirical pile driving formulas. More recently, this discusser proposed an empirical relationship[28] based on a limited statistical investigation of piles loaded to failure. Although containing but two simple parameters, this relationship gives more consistently accurate results than the most complex dynamic formula yet advanced. For piles driven with a Vulcan #1 hammer this formula is:

$$B = 48 \log \frac{10}{s} \qquad (37)$$

in which B is the ultimate bearing capacity in tons and s is the customary set per blow for the last 6 in. or twenty blows, in inches. A safety factor of from two to three is recommended.

The application of statistical practice to pile driving has been inexcusably neglected. A concerted effort in this direction can yield a reliable pile bearing formula, based on the wealth of data already on hand, within six months.

The use of the wave equation to solve for driving stresses most certainly deserves serious consideration. As a result of Mr. Smith's intimate acquaintance with this subject he has devised a most ingenous analogy; the weights and springs concept. This expedient will simplify for many, who might otherwise have remained unaware, the principals of the wave equation. The use of electronic computors to facilitate the mathematical work is a natural consequence; and indeed is virtually a necessity. It is regrettable, however, that Mr. Smith has not yet compared his theoretical results with those obtained by other investigators from field tests. This suggestion was made previously[29] and the source of valuable field data,[30] obtained by affixing strain gauges to driven piles was cited. One of the many interesting results reported in the last cited reference is the small increase in stress at the head and sharp decrease in stress at the tip, with increased pile penetration and driving resistance. This should serve a signal of caution to those who would apply the wave equation without further investigation.

The application of a fundamental mathematical theory to practice is frequently negated because of the necessity to make at least partially invalid

---

27 "Pile Foundations," by R. D. Chellis, McGraw-Hill Book Co., Inc., New York, N.Y., 1951.

28 Empirical Formula for Predicting Pile Bearing Capacity, Civil Engineering, March, 1957, pp. 65-66.

29 Letter to Mr. Smith, May, 1958.

30 Proceedings, American Railway Engineering Association, September, 1950.

assumptions and over-simplifications. This bane is evident to some degree in Mr. Smith's paper. According to Cummings,[19] the application of the wave equation to pile driving assumes that:

1. The sides of the pile are free and that there is no side friction which would affect the stress waves running up and down the pile.
2. Stress waves in the hammer may be neglected.
3. There are no flexural vibrations of the pile.
4. The pile behaves as a linearly elastic rod.
5. The hammer strikes directly on the head of the pile and that the surfaces of contact are two ideally smooth parallel planes.
6. The lower end of the pile is fixed.

In addition to these assumptions, the theory does not include the effect of dissipation of energy due to propagation losses in the pile.

Cummings' further comments should be studied before any attempt is made to apply the wave equation; albeit in his paper, too, certain concepts are not clearly explained. One generalization, based on Cummings' analysis bears repeating here. The six foregoing assumptions all lead to conservative answers. That is, the computed driving stresses are greater than actually occur. This fact has been substantiated by investigators in the field. Therefore, any attempt to correlate these computed stresses to bearing capacity will, naturally, yield unsafe results.

Looking now to the problem solved by Mr. Smith, we find that for the conditions specified, a Vulcan #1 hammer driving a 12BP53 to a count of five blows to the inch, at a pile penetration of 100 ft, develops a ground resistance to driving, at the tip, of 200,000 lb. Substituting the set, 0.2 in., in Eq. 37 yields a value of 164,000 lb. Considering that Mr. Smith's answer is too great for the reasons outlined previously, the likelihood is that Eq. 37 is as dependable as Mr. Smith's method.

The compressive forces are shown as increasing rapidly towards the tip of the pile. This conclusion is diametrically opposed to the results obtained from the field tests previously cited.[30] This same paper also concludes that:

1. The measured driving stresses in the top of the steel piles increased with an increase in pile penetration, and attained a maximum value equal to 20 to 34 times the static weight of the hammer ram with a 3-ft stroke.
2. Only about 7 per cent of the driving stress measured in the top of the single friction steel pile was observed at the point of the pile.
3. Only about a third of the total driving stress measured in the top of the 110-ft steel pile driven through 90 feet of clay, silt and silt clay into sand was observed at the pile point.

If these conclusions and observations are correct, then the maximum stress which will obtain with a Vulcan #1 hammer is between 100,000 and 170,000 lb. The higher value is about 60% of the head value and 40% of the point value reported by Mr. Smith. The other two conclusions have already been discussed.

There are other questionable aspects in Mr. Smith's method; most notable being the need to preassign not only the factor R_u but also the penetration at which this value occurs. The ability to accurately predict what Mr. Smith implicitly takes for granted, would, in itself, be a major breakthrough in the field of pile driving analysis.

The ultimate solution to this problem lies in the field, the laboratory of the foundation engineer. No theory, however rigorous mathematically, can satisfactorily explain the pile driving phenomenon, unless it is modified to reflect the heterogenous nature of each pile driving operation.

Mr. Smith should enlist the aid of others, if necessary, to verify experimentally his theoretical conclusions and modify them accordingly. The fact that he has been slow to do so detracts only from the immediate application of his efforts. He must still be commended for laying an important building block in the theoretical area of foundation engineering.

PROCEEDINGS PAPERS

The technical papers published in the past year are identified by number below. Technical-division sponsorship is indicated by an abbreviation at the end of each Paper Number, the symbols referring to: Air Transport (AT), City Planning (CP), Construction (CO), Engineering Mechanics (EM), Highway (HW), Hydraulics (HY), Irrigation and Drainage (IR), Pipeline (PL), Power (PO), Sanitary Engineering (SA), Soil Mechanics and Foundations (SM), Structural (ST), Surveying and Mapping (SU), and Waterways and Harbors (WW), divisions. Papers sponsored by the Department of Conditions of Practice are identified by the symbols (PP). For titles and order coupons, refer to the appropriate issue of "Civil Engineering." Beginning with Volume 82 (January 1956) papers were published in Journals of the various Technical Divisions. To locate papers in the Journals, the symbols after the paper number are followed by a numeral designating the issue of a particular Journal in which the paper appeared. For example, Paper 2270 is identified as 2270(ST9) which indicates that the paper is contained in the ninth issue of the Journal of the Structural Division during 1959.

VOLUME 85 (1959)

DECEMBER: 2271(HY12)[c], 2272(CP2), 2273(HW4), 2274(HW4), 2275(HW4), 2276(HW4), 2277(HW4), 2278(HW4), 2279(HW4), 2280(HW4), 2281(IR4), 2282(IR4), 2283(IR4), 2284(IR4), 2285(PO6), 2286(PO6), 2287(PO6), 2288(PO6), 2289(PO6), 2290(PO6), 2291(PO6), 2292(SM6), 2293(SM6), 2294(SM6), 2295(SM6), 2296(SM6), 2297(WW4), 2298(WW4), 2299(WW4), 2300(WW4), 2301(WW4), 2302(WW4), 2303(WW4), 2304(HW4), 2305(ST10), 2306(CP2), 2307(CP2), 2308(ST10), 2309(CP2), 2310(HY12), 2311(HY12), 2312(PO6), 2313(PO6), 2314(ST10), 2315(HY12), 2316(HY12), 2317(HY12), 2318(WW4), 2319(SM6), 2320(SM6), 2321(ST10), 2322(ST10), 2323(HW4)[c]. 2324(CP2)[c], 2325(SM6)[c], 2326(WW4)[c], 2327(IR4)[c], 2328(PO6)[c], 2329(ST10)[c], 2330(CP2).

VOLUME 86 (1960)

JANUARY: 2331(EM1), 2332(EM1), 2333(EM1), 2334(EM1), 2335(HY1), 2336(HY1), 2337(EM1), 2338(EM1), 2339(HY1), 2340(HY1), 2341(SA1), 2342(EM1), 2343(SA1), 2344(ST1), 2345(ST1), 2346(ST1), 2347(ST1), 2348(EM1)[c], 2349(HY1)[c], 2350(ST1), 2351(ST1), 2352(SA1)[c], 2353(ST1)[c], 2354(ST1).

FEBRUARY: 2355(CO1), 2356(CO1), 2357(CO1), 2358(CO1), 2359(CO1), 2360(CO1), 2361(PO1), 2362(HY2), 2363(ST2), 2364(HY2), 2365(SU1), 2366(HY2), 2367(SU1), 2368(SM1), 2369(HY2), 2370(SU1), 2371(HY2), 2372(PO1), 2373(SM1), 2374(HY2), 2375(PO1), 2376(HY2), 2377(CO1)[c], 2378(SU1), 2379(SU1), 2380(SU1), 2381(HY2)[c], 2382(ST2), 2383(SU1), 2384(ST2), 2385(SU1)[c], 2386(SU1), 2387(SU1), 2388(SU1), 2389(SM1), 2390(ST2)[c], 2391(SM1)[c], 2392(PO1)[c].

MARCH: 2393(IR1), 2394(IR1), 2395(IR1), 2396(IR1), 2397(IR1), 2398(IR1), 2399(IR1), 2400(IR1), 2401(IR1), 2402(IR1), 2403(IR1), 2404(IR1), 2405(IR1), 2406(IR1), 2407(SA2), 2408(SA2), 2409(HY3), 2410(ST3), 2411(SA2), 2412(HW1), 2413(WW1), 2414(WW1), 2415(HY3), 2416(HW1), 2417(HW3), 2418(HW1)[c], 2419(WW1)[c], 2420(WW1), 2421(WW1), 2422(WW1), 2423(WW1), 2424(SA2), 2425(SA2)[c], 2426(HY3)[c], 2427(ST3)[c].

APRIL: 2428(ST4), 2429(HY4), 2430(PO2), 2431(SM2), 2432(PO2), 2433(ST4), 2434(EM2), 2435(PO2), 2436(ST4), 2437(ST4), 2438(HY4), 2439(EM2), 2440(EM2), 2441(ST4), 2442(SM2), 2443(HY4), 2444(ST4), 2445(EM2), 2446(ST4), 2447(EM2), 2448(SM2), 2449(HY4), 2450(ST4), 2451(HY4), 2452(HY4), 2453(EM2), 2454(EM2), 2455(EM2)[c], 2456(HY4)[c], 2457(PO2)[c], 2458(ST4)[c], 2459(SM2)[c].

MAY: 2460(AT1), 2461(ST5), 2462(AT1), 2463(AT1), 2464(CP1), 2465(CP1), 2466(AT1), 2467(AT1), 2468(SA3), 2469(HY5), 2470(ST5), 2471(SA3), 2472(SA3), 2473(ST5), 2474(SA3), 2475(ST5), 2476(SA3), 2477(ST5), 2478(HY5), 2479(SA3), 2480(ST5), 2481(SA3), 2482(CO2), 2483(CO2), 2484(HY5), 2485(HY5), 2486(AT1)[c], 2487(CP1)[c], 2488(CO2)[c], 2489(HY5)[c], 2490(SA3)[c], 2491(ST5)[c], 2492(CP1), 2493(CO2).

JUNE: 2494(IR2), 2495(IR2), 2496(ST6), 2497(EM3), 2498(EM3), 2499(EM3), 2500(EM3), 2501(SM3), 2502(EM3), 2503(PO3), 2504(WW2), 2505(EM3), 2506(HY6), 2507(WW2), 2508(PO3), 2509(ST6), 2510(EM3), 2511(EM3), 2512(ST6), 2513(HW2), 2514(HY6), 2515(PO3), 2516(EM3), 2517(WW2), 2518(WW2), 2519(EM3), 2520(PO3), 2521(HY6), 2522(SM3), 2523(ST6), 2524(HY6), 2525(HY6), 2526(HY6), 2527(IR2), 2528(ST6), 2529(HW2), 2530(IR2), 2531(HY6), 2532(EM3)[c], 2533(HW2)[c], 2534(WW2), 2535(HY6)[c], 2536(IR2)[c], 2537(PO3)[c], 2538(SM3)[c], 2539(ST6)[c], 2540(WW2)[c].

JULY: 2541(ST7), 2542(ST7), 2543(SA4), 2544(ST7), 2545(ST7), 2546(HY7), 2547(ST7), 2548(SU2), 2549(SA4), 2550(SU2), 2551(HY7), 2552(ST7), 2553(SU2), 2554(SA4), 2555(ST7), 2556(SA4), 2557(SA4), 2558(SA4), 2559(ST7), 2560(SU2)[c], 2561(SA4)[c], 2562(HY7)[c], 2563(ST7)[c].

AUGUST: 2564(SM4), 2565(EM4), 2566(ST8), 2567(EM4), 2568(PO4), 2569(PO4), 2570(HY8), 2571(EM4), 2572(EM4), 2573(EM4), 2574(SM4), 2575(EM4), 2576(EM4), 2577(HY8), 2578(EM4), 2579(PO4), 2580(EM4), 2581(ST8), 2582(ST8), 2583(EM4)[c], 2584(PO4)[c], 2585(ST8)[c], 2586(SM4)[c], 2587(HY8)[c].

SEPTEMBER: 2588(IR3), 2589(IR3), 2590(WW3), 2591(IR3), 2592(HW3), 2593(IR3), 2594(IR3), 2595(IR3), 2596(HW3), 2597(WW3), 2598(IR3), 2599(WW3), 2600(WW3), 2601(WW3), 2602(WW3), 2603(WW3), 2604(HW3), 2605(SA5), 2606(WW3), 2607(SA5), 2608(ST9), 2609(SA5)[c], 2610(IR3), 2611(WW3)[c], 2612(ST9)[c], 2613(IR3)[c], 2614(HW3)[c].

OCTOBER: 2615(EM5), 2616(EM5), 2617(ST10), 2618(SM5), 2619(EM5), 2620(EM5), 2621(ST10), 2622(EM5), 2623(SM5), 2624(EM5), 2625(SM5), 2626(SM5), 2627(EM5), 2628(EM5), 2629(ST10), 2630(ST10), 2631(PO5)[c], 2632(EM5)[c], 2633(ST10), 2634(ST10), 2635(ST10)[c], 2636(SM5)[c].

NOVEMBER: 2637(ST11), 2638(ST11), 2639(CO3), 2640(ST11), 2641(SA6), 2642(WW4), 2643(ST11), 2644(HY9), 2645(ST11), 2646(HY9), 2647(WW4), 2648(WW4), 2649(WW4), 2650(ST11), 2651(CO3), 2652(HY9), 2653(HY9), 2654(ST11), 2655(HY9), 2656(HY9), 2657(SA6), 2658(WW4), 2659(WW4)[c], 2660(SA6), 2661(CO3), 2662(CO3), 2663(SA6), 2664(CO3)[c], 2665(HY9)[c], 2666(SA6)[c], 2667(ST11)[c].

DECEMBER: 2668(ST12), 2669(IR4), 2670(SM6), 2671(IR4), 2672(IR4), 2673(IR4), 2674(ST12), 2675(EM6), 2676(IR4), 2677(HW4), 2678(ST12), 2679(EM6), 2680(ST12), 2681(SM6), 2682(IR4), 2683(SM6), 2684(SM6), 2685(IR4), 2686(EM6), 2687(EM6), 2688(EM6), 2689(EM6), 2690(EM6), 2691(EM6)[c], 2692(ST12), 2693(ST12), 2694(HW4)[c], 2695(IR4)[c], 2696(SM6)[c], 2697(ST12)[c].

c. Discussion of several papers, grouped by divisions.

AMERICAN SOCIETY OF CIVIL ENGINEERS

OFFICERS FOR 1961

PRESIDENT
GLENN W. HOLCOMB

VICE-PRESIDENTS

Term expires October 1961:
CHARLES B. MOLINEAUX
LAWRENCE A. ELSENER

Term expires October 1962:
DONALD H. MATTERN
WILLIAM J. HEDLEY

DIRECTORS

Term expires October 1961:
THOMAS J. FRATAR
EARL F. O'BRIEN
DANIEL B. VENTRES
CHARLES W. BRITZIUS
WAYNE G. O'HARRA
FRED H. RHODES, JR.
N. T. VEATCH

Term expires October 1962:
ELMER K. TIMBY
SAMUEL S. BAXTER
THOMAS M. NILES
TRENT R. DAMES
WOODROW W. BAKER
BERNHARD DORNBLATT

Term expires October 1963:
ROGER H. GILMAN
HENRY W. BUCK
EARLE T. ANDREWS
JOHN B. SCALZI
JOHN D. WATSON
HARMER E. DAVIS

PAST PRESIDENTS
Members of the Board

FRANCIS S. FRIEL
FRANK A. MARSTON

EXECUTIVE SECRETARY
WILLIAM H. WISELY

TREASURER
E. LAWRENCE CHANDLER

ASSISTANT SECRETARY
DON P. REYNOLDS

ASSISTANT TREASURER
LOUIS R. HOWSON

PROCEEDINGS OF THE SOCIETY

HAROLD T. LARSEN
Manager of Technical Publications

PAUL A. PARISI
Editor of Technical Publications

MARVIN L. SCHECHTER
Associate Editor of Technical Publications

IRVIN J. SCHWARTZ
Assistant Editor of Technical Publications

COMMITTEE ON PUBLICATIONS

THOMAS M. NILES, *Chairman*

WAYNE G. O'HARRA, *Vice-Chairman*

BERNHARD DORNBLATT
JOHN D. WATSON
HENRY W. BUCK
HARMER E. DAVIS

PART 2

DECEMBER 1960 — 46
VOLUME 86

NO. SM6
PART 2

Your attention is invited

NEWS
OF THE
SOIL
MECHANICS
AND
FOUNDATIONS
DIVISION
OF
ASCE

AMERICAN SOCIETY OF CIVIL ENGINEERS
FOUNDED 1852

JOURNAL OF THE SOIL MECHANICS AND FOUNDATIONS DIVISION
PROCEEDINGS OF THE AMERICAN SOCIETY OF CIVIL ENGINEERS

DIVISION ACTIVITIES
SOIL MECHANICS AND FOUNDATIONS DIVISION
Proceedings of the American Society of Civil Engineers

NEWS

December, 1960

NEWS ON RESEARCH ACTIVITIES FROM THE BUREAU OF RECLAMATION

A. 1960 Edition of the Earth Manual

The Bureau of Reclamation has published a new 1960 Edition of its Earth Manual, a successor to the 1951 Edition. The new edition provides current technical information relating to field and laboratory investigations of soils used as foundations in materials for dams, canals, and many other types of structures built on Reclamation projects in the United States. More than 6,000 copies of the 1951 edition have been distributed worldwide. The new edition has been completely revised and is published with an attractive bound cover, 4-$\frac{1}{4}$ inches by 7 inches in size. Copies of the publication may be obtained from the Superintendent of Documents, U. S. Government Printing Office, Washington 25, D. C., or the Bureau of Reclamation, Denver Federal Center, Denver, Colorado, Attention 841. The price is $3.75 postpaid.

B. Undisturbed Sampling of In-place vane Shear Tests

In a recent field exploration program, undisturbed samples were taken of the soil which had been subjected to the vane shear test. This permitted a rare opportunity to examine the shear surfaces cut by the vanes. The vane test is performed by inserting a 4-bladed vane into the soil and measuring the torque necessary to cut cylindrical surfaces (Test Designation E-20, USBR Earth Manual 1960). Figure 1 shows the cylindrical sheared surface observed in one of the samples. The interesting features of this observation are that the cylindrical failure surface forms a relatively thin line and the soil in the quarters formed by the vanes appears undisturbed, giving confidence in the mathematical theory for computing the shearing resistance of the soil.

C. Effect of Negative Pore Pressures in Unsaturated Soils

The effect of negative pore pressures in unsaturated soils is being studied extensively by the Earth Laboratory. The initial results of this study were reported in the Bureau's paper (for the ASCE Research Conference on Shear

Note.—No. 1960-46 is Part 2 of the copyrighted Journal of the Soil Mechanics and Foundations Division, Proceedings of the American Society of Civil Engineers, Vol. 86, No. SM 6, December, 1960.

Strength of Cohesive Soils), entitled "Shear Strength of Cohesive Soil".[1] Much useful information has been gained from this program and the research is being continued.

D. Continuing Research on Gravelly Soils

The Earth Laboratory's research program on gravelly soils is being continued and the most recent report is a paper accepted for the Fifth International Conference on Soil Mechanics and Foundation Engineering at Paris, France. The paper by W. G. Holtz[2] and Willard Ellis[3] is entitled "Triaxial Shear Characteristics of Clayey Gravel Soils."

E. Revised Relative Density Test for Granular Soils

The Denver Earth Laboratory of the Bureau of Reclamation is one of the participants in a cooperative research program being conducted by the American Society for Testing Materials for the development of a standard relative density test procedure for cohesionless free-draining soils. The program involves the development of both a maximum density and a minimum density test procedure. The Bureau's research has resulted in the development of a tentative procedure which has been adopted as an alternate to the Bureau of Reclamation's standard test, Designation E-12. The alternate procedure involves the use of an electromagnetic table-type vibrator, 8 minutes of vibration, a 0.1- or 0.5-cubic-foot container, 2 psi guided dead-weight surcharge, a method of measuring the thickness of the compacted soil specimen and the use of ovendry or saturated soil. The equipment was designed for use with soils containing a maximum particle size of 3 inches. A complete set of equipment for the maximum and minimum density test is shown in Figure 2.

NEW DELHI CONFERENCE ON BEARING CAPACITY OF SOILS

Under the joint auspices of the Central Building Research Institute, Roorkee and the National Buildings Organization, New Delhi, two sister organizations of the Government of India for the promotion of research and dissemination of knowledge on Buildings, a Symposium on Load Bearing Capacity of Soils will be held in New Delhi on the 23rd and 24th of January in 1961. About thirty papers are expected to be discussed, and besides Indian research workers, papers are being contributed by workers in Japan, France, U.S.A., Israel and U.K. It is proposed to publish the papers and circulate them to the delegates in advance. The discussion will be published in a separate volume after the symposium. Further particulars may be obtained from Mr. Dinesh Mohan, Deputy Director and Head, Soil Engineering Division, Central Building Research Institute, Roorkee, U.P. (India).

---

1 This paper will be published as a part of the final proceedings of the conference.
2 Chief, Earth Laboratory Branch, Bureau of Reclamation, Denver, Colorado.
3 Civil Engineer (Soil Mechanics), Earth Laboratory Branch, Bureau of Reclamation, Denver, Colorado.

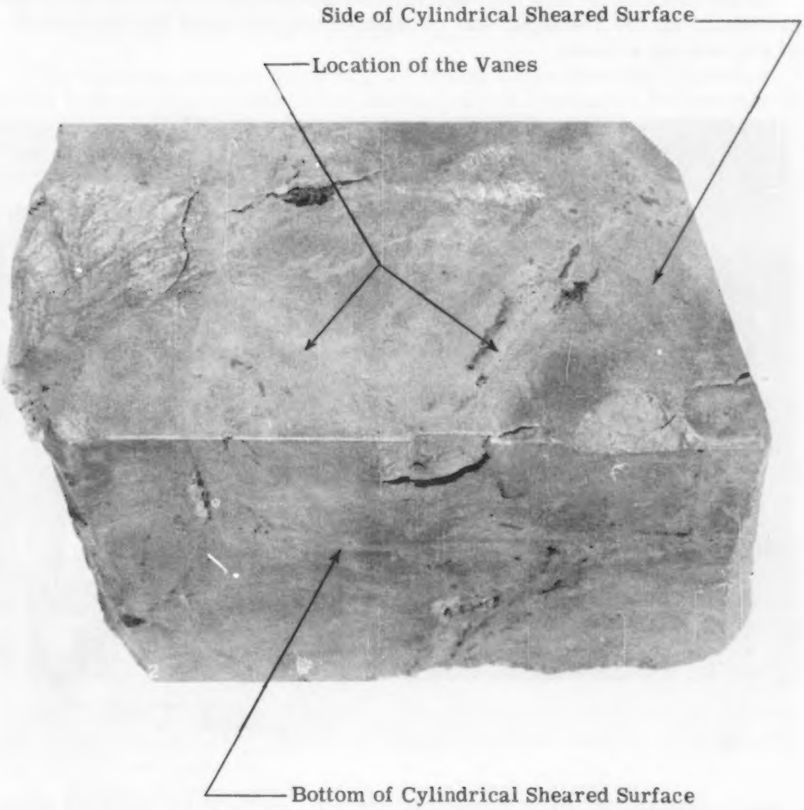

FIG. 1.—AN UNDISTURBED SOIL SAMPLE REMOVED FROM THE SITE OF A VANE SHEAR TEST

TERZAGHI MEMORIAL VOLUME

At the annual meeting of the Society held in Boston in October, Dr. Karl Terzaghi was presented a copy of From Theory to Practice in Soil Mechanics by his distinguished student and long-time friend, Dr. Arthur Casagrande. The presentation was made during the Soil Mechanics and Foundation Division meetings which included a number of excellent papers by both these and other men.

The book contains selections from the writings of Dr. Terzaghi, with bibliography and contributions on his life and achievements, prepared by L. Bjerrum, A. Casagrande, R. B. Peck, and A. W. Skempton.

In the last century no civil engineer has exerted so much influence on his profession as Dr. Terzaghi, who established and developed this new branch of engineering science.

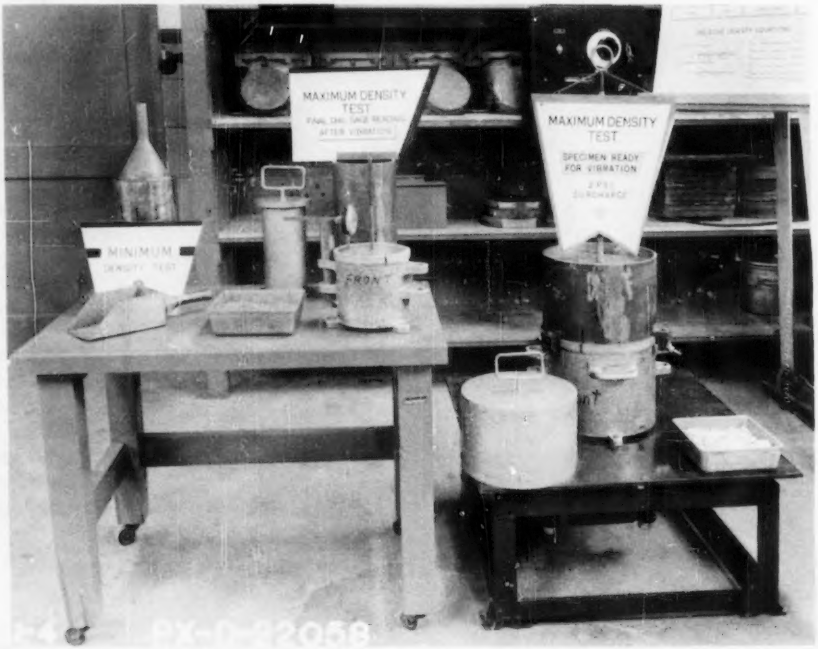

FIG. 2.—RELATIVE DENSITY TEST EQUIPMENT. A 0.5-CU-FT MEASURE WITH GUIDE SLEEVE AND 2-PSI SURCHARGE IS ATTACHED TO THE VIBRATORY TABLE ON THE RIGHT. A 2-PSI SURCHARGE WEIGHT IS EXHIBITED ON THE FRONT LEFT CORNER OF THE VIBRATORY TABLE.

For the first time in one volume, an account is given of this man's life and his method of working. The representative selection of papers, which are in English for the most part, includes those that established the science of soil mechanics, a selection of his professional reports that indicate his methods of dealing with specific jobs and a complete bibliography of his works.

The collection contains papers that were previously hard to find in the literature and others that have been translated for this book. They provide a special insight into how Dr. Terzaghi approached and solved foundation, landslide, tunneling, and earth dam problems.

UNITED STATES NATIONAL COMMITTEE FOR THE INTERNATIONAL SOCIETY OF SOIL MECHANICS AND FOUNDATION ENGINEERING

The following statutes regarding the United States National Commitee for the International Society of Soil Mechanics and Foundation Engineering as adopted August 31, 1960 have been received from Mr. John Lowe, Secretary of the Committee. They are presented to acquaint division members with this organization and its function:

Article I. Name, Sponsorship and Headquarters

1. The name of the Society is the "United States National Committee for the International Society of Soil Mechanics and Foundation Engineering," hereinafter called the United States National Committee.
2. Sponsorship. The United States National Committee is an Administrative Committee of the Soil Mechanics and Foundations Division of the American Society of Civil Engineers.
3. Headquarters. The headquarters of the U. S. National Committee shall be that of the American Society of Civil Engineers. The mailing address however, shall be the mailing address of the Secretary of the United States National Committee (375 Park Avenue (Room 900), New York 22, New York).

Article II. Purpose

The purpose of the United States National Committee is to represent the United States of America in the International Society of Soil Mechanics and Foundation Engineering and to foster international cooperation among engineers and scientists in the field of soil mechanics and foundation engineering. Specific activities of the U. S. National Committee include:

a. Designating a delegate and alternative delegate to represent the U. S. National Committee in the Executive Committee of the International Society.
b. Cooperating in the holding of periodic International Conferences both world-wide and regional.
c. Appointing members to act on international committees.
d. Publicizing international conferences in Soil Mechanics and Foundation Engineering.
e. Reviewing and selecting papers for presentation at international conferences.

Article III. Membership

1. The membership of the United States National Committee shall include those members of the Soil Mechanics and Foundations Division of the American Society of Civil Engineers who are residents or citizens of the United States of America and who indicate their desire to be listed on the roster of the United States National Committee.
2. The membership of the United States National Committee shall include those members of the Soil Mechanics and Foundations Division of the ASCE

who are not residents of the U.S.A. and who are not represented by a national society in the International Society of Soil Mechanics and Foundation Engineering and whose application is approved by the Secretary of the United States National Committee.

Article IV. Executive Committee

1. The management of the United States National Committee shall be vested in an executive committee consisting of five members. Four of the members shall be the four members of the Executive Committee of Soil Mechanics and Foundations Division of the ASCE. These four members are appointed by the ASCE Committee on Division Activities in accordance with the ASCE Constitution, Bylaws and Rules of Policy and Procedure. Each member is to hold office for four years, with one member retiring annually at the close of the annual ASCE meeting, at which time the newly appointed member takes office. The fifth member shall be a secretary of the committee, elected by the four above mentioned members. The term of office of the secretary shall be one year; but there shall be no limit to the number of consecutive terms a secretary may be elected to serve.

2. The officers of the executive committee are a chairman, a vice-chairman and a secretary. The chairman and vice-chairman of the Executive Committee of the Soil Mechanics and Foundations Division shall serve also as the chairman and vice-chairman of the Executive Committee of the United States National Committee. The secretary shall be elected as described in Article IV-1.

3. Meetings of the Executive Committee shall be held at the call of the chairman or of any three members of the committee. Three members of the Executive Committee shall constitute a quorum. When voting is required on a particular question and circumstances do not permit the calling of a meeting, the membership of the Executive Committee may be polled by letter ballot. Voting in all cases shall be decided by a simple majority.

Article V. Dues and Finances

1. Dues. There are no membership contributions in addition to the yearly ASCE dues.

2. Finances. Each year the U. S. National Committee shall prepare an estimate of its expenses for the coming year and submit it to the Soil Mechanics and Foundations Division for inclusion in the Division's budget request. Neither the U. S. National Committee nor any of its subcommittees shall incur any financial obligations chargeable to the ASCE unless specifically authorized by the ASCE.

Article VI. International Society Obligations

Annually, at a date fixed by the Executive Committee of the International Society, the Secretary of the United States National Committee shall transmit to the Secretary of the International Society the following:

a. The amount of the National Society's contribution as set forth by the Executive Committee of the International Society.

b. Copies of the statutes of the United States National Committee if they have been modified during the current year.

c. The current list of the membership of the United States National Committee, their occupations and addresses.

Article VII. Committees

1. As required by the International Society, the U. S. National Committee shall appoint members to represent the U. S. National Committee on committees of the International Society. Appointment of these representatives shall be by the Executive Committee of the U. S. National Committee. Members appointed to international committees shall make annual reports to the U. S. National Committee and shall submit their budget for any anticipated expenses to the U. S. National Committee for inclusion in its budget.

2. Committees for review of papers for International Conferences shall be appointed as required. Alternatively, review of papers may be accomplished by the Publications Committee of the Soil Mechanics and Foundations Division. In either case, final approval of papers shall be by the Executive Committee with due consideration of the recommendations of the Review Committee.

Article VIII. Amendments to Present Statutes

The statutes of the United States National Committee may be amended only by the Executive Committee of the United States National Committee.

DEFINITION OF TERMS AND SYMBOLS RELATING TO SOIL MECHANICS

In 1947, the Committee on Glossary of Terms and Definitions in Soil Mechanics was formed under the chairmanship of R. E. Fadum, for the purpose of preparing an up-to-date glossary. During the same year, Subcommittee G-3 on Nomenclature and Definitions of ASTM Committee D-18 was formed for a similar purpose under the chairmanship of E. A. Abdun-Nur, and later C. R. Foster. It was realized that joint action by these two groups would be desirable. This was achieved through the membership of the Subcommittee G-3 chairman on the ASCE Committee.

After numerous meetings and considerable personal work on the part of the members, the committees completed a glossary acceptable to both. The results of their work has been published by both societies. "Definition of Terms and Symbols Relating to Soil Mechanics" (Designation D-653-58T) was adopted as a Tentative Standard by the ASTM in 1958 and as a Standard in 1960, and has been published in Part IV of the ASTM Standards, 1948. The "Glossary of Terms and Definitions in Soil Mechanics" was published as ASCE Proceedings, Paper No. 1826, Journal of the Soil Mechanics and Foundations Division, October 1958.

The compilation of papers for the ASCE Shear Conference revealed a lack of uniformity of definitions and symbols used by the authors. This tends to make the review and reading of the papers difficult. Authors of papers are urged to use the Definitions of Terms and Symbols adopted by the joint action of the ASTM and ASCE groups as much as possible.

It is planned that these groups will continue their efforts in this field to periodically review and revise the glossary to keep pace with future developments. Comments on the glossary are solicited and members should feel free to express their ideas on this subject. The committee on Definitions and Standards of the ASCE, Soil Mechanics and Foundations Division, is now under the Chairmanship of Gerald A. Leonards. Sub-committee G-3 of ASTM, Committee D-18, is now under the Chairmanship of R. G. Ahlvin.

To coordinate the work of these two committees, the Boards of Direction of the two Societies authorized (June 1960) the formation of a joint ASCE-ASTM Committee on Glossary of Terms and Definitions in Soil Mechanics. The joint committee consists of the members of ASCE's Committee on Definitions and Standards and Sub-committee G-3 of ASTM's Committee D-18.

NEWS FROM THE ILLINOIS SECTION

The Soil Mechanics and Foundations Division of the Illinois Section, ASCE featured Mr. Vern McClurg, Senior Partner of McClurg, Shoemaker, McClurg; Mr. Normal Scott, Executive Secretary, Prestressed Concrete Institute; and Mr. Eugene Guillard, Research Engineer of the Armour Research Foundation who discussed the results of load tests on timber, prestressed concrete and steel H-piles respectively. Their talks were followed with a discussion period during which the "whys" of the results were probed. This meeting provided an excellent opportunity to compare the various pile types and to study their advantages.

The October meeting featured Mr. E. G. Robbins, Supervising Engineer, Paving Bureau, Portland Cement Association who spoke on "Treating Soils Materials with Portland Cement." Mr. Robbins reviewed the design procedures used for soil cement, explaining the cement content required for adequate stabilization varies primarily with soil type and is affected very little by the other variables. His talk was illustrated with slides which showed the developments in soil cement construction from mule teams to the modern one-pass paver which is capable of laying up to 3.5 miles of roadway per day.

FEBRUARY NEWSLETTER

Deadline date for arrival at this office of contributions for the February Newsletter: December 23, please.

Bernard B. Gordon, Assistant Editor
Porter, Urquhart, McCreary, and O'Brien
1140 Howard Street
San Francisco 3, California

Wilbur M. Haas, Assistant Editor
Michigan College of Mining and Technology
Houghton, Michigan

J. H. Schmertmann, Assistant Editor
College of Engineering
University of Florida
Gainesville, Florida

Alfred C. Ackenhell, Editor
University of Pittsburgh
Civil Engineering Department
Pittsburgh 13, Pennsylvania

ASCE SYMPOSIUM ON ROCKFILL DAMS

At the meeting of the ASCE Board of Direction, in Reno in June 1960, it was arranged that the complete Symposium on Rockfill Dams of some eight hundred pages be published in one bound volume as ASCE TRANSACTIONS, 1960, Vol. 125, Part II (Symposium on Rockfill Dams).

The volume will include all ASCE literature on the subject of rockfill dams from October 1954 to October 1960. It will consist of 24 papers and 68 discussions and closures; the discussion following each paper. This special volume of 1960 ASCE TRANSACTIONS will provide a comprehensive, up-to-date and convenient reference volume on rockfill dams.

ASCE TRANSACTIONS, 1960, Vol. 125, Part II (Symposium on Rockfill Dams) will be available in January 1961 and will be priced at $12, making it available to ASCE members at $6 with the usual 50% discount.

To reserve a copy, please write to Executive Secretary, ASCE, 33 West 39th Street, New York 18, New York, with advance payment. This will assure you of a copy at the earliest possible date. For your convenience, an advance order form is provided herewith.

The Symposium has been planned to assemble design, construction and performance data on most of the world's higher rockfill dams. The presentation of settlement data has been emphasized and detailed data on many high dams has been made available for the first time in the papers and discussions.

For purposes of the Symposium, a rockfill dam was defined to be one that relies on rock, either dumped or compacted in layers, as a major structural element. Included are rockfill dams of the types with (1) impervious face membranes, (2) sloping earth cores, (3) thin central cores, and (4) thick central cores. Some of the notable dams covered in the Symposium and listed by the above types are: (1) Dix River, Salt Springs, Montgomery, Cogswell, San Gabriel, Lower Bear River, Paradela, Wishon, Courtright, Pinzanes, Nozori, and Ishibuchi; (2) Natahala, Kenney, Brownlee, Bersimis, Dalles Closure, Trangslet, Miboro, Hirfanli, Queens Creek, Cedar Cliss, Bear Creek and Furnas; (3) Makio, Derbendi Khan, Kajakai, Mud Mountain, Goschener, Messaure and Cougar; and (4) Nottely, Watauga, South Holston and Cherry.

Rockfill dams are being increasingly adopted throughout the world and are being constructed to ever-increasing heights. This Symposium will certainly contribute toward improved, more economic and higher rockfill dams of all types.

---------------------------- CUT HERE ----------------------------

Executive Secretary
American Society of Civil Engineers
33 West 39th Street
New York 18, New York.

Please send me . . . copy(s) of ASCE TRANSACTIONS, Volume 125 (1960) - Part II (Rockfill Dams). Enclosed is my remittance of $. . . . My ASCE membership grade is . . . . List price: $12.00

- -

____
Print Name

____
Address

____
City Zone State 1960T-II

COMBINED INDEX TO ASCE PUBLICATIONS

For complete coverage of the Society's 1959 year in print, there is now a Combined Index covering the Division Journals, Transactions, and Civil Engineering. Also included are reprints of the Proceedings Abstracts that are published each month in Civil Engineering. The price of the Combined Index (ASCE publication 1960-10) is $2.00 with the usual 50% discount to members. The coupon herewith will make ordering easy:

------------------------------ CUT HERE ------------------------------

American Society of Civil Engineers
33 West 39th Street
New York 18, New York

Please send me . . . . copy(s) of ASCE 1960-10. Enclosed is my remittance of $. . . . My ASCE membership grade is . . . . List price: $2.00.

- -

Print Name

Address

City Zone State

. . . . of 1960-10

NEW DIRECTORY IS AVAILABLE TO MEMBERS

The 1960 Directory is now available to members on request. The Directory lists the entire membership of the Society, giving the membership grade, position, and mailing address of each. In addition, there is a complete listing of the Honorary Members, past and present, and the Life Members. A useful geographical listing of the members is also included.

It goes without saying that the information contained in the Directory is of value to every member, and every member can obtain this valuable information. To receive your free copy of the Directory simply fill out the coupon below. Prompt delivery depends on prompt return of the coupon.

The Society publishes the membership Directory every other year. The next edition will be issued in 1962.

DIRECTORY 1960

ASCE members are entitled to receive, free of charge, the 1960 ASCE Directory. To obtain the directory simply clip this coupon and mail to: American Society of Civil Engineers, 33 West 39th Street, New York 18, N.Y.

Please make the mailing label legible--correct delivery depends on you.

---------------------------- CUT HERE ----------------------------

____
Print Name

____
Address

____
City Zone State

1960-Dir.